

# **The role of HAX1 in neutrophil homeostasis**

**Von der Naturwissenschaftlichen Fakultät  
der Gottfried Wilhelm Leibniz Universität Hannover  
zur Erlangung des Grades**

**Doktor der Naturwissenschaften**

**Dr.rer.nat.**

**genehmigte Dissertation**

**Von**

**Master of Science Giridharan Appaswamy  
geboren am 07. Oktober 1980 in Nagercoil, Indien  
Hannover  
2010**

Referee 1 : Prof. Dr. Rita Gerardy-Schahn  
Institute for Cellular Chemistry  
Hannover Medical School  
Carl-Neuberg-Str. 1  
D-30625 Hannover  
Germany

Referee 2 : Prof. Dr. Christoph Klein  
Department of Pediatric Hematology and Oncology  
Hannover Medical School  
Carl-Neuberg-Str. 1  
D-30625 Hannover  
Germany

Referee 3 : Prof. Dr. Hans Joerg Jacobsen,  
Department of Plant Genetics  
Gottfried Wilhelm Leibniz university  
Herrenhaeuser str. 2  
30419 Hannover  
Germany

Tag der promotion: 19<sup>th</sup> October 2010

*Dedicated to my hero, my **DAD**.*

**Erklärung zur Dissertation:** Hierdurch erkläre ich, dass ich meine Dissertation mit dem Titel "The role of HAX1 in neutrophil homeostasis" selbständig verfasst und die benutzten Hilfsmittel und Quellen sowie gegebenenfalls die zu Hilfeleistungen herangezogenen Institutionen vollständig angegeben habe.

Die Dissertation wurde nicht schon als Masterarbeit, Diplomarbeit oder andere Prüfungsarbeit verwendet

Giridharan Appaswamy



# Contents

<b>1. Introduction</b> .....	<b>8</b>
<b>1.1 Clinical disease</b> .....	<b>8</b>
1.1.1 Neutropenia.....	8
<b>1.2 APOPTOSIS</b> .....	<b>11</b>
1.2.1 Mitochondria in apoptosis .....	13
1.2.2 Bcl-2 proteins .....	15
1.2.3 Caspases.....	16
1.2.4 Inhibitor of apoptosis proteins .....	17
1.2.5 Endoplasmic reticulum in apoptosis .....	17
1.2.6 CHOP.....	19
1.2.7 BiP.....	19
<b>1.3 Autophagy</b> .....	<b>20</b>
1.3.1 Autophagy related genes .....	22
<b>1.4 HAX1</b> .....	<b>24</b>
<b>2. Focus of the current study</b> .....	<b>25</b>
<b>3. Materials</b> .....	<b>26</b>
3.1 Antibodies.....	27
3.2 Cytokines.....	27
3.3 Cell culture reagents.....	27
3.4 Chemicals .....	27
3.5 Enzymes, DNA and protein ladder .....	28
3.5 Laboratory equipments .....	29
3.7 Kits .....	29
3.8 Preparation of buffers and media.....	29
<b>4. Methods</b> .....	<b>30</b>
<b>4.1 Sequence analysis of <i>HAX1</i></b> .....	<b>30</b>
<b>4.2 Cells and cell culture</b> .....	<b>31</b>
4.2.1 Isolation of neutrophil and PBMCs.....	31
4.2.2 Isolation of CD34+ cells from the bone marrow .....	31
4.2.3 Culturing of BM derived CD34+ cells .....	32
4.2.4 <i>In vitro</i> differentiation of BM derived CD34+ cells to neutrophils .....	32
4.2.5 Culturing of fibroblasts and HEK293T cells .....	33
<b>4.3 Apoptosis assay</b> .....	<b>33</b>
<b>4.4 Mitochondria membrane potential assay</b> .....	<b>33</b>
<b>4.5 Assay of mitochondrial mass</b> .....	<b>34</b>
<b>4.6 Cytosolic ROS assay</b> .....	<b>34</b>
<b>4.7 Protein isolation and western blot analysis</b> .....	<b>35</b>
<b>4.8 Flow cytometry analysis</b> .....	<b>35</b>
<b>4.9 Immunofluorescence and light microscopy</b> .....	<b>36</b>
<b>4.10 RNA isolation, cDNA synthesis and Real Time PCR</b> .....	<b>36</b>
<b>4.11 Molecular cloning</b> .....	<b>37</b>
4.11.1 Generataion of <i>HAX1</i> expression constructs .....	37
4.11.2 Generataion of shRNA constructs targeting <i>HAX1</i> .....	39
<b>4.12 Retroviral gene transfer</b> .....	<b>40</b>
<b>4.13 Electron microscopy</b> .....	<b>41</b>
<b>5. Results</b> .....	<b>42</b>

5.1 Identification of mutations in <i>HAX1</i> genomic DNA.....	42
5.2 Bone marrow of <i>HAX1</i> mutated patients show a phenotype of SCN.....	43
5.3 Mutations identified in <i>HAX1</i> results in complete absence of the protein.....	44
5.4 Intracytoplasmic localization of HAX1 .....	46
5.5 HAX1 deficient cells show an increased rate of apoptosis .....	47
5.6 HAX1 deficient cells show a rapid loss of MMP ( $\Delta\Psi_m$ ).....	50
5.7 HAX1 deficient cells show increased caspase activation. ....	53
5.8 Silencing of <i>HAX1</i> mRNA is inadequate.....	55
5.9 Reconstitution of $\Delta\Psi_m$ by retroviral gene transfer of <i>HAX1</i> .....	56
5.10 HAX1 deficient neutrophils show reduced mitochondrial mass.....	59
5.11 HAX1 deficient neutrophils have decreased cellular ATP.....	60
5.12 HAX1 deficient neutrophils show increased ROS production.....	60
5.13 HAX1 deficient neutrophils show hampered antioxidant defense.....	62
5.14 HAX1 deficient granulocytes exhibit enhanced autophagy .....	63
<b>6. DISCUSSION.....</b>	<b>67</b>
6.1 Individuals with autosomal recessive severe congenital neutropenia reveal mutations in <i>HAX1</i> .....	67
6.2 HAX1 deficiency results in increased apoptosis through defective maintenance of mitochondrial membrane potential (MMP/ $\Delta\Psi_m$ ) .....	68
6.3 Deficiency of HAX1 results in mitochondrial dysfunction and induces oxidative stress.....	70
6.4 Deficiency of HAX1 results in Beclin-1 dependent autophagy in neutrophil granulocytes .....	71
<b>7. Bibliography.....</b>	<b>73</b>
<b>Abbreviations .....</b>	<b>82</b>
<b>Acknowledgements .....</b>	<b>84</b>
<b>Curriculum Vitae .....</b>	<b>85</b>
<b>Publications .....</b>	<b>86</b>

## Abstract

Severe congenital neutropenia (SCN) is a heterogeneous disorder with the phenotypic hallmark of "myeloid maturation arrest". Although a large group of the neutropenia patients have mutations in *ELANE/ELA2*, the genetic defects underlying Kostmann syndrome, characterized by autosomal recessive mode of inheritance remained largely unknown.

The present study illustrates that mutations in HS-1 associated protein X1 (*HAX1*) leading to absence of the respective protein, results in SCN. We identified that *HAX1* a ubiquitously expressed mitochondrial protein, exerts its antiapoptotic function through maintenance of mitochondrial membrane potential (MMP/ $\Delta\Psi$ M). *HAX1* deficient neutrophils showed an increased rate of ROS production and accelerated degradation of catalase, a primary antioxidant defense protein. *HAX1* deficient neutrophils show defective mitochondrial biogenesis marked by elevated AMP/ATP ratio as exemplified by increased activation of AMP activated protein kinase  $\alpha$  (AMPK $\alpha$ ) and decrease in mitochondrial mass. Expression of beclin-1, an autophagy essential protein was increased in *HAX1* deficient neutrophils, accompanied by an increase in the ATG12-5 complex formation as compared to healthy control cells. Furthermore, transmission electron microscopy studies revealed evidence of increased autophagy in *HAX1* deficient neutrophils. These observed effects are specific to *HAX1* deficiency, as these biochemical aberrations were not observed in patients with mutation in *ELA2* or SCN patients expressing functional *HAX1*. Moreover the phenotype was observed only in neutrophils and not in *HAX1* deficient lymphoid or monocytic cells.

Our results unravel a novel role of the antiapoptotic protein *HAX1* in maintenance of cellular homeostasis in neutrophil granulocytes, by simultaneously regulating apoptosis (PCD-I) and autophagy (PCD-II).

**Keywords:** Severe congenital neutropenia, neutrophils, HS-1 associated protein X1 (*HAX1*), mitochondria, apoptosis, autophagy

## Zusammenfassung

Die schwere kongenitale Neutropenie (SCN) stellt ein heterogenes Krankheitsbild dar, welches phänotypisch durch einen Reifungsstopp der myeloiden Differenzierung charakterisiert ist. Obwohl eine große Gruppe von Neutropenie-Patienten eine Mutation im Gen der Neutrophilen-Elastase (*ELANE/ELA2*) aufweist, sind die genetischen Ursachen des klassischen, autosomal-rezessiv vererbten Kostmann-Syndroms weitgehend unbekannt.

Im Rahmen dieses Promotionsvorhabens konnte dargelegt werden, dass homozygote Mutationen in dem Gen *HAX1* (*HS1-Associated protein X1*) zu einer ausbleibenden Proteinexpression dieses Gens führen, was schließlich in einer SCN resultiert. Hierbei konnten wir zeigen, dass es sich bei *HAX1* um ein ubiquitär exprimiertes mitochondriales Protein handelt, welches eine anti-apoptotische Wirkung in myeloiden Zellreihen durch Aufrechterhaltung des mitochondrialen Membran potentials ( $MMP/\Delta\Psi_m$ ) vermittelt. So konnten wir veranschaulichen, dass *HAX1* defiziente Neutrophile eine erhöhte ROS-Produktion und einen beschleunigten Abbau von Catalase, einem primären antioxidativen Abwehrprotein, aufweisen. Des Weiteren konnte eine defiziente mitochondriale Biogenese in *HAX1* defizienten Neutrophilen dokumentiert werden, was sich in einem erhöhten AMP/ATP Verhältnis widerspiegelte. Beispielsweise konnte in diesem Zusammenhang eine gesteigerte Aktivierung der AMP-aktivierten Proteinkinase  $\alpha$  ( $AMPK\alpha$ ) und eine Verringerung der mitochondrialen Masse detektiert werden.

Darüber hinaus konnten wir in *HAX1* defizienten Neutrophilen zeigen, dass die Expression von Beclin-1, einem essentiellen Protein für den zelluläre Prozess der Autophagie, im Vergleich zu gesunden Kontrollzellen gesteigert war. Ferner war dieser Befund mit einer Erhöhung der ATG12-5-Komplexbildung assoziiert. Der Phänotyp einer gesteigerten Autophagie in *HAX1* defizienten Neutrophilen konnte zudem durch Transmissions Elektronenmikroskopische Untersuchungen bestätigt werden. Interessanterweise sind diese beobachteten Effekte spezifisch für die *HAX1* Defizienz, da diese biochemischen Veränderungen nicht bei Patienten mit *ELA2* Defizienz oder SCN Patienten mit funktioneller *HAX1* Expression nachgewiesen werden konnten. Des

Weiteren wurde dieser Phänotyp nur in Neutrophilen und nicht in lymphoiden oder monozytären Zellen beobachtet.

Unsere Forschungsergebnisse zeigen eine neue Rolle des anti apoptotischen Proteins HAX1 in der simultanen Regulierung von Apoptose (PCD-1) und Autophagie (PCD-II) auf und verdeutlichen die essentielle Bedeutung von HAX1 für die Aufrechterhaltung der zellulären Homöostase neutrophiler Granulozyten.

**Keywords:** schwere kongenitale Neutropenie (SCN), neutrophiler Granulozyten, HS-1 associated protein X1 (*HAX1*), mitochondrialen, Apoptose, Autophagie

# **1. Introduction**

## **1.1 Clinical disease**

A proper balance of immunity and tolerance represents a functionally sound immune system. Disrupted cellular homeostasis leading to aberrant function of the immune system, impairing biological activity of a cell, tissue or an organism manifests clinically evident symptoms. A tilt in the balance of the immune system results either in hyperreactivity or a dysfunction leading to a state of autoimmunity or immunodeficiency.

Immunodeficiency, a state of compromised ability of the immune system is further classified as primary or acquired immunodeficiency. Primary immunodeficiency includes rare lymphoid and myeloid disorders such as Congenital Neutropenia, in which the individual's immune system is compromised and hence is highly susceptible to infections. Immunodeficiency such as Acquired Immuno Deficiency Syndrome (AIDS), caused by the Human Immuno Deficiency Virus (HIV) is the result of an indirect impairment of the immune response. Majority of the immunodeficiencies are acquired and are referred to as secondary immunodeficiency.

### **1.1.1 Neutropenia**

Neutrophils, account for 50-70% of the circulating white blood cells and serve as the primary source of defense against varied infectious bacteria. Neutrophils extend their defense against microorganisms by a mode of intracellular killing, termed phagocytosis. During phagocytosis, the neutrophils engulf and degrade the microorganisms using an array of cytotoxic agents and serine proteases such as neutrophil elastase [1, 2], cathepsinG [3] and proteinase3 [4].

Neutrophils encompass a variety of granules, which are sequentially developed during their differentiation in the bone marrow. These granules distinguished based on their proteinaceous content, contribute to the microbicidal activity of these neutrophils [5]. In addition, neutrophils release serine proteases along with chromatin into the

extracellular matrix to form neutrophils extracellular traps (NETs), which further help in trapping and killing the bacteria [6].

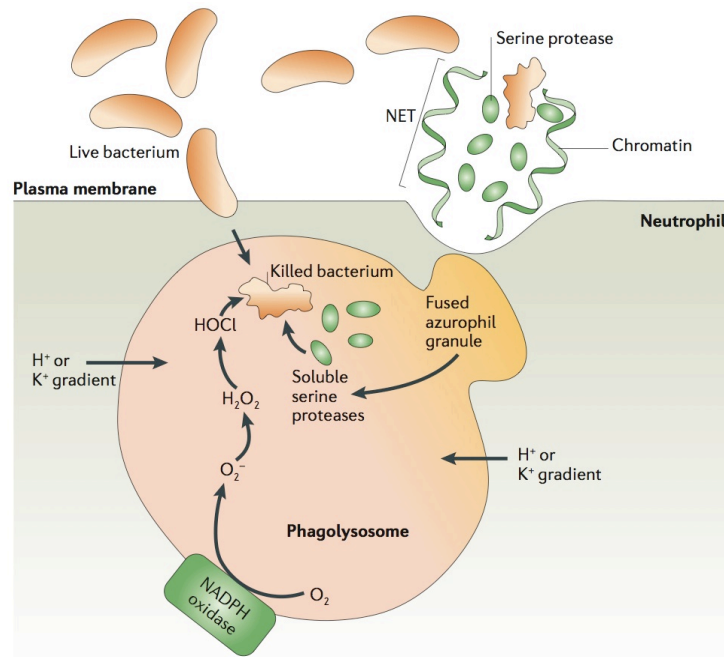


### Fig 1. Microbicidal activity of neutrophil granulocytes

Neutrophils ingest and transport the bacteria inside the phagolysosome, whereby they are directly degraded by the cationic serine proteases. Neutrophil extracellular traps (NETs), which are composed of serine proteases and nuclear constituents, trap and kill bacteria by degrading their virulence factors. (Source: Christine T. N. Pham, Nature reviews Immunology; 2006)

The recruitment of neutrophils to the site of inflammation is the first line of host defence against an infection, whereby the recruited neutrophils perform their function by bacterial phagocytosis and chemokine signaling, thus initiating an inflammatory response [7].

Persistent quantitative and qualitative abnormalities in mature neutrophils result in lack of neutrophil function, leading to life threatening infections. A variety of human diseases including neutropenia, papillon-Lefevre Syndrome (PLS), acute promyelocytic leukaemia (APL) and Wegner's granulomatosis have been associated with the malfunction of neutrophilic serine proteases [7].

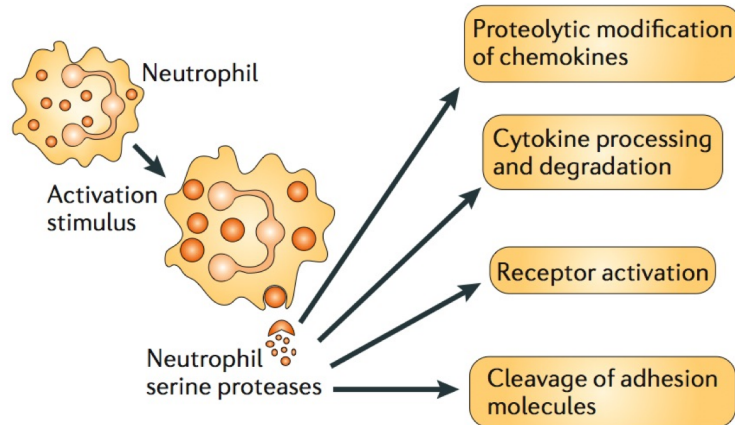


### Fig 2. Immune response by neutrophil granulocytes

Activated neutrophils release their serine proteases to the extracellular environment whereby they can proteolytically modify chemokine activity, activate and inactivate cytokines, activate specific receptors, and potentially participate in neutrophil migration by cleaving adhesion molecules. (Source: Christine T. N. Pham, *Nature reviews Immunology*; 2006)

Neutropenia defines a state of abnormally low number of neutrophils in the peripheral blood. Severe congenital neutropenia (SCN) originally described by Kostmann in 1956 [8], is characterized by paucity of mature neutrophils in the peripheral blood, accompanied by an early onset of life threatening bacterial infections [9]. SCN, marked by promyelocytic or myelocytic granulocytic differentiation arrest differs from cyclic neutropenia [10], a related disorder of granulopoiesis characterized by periodic oscillations in the number of circulating neutrophils [11]. The quantitative decrease of neutrophils in peripheral blood result from defective myeloid differentiation and migration of the differentiated neutrophils from bone marrow and in some reported cases, impaired survival. The qualitative abnormalities arise due to defective chemotaxis of mature neutrophils accompanied by insufficient clearance of pathogenic bacteria. Advancements in neutropenia research over the past years have identified mutations in genes encoding *ELA2* [12], *WAS* [13, 14], *GFI1* [15] and *P14* [16] as the cause of severe congenital neutropenia.



## 1.2 APOPTOSIS

Programmed cell death commonly referred as apoptosis, is an evolutionarily conserved biochemical process [17-19]. Dysregulation of apoptosis results in disturbances of cellular homeostasis causing a number of human pathologies including cancer [20, 21], autoimmune diseases, immunodeficiency [22] and neurodegenerative disorders [10, 23]. Apoptosis is marked by a well defined sequence of morphological changes in a cell. Apoptosis occurs through two major pathways, the extrinsic and intrinsic pathway, classified based on the source of death stimuli. Both the intrinsic and extrinsic pathways of apoptosis culminate the activation of a series of death proteases termed caspases (cysteine-aspartic acid proteases) [24].

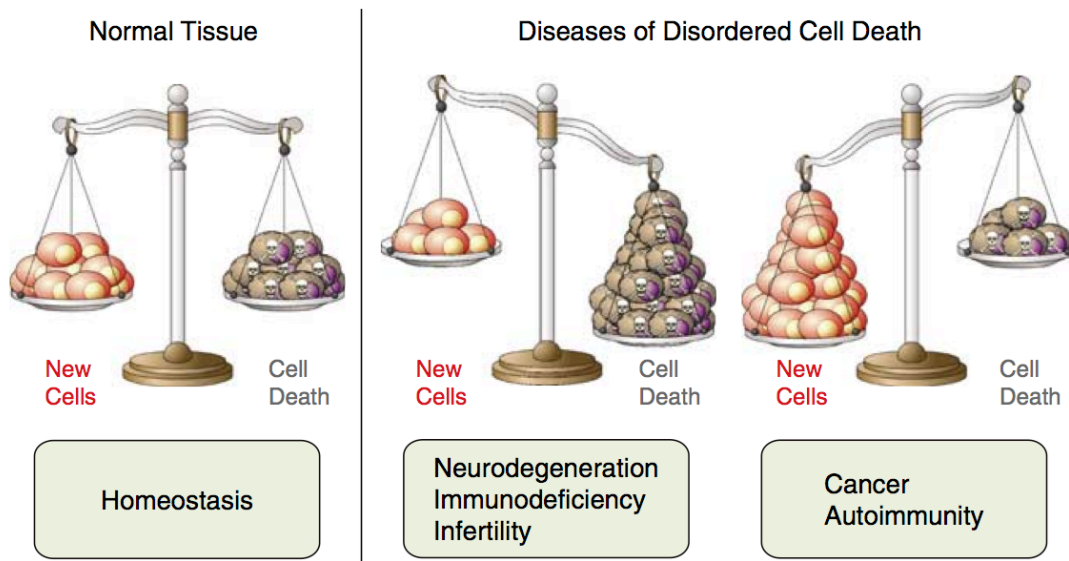


**Fig 3. Role of apoptosis in tissue homeostasis**

Apoptosis maintains tissue homeostasis by balancing cellular life and death. Dysregulated apoptotic pathways disrupt the balance, resulting in diseases of premature cell loss or unrelenting cell survival. (Source: LD Walensky, *Cell Death and Differentiation*; 2006)

The extrinsic pathway of apoptosis begins at the cell surface, involving ligand induced activation of death receptors [20, 25]. Extracellular death stimuli such as the Fas ligand directly activate the death receptors located on cell surface [26, 27].

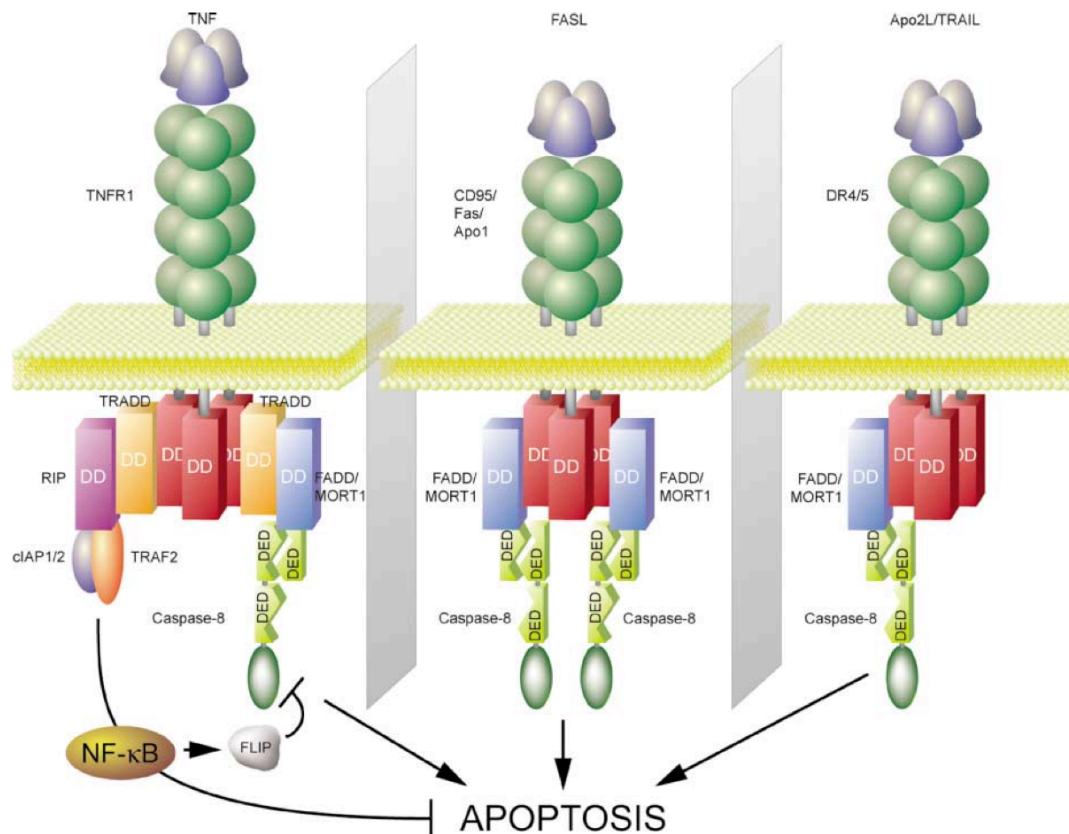


#### Fig 4. Extrinsic pathway of apoptosis

The figure illustrates the distinct composition of the Death-Inducing-Signaling Complex (DISC) downstream of the various death receptors TNFR1, CD95, and DR4/5. (Source: Nika N. Danial and Stanley J. Korsmeyer, Cell; 2004)

Death receptors characterized by the presence of extracellular cysteine rich domains (CRD's) such as TNFR1, Fas and DR3 contain a death domain (DD) in the intracellular compartment [25] and recruits adapter proteins, such as Fas associated death domain (FADD) through homotypic interactions [10]. The activated homotrimeric death ligands, upon binding with the death receptors, induce their oligomerization. The receptor associated adapter molecule, such as FADD recruits the initiator caspase procaspase-8 or procaspase-10 to DISC for activation [25]. The activated caspase-8 subsequently

cleaves and activates the effector caspases, caspase -3 and -7. Alternatively, activated caspase-8 also physiologically targets Bid (BH3 interacting death domain agonist), a member of the Bcl-2 family of proteins, resulting in the cleavage of the c-terminal of Bid. The resulting tBid (truncated c-terminal of Bid) translocates to the outer membrane of the mitochondria and induces the release of proapoptotic factors, which then initiates an intrinsic cell death. Thus the extrinsic pathway of apoptosis also culminates at the intrinsic pathway of apoptosis [28].

The intrinsic pathway of apoptosis begins with intracellular stress signals that target cellular organelles such as mitochondria for the release of cytochrome *c* and other apoptotic factors, which when released activates the caspase via the apoptotic protease activating factor-1 (Apaf-1). The intrinsic pathway of apoptosis results due to a variety of stimuli such as nutrient deprivation, DNA damage, Hypoxia, ER stress [29] or unfolded protein response (UPR).

### **1.2.1 Mitochondria in apoptosis**

Mitochondria, the powerhouse of the cell are membrane enclosed organelles that principally generate adenosine triphosphates (ATP) through the process of aerobic respiration, more commonly referred to as oxidative phosphorylation [30]. In addition to supplying cellular energy, the mitochondria are involved in a variety of other cellular processes such as signaling, differentiation, cell cycle, growth and cell death [31, 32]. A mitochondrion, majorly composed of phospholipid bilayers and proteins is compartmentalized as outer mitochondrial membrane, intermembrane space, inner membrane, cristae and the matrix [33].

Although most of cellular DNA is contained in the nucleus, the mitochondria have their own independent genome and hence the mitochondrial proteome is dynamically regulated [30, 31]. Despite its predominant role in ATP synthesis, mitochondria are being majorly studied for their role in apoptosis [32]. The intrinsic pathway of apoptosis, initiated by stress stimuli originating from different intercellular organelles such as the nucleus, lysosomes, endoplasmic reticulum or mitochondria, begins with the permeabilization of the mitochondrial outer membrane [28, 34] by proapoptotic

members of the Bcl-2 family [35-38]. Hence the intrinsic pathway is also most commonly referred to as the mitochondrial pathway of apoptosis.

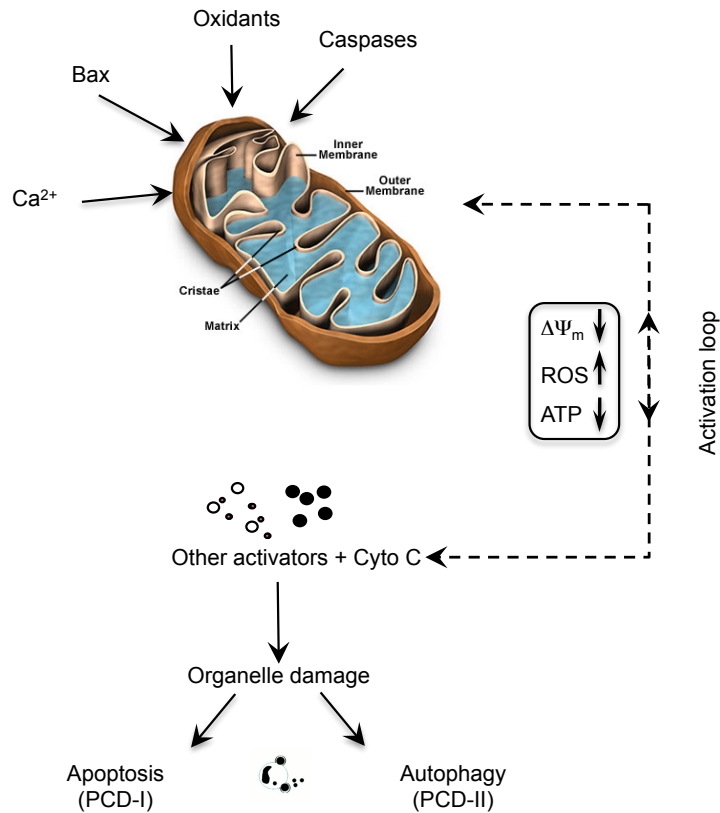


**Fig 5. Mitochondria and intrinsic pathway of apoptosis**

Pathway regulating mitochondrial stress, ATP,  $\Delta\Psi_m$ , ROS levels, autophagy, cell survival and apoptosis (Modified from source: Huafeng Zhang *et al.*, JBC; 2008)

Mitochondrial defect leading to the opening of the PTP is a central component of the intrinsic mitochondrial death pathway [37, 39] and this opening of the PTP has also been reported in case of hypoxia, increased intracellular calcium, as well as oxidative stress injury [38]. Once the mitochondrion is permeabilized, cell death proceeds regardless of caspase activation or eventual loss of mitochondrial functions [40]. Upon induction of apoptosis, the mitochondrion releases apoptogenic factors that activate a family of cysteine proteases called caspases [41]. Cytochrome *c*, one of the released proapoptotic factors, interacts with Apaf-1 and facilitates a conformational change resulting in its oligomerization and recruitment of caspase-9 to form the apoptosome [28]. The apoptosome associated caspase-9 is thereby activated and in turn cleaves and activates the executioner caspases, caspase-3 and caspase-7. These activated

executioner caspases then cleave key substrates in the cell, creating an avalanche of biochemical events resulting in cell death [41]. Both the extrinsic and intrinsic pathway of death converges at mitochondrial membrane permeabilization (MMP/ $\Delta\Psi_m$ ) [34] and is tightly regulated by the Bcl-2 family proteins [28, 42].

### **1.2.2 Bcl-2 proteins**

The Bcl-2 (B-cell lymphoma-2) family of proteins plays a central role in apoptosis by regulating the release of apoptotic factors from mitochondria [43]. The antiapoptotic protein Bcl-2 extends survival against varied apoptotic signals including nutrient deprivation, UV radiation, calcium ionophores and free radicals [23]. Intracellular death stimuli such as oxidative stress or DNA damage generally results in the activation of BH3-only Bcl-2 proteins, which causes the release of apoptotic factors such as cytochrome-*c* from the mitochondrial intermembrane space to the cytoplasm. The release of such apoptotic factors is mediated by the proapoptotic Bcl-2 proteins, Bax and Bak and is antagonized by the antiapoptotic Bcl-2 and Bcl-X<sub>L</sub> proteins [43].

On the basis of their anti or proapoptotic function and their sequence homology to Bcl-2 homology (BH) domains, Bcl-2 proteins are subdivided as the antiapoptotic multidomain, proapoptotic multidomain and the proapoptotic BH3 only domain proteins. Based on their specific role, they are further classified as sensitizers, derepressors and activators [44]. The antiapoptotic multidomain proteins such as Bcl-2 and Bcl-X<sub>L</sub> that contain all the four-conserved Bcl-2 homology (BH) domains, BH1, BH2, BH3, and BH4, prevent the release of the mitochondrial proteins and other apoptotic factors from the mitochondria [34]. The proapoptotic multidomain Bcl-2 proteins such as Bax and Bak contain the conserved BH1, BH2 and BH3 domains, but lack the BH4 domain. They exist as monomers in the absence of apoptotic signals [45]. upon activation by an apoptotic stimulus, they form homo oligomers and induce pore formation in the mitochondria, leading to release of apoptogenic mitochondrial proteins such as cytochrome *c* [37]. The BH3 only proteins such as Bid, Bim and Bad can promote apoptosis by antagonizing the antiapoptotic proteins or facilitating proapoptotic Bcl-2 members [10, 36, 46].

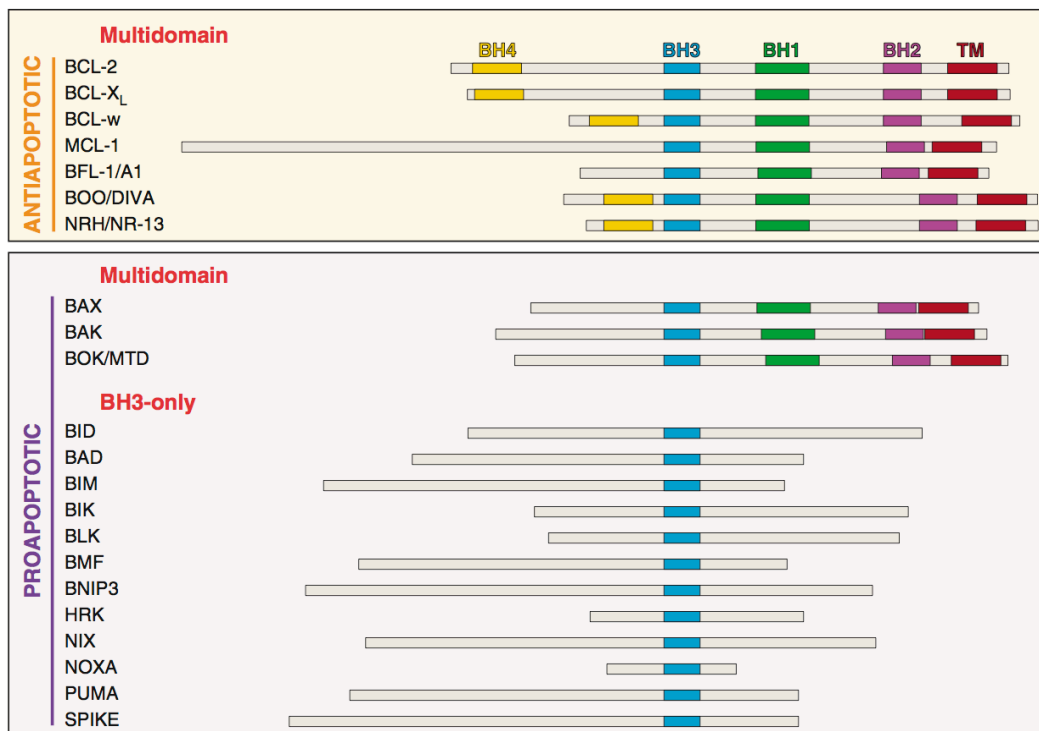


**Fig 6. Classification of Bcl-2 protein family**

BCL-2 family proteins are structurally defined by their BCL-2 homology domains (BH domains) and functionally categorized by their ability to inhibit or activate cell death. (Source: LD Walensky, *Cell Death and Differentiation*; 2006)

Mcl-1 an antiapoptotic member of the Bcl-2 family exerts its antiapoptotic effects by interacting with and antagonizing the proapoptotic Bcl-2 proteins such as Bax [47]. Thus the large Bcl-2 family, including both pro and antiapoptotic proteins form a complex network regulating cell survival and cell death [21, 45].

### 1.2.3 Caspases

Caspases are a class of intracellular death proteases, participating in both extrinsic and intrinsic pathway of apoptosis [48]. Apart from their prominent role in apoptosis, caspases have a variety of other biological functions ranging from cell cycle progression to immune cell development [48, 49]. Nearly 14 distinct mammalian caspases of varied biological function have been identified so far. Caspases that are involved in apoptosis comprise two groups: the initiator caspases, (caspase -2, -8, -9, and -10) and the effector caspases, (caspase -3, -6 and -7) [48, 50] which are targets of initiator caspases. Also a phylogenetically distinct class of caspases which comprise caspase -1, -4, -5, -11 and -12

triggers the release of inflammatory mediators through the proteolytic processing of the precursors of the inflammatory cytokines IL-1 $\beta$  and IL-18 [48, 51]. Caspases are synthesized in a cell as catalytically inactive zymogens and undergo proteolytic activation during apoptosis [52]. The activation of effector caspases such as caspase-3 or -7 is performed by an initiator caspase such as caspase-9, through internal cleavage to separate the large and the small subunits [41, 48, 49, 53, 54]. Unlike the effector caspases, which are activated by proteolytic cleavage, the enzymatic activity of initiator caspases is initiated by oligomerization through protein-protein interactions mediated by death effector domains (DEDs) or caspase recruitment domains (CARDs) present in these caspases [10, 41].

#### **1.2.4 Inhibitor of apoptosis proteins**

The inhibitor of apoptosis (IAP) family of proteins suppresses apoptosis by negatively regulating caspases [35, 54, 55]. There are eight distinct mammalian IAP's: XIAP, CIAP-1, c-IAP-2, ML-IAP/Livin, ILP-2, NAIP, Bruce/Apollon and survivin. The unique and characteristic property of an IAP is the presence of BIR (baculoviral IAP repeat) domain, which possess the ability to bind zinc. Most IAP's contain more than one BIR domain, with each BIR domains exhibiting distinct functions [55]. In case of XIAP, the third BIR domain (BIR3) inhibits caspase-9 whereas the linker region between BIR1 and BIR2 specifically targets caspase-3 and -7 [56].

#### **1.2.5 Endoplasmic reticulum in apoptosis**

The endoplasmic reticulum (ER) is a membranous labyrinth comprising a network of tubules, vesicles and sacs that are interconnected in the cytoplasm [57, 58]. The endoplasmic reticulum occurs in two forms as the rough and the smooth ER. They are differentiated based on their appearance resulting from the presence and absence of ribosomes. The ER performs specialized functions in a cell ranging from protein synthesis, calcium sequestration, glycogen synthesis and protein folding [57, 59]. Folding and assembly of a protein in the endoplasmic reticulum is a key component in protein trafficking to the golgi apparatus and lysosomes [60]. The ER contains numerous resident chaperone proteins, which function towards efficient folding of

newly synthesized proteins. These ER resident proteins involved in the process of protein folding can be classified into two categories based on their specific functions. A first class of proteins referred to as the catalyzers, such as disulfide isomerase (PDI), which catalyze the protein folding reactions [61, 62]. A second class of proteins called chaperones, such as the ER resident immunoglobulin binding protein (BiP) or GRP78 stabilizes energetically unfavorable conformations of polypeptides to minimize misfolding and facilitate the folding of the newly synthesized proteins to attain their final conformation [63, 64]. Thus the catalyzers and the chaperones together facilitate the maintenance of proteins, preventing aggregation of the folding intermediates and protein misfolding.

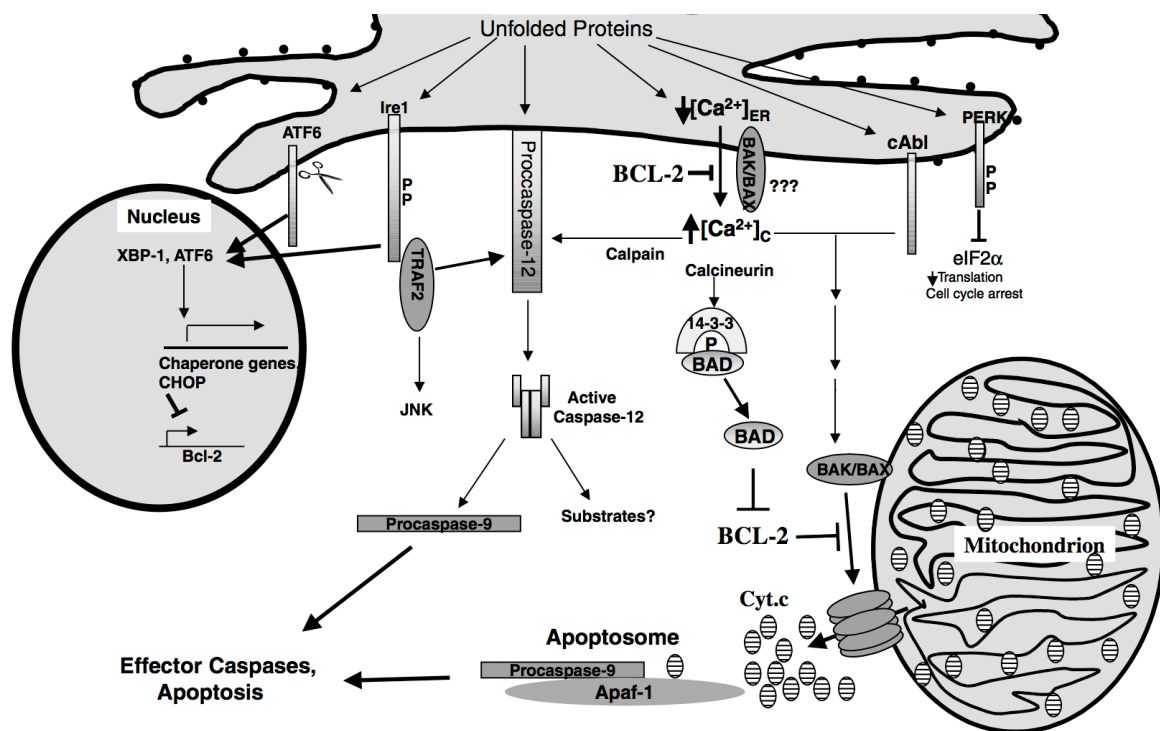


**Fig 7. Endoplasmic reticulum and intrinsic pathway of apoptosis**

Activation of the unfolded protein response (UPR) increases the expression of ER chaperones, such as GRP78, which bind to unfolded protein to prevent further accumulation. Although unfolded protein might undergo refolding to promote cell survival. ER stress beyond a certain threshold causes severe DNA damage resulting in apoptosis and autophagy. (Source: David G Breckenridge *et al.*, *Oncogene*; 2003)



ER stress has been implicated in a variety of common diseases such as diabetes, ischemia and neurodegenerative disorders [65-69]. Alterations in the ER environment occurring with nutrient, glucose or oxygen deprivation, interference in glycosylation or calcium flux across membranes, dramatically affects protein folding, resulting in accumulation of unfolded proteins [57, 70]. A perturbation of the ER homeostasis transduces signal cascades collectively referred to as the unfolded protein response (UPR) and is further characterized by the induced expression of ER chaperones to control the UPR stress [64, 71].

### **1.2.6 CHOP**

Growth arrest and DNA damage 153 (GADD 153) commonly referred to as C/EBP homology protein (CHOP) has been implicated in the cellular response to stress [72-74]. CHOP expression is induced by cellular stress signals such as alkylating agents and ultraviolet radiation (UV) [75]. CHOP encodes a small nuclear protein that dimerizes with members of the C/EBP family of transcription factors. The resulting CHOP-C/EBP heterodimers bind specific DNA sequences and activate a set of downstream target genes such as DOCs leading to cell cycle arrest and thus promoting apoptosis [70].

### **1.2.7 BiP**

Immunoglobulin heavy chain binding protein (BiP), identified as an ER localized protein prevents the secretion of incompletely assembled immunoglobulins in B lymphocytes. The protein family is highly upregulated upon conditions of glucose deprivation [63, 64] and is hence named as glucose regulated protein family (GRPs). BiP is a classical example of the ER resident chaperone, which stabilizes energetically unfavorable conformations of polypeptides to minimize misfolding [57]. In addition to changes in the transcriptional machinery, the immediate response to accumulated unfolded proteins in the ER occurs at the translational level [57, 68, 70] through one or more protein kinases that specifically phosphorylate eukaryotic translation initiation factor 2 (eIF-2 alpha) to inhibit protein synthesis, thereby preventing further accumulation of unfolded proteins as well as preserving nutrients and energy [76].

ER stress also induces conformational changes of Bax and Bak resulting in their translocation to the mitochondria and the endoplasmic reticulum [70, 72, 77-79]. This translocated Bak further depletes the ER  $\text{Ca}^{2+}$  mediating a caspase dependent apoptosis [72, 80, 81]. Thus the intrinsic pathway of apoptosis irrespective of the originating organelle, targets the mitochondria for initiation of apoptosis.

### **1.3 Autophagy**

The eukaryotic cells comprise two major intracellular degradation pathways as mediated by the proteasome and the lysosome. The proteasome is a self compartmentalized complex with catalytic protease activity inside its central proteinaceous chamber and plays a central role in the degradation of short lived and abnormal proteins. In contrast, the lysosome is a vesicle that contains many hydrolases, which are separated from the cytosol by a limiting membrane. In the lysosomal pathway, degradation of plasma membrane proteins and extracellular proteins is mediated by endocytosis, whereas degradation of cytoplasmic components is achieved through autophagy. Autophagy is a bulk degradation process which is the main route for sequestration of the cytoplasm into the lysosome. Thus the degradation of cellular constituents facilitating energy conservation or preventing organelle damage is achieved by sequestered and distinctly organized events, collectively referred to as autophagy.

Autophagy, generally induced under physiological stress conditions in a cell such as starvation, promotes cellular survival by purging the cell of damaged organelles [82, 83], toxic metabolites [82] and intracellular pathogens [83-87]. However, autophagy may also be involved in apoptosis, as excessive autophagy can also promote cell death through self digestion and degradation of essential cellular constituents [85]. Autophagy is reported to be essential by a number of autophagy regulated genes [90] and the Bcl-2 proteins. A few Bcl-2 proteins, apart from their role in apoptosis express anti autophagic properties by inhibiting Beclin-1 mediated autophagy [88-90]. In contrast, overexpression of a few members of the antiapoptotic Bcl-2 protein family such as BCL-X<sub>L</sub> and BCL-2 enhances autophagy [91]. Beclin-1, initially identified as a protein that

interacts with Bcl-2 is an autophagy essential protein and cooperates with Bif-1 and UVRAG to activate Vps34, thus inducing autophagy [92]. Autophagy promotes cellular survival under metabolic stress [76] and upon limitation of intracellular nutrients. Autophagy related genes maintain cellular energy and survival [90] and a compromised state of autophagy promotes tumorigenesis or neurological disorder [82, 85, 86, 93-95].

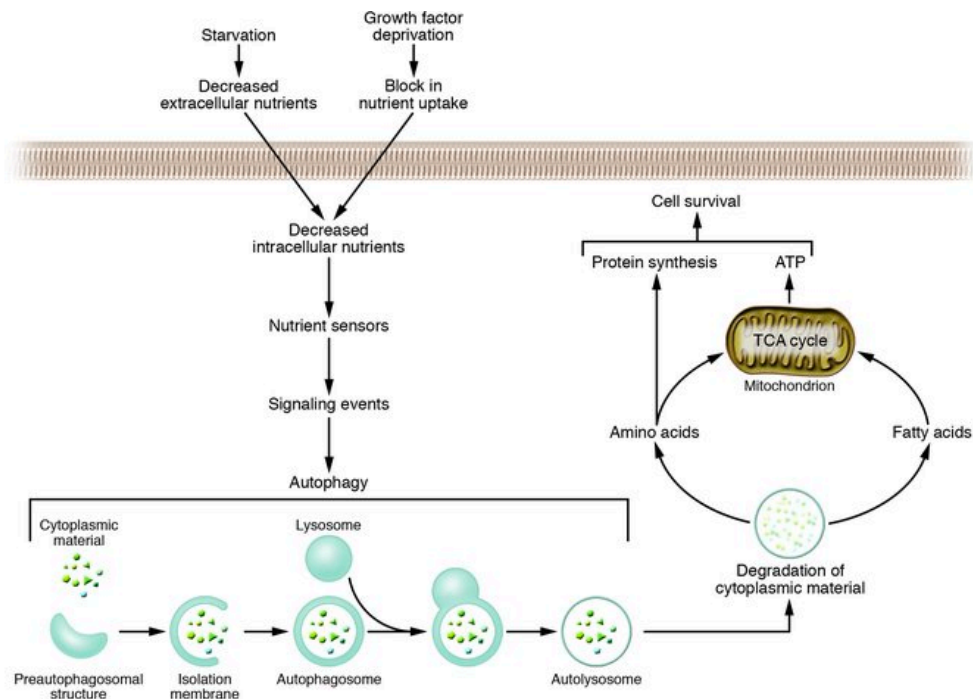


**Fig 8. The autophagy pathway in cellular adaptation to nutrient deprivation**  
 Decrease in intracellular nutrients and activation of nutrient sensing signaling pathways stimulate autophagy. Autophagy involves the sequestration of cytoplasmic material by an isolation membrane to form the autophagosome. The autophagosome undergoes fusion with a late endosome or lysosome, to form an autolysosome, in which the sequestered membrane lipids and proteins are degraded by the autolysosome. This in turn generates free fatty acids and amino acids that can be reused by the cell to maintain mitochondrial ATP energy production and protein synthesis and thereby promotes cell survival. **(Source: Beth Levine and Junying Yuan, JCI, 2005)**

The initial step of autophagy is the elongation of an isolation membrane which enwraps cytoplasmic constituents such as proteins or organelles and delivers it to the lysosome. The edges of the isolation membrane then fuse to form a double membranous autophagosome, which subsequently fuses with the lysosome [96]. Lysosomes can directly engulf cytoplasmic constituents by invagination, protrusion and septation of the lysosomal limiting membrane. The sequestered cytoplasmic components are degraded

by the enclosed hydrolases, together with the inner membrane of the autophagosomes [97, 98]. Thus the process of autophagy is characterized by the formation of double membrane cytosolic vesicles, known as autophagosomes that are later targeted for fusion with lysosomes. and degraded by the resulting autophagolysosome [76, 83, 96, 99-102].

### **1.3.1 Autophagy related genes**

Several kinases have been reported in the regulation of autophagy [89, 103]. The mammalian target of rapamycin (mTOR) is a well characterized protein which negatively regulates the autophagy pathway [89, 104-106]. Correspondingly a variety of mTOR inhibitors activate autophagy. Numerous upstream signalling factors regulating the mTOR pathway include PI3K/Akt, MAP kinases, AMP dependent protein kinases, small GTPases, and the trimeric G proteins [106, 107]. Continuous presence of autocrine growth factors activate receptor tyrosine kinases (RTKs) associated signal transduction of the small GTPase Ras and the phosphatidylinositol 3- kinase (PI3K). The Ras and the PI3K converge to activate mTOR, stimulating cell growth and inhibiting autophagy [106, 108]. A number of autophagy related genes, potentially regulating the autophagic process have been identified and termed Atg proteins [109-111]. Genetic studies in yeast have identified at least 16 autophagy related genes (Atg) that encode components of the autophagic machinery [109, 112]. The autophagy proteins functionally comprise a protein kinase autophagy regulatory complex that responds to cellular signal cascade; a lipid kinase signaling complex that mediates vesicle nucleation, a ubiquitin-like protein conjugation required for vesicle expansion and a retrieval pathway required for the disassembly of Atg protein complexes from matured autophagosomes [113].

The phagophore formation during autophagic initiation is marked by the increased Atg12-5 complex formation, whereby Atg12 conjugates at its carboxy terminal glycine to lysine 149 of Atg5, thus covalently attaching to Atg5 [114, 115]. After the formation of Atg12-Atg5 conjugate, Atg16 attaches to Atg5 to form the Atg12-Atg5-Atg16 complex essential for autophagy. LC3, a mammalian homologue of Apg8/Aut7 is a protein of the autophagosome membrane [112], when synthesized is subsequently processed to form

cytosolic LC3-I and further converted as LC3-II, by a posttranslational modification. This converted LC3-II is membrane bound to the outer membrane of the autophagosome.

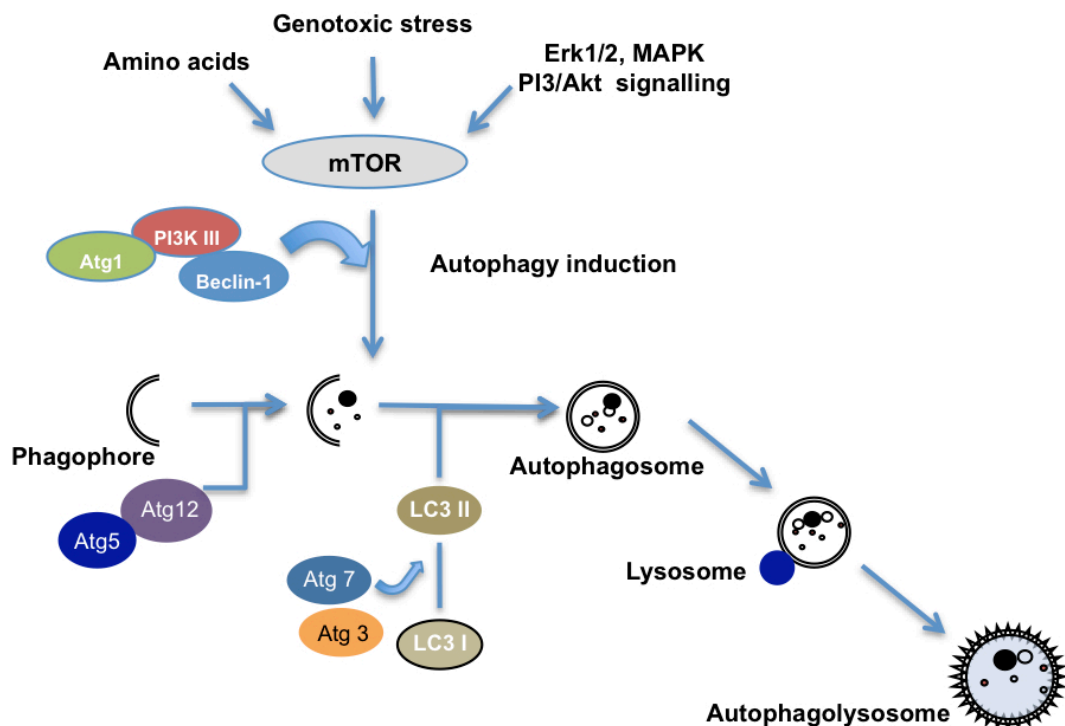


### Fig 9. The molecular mechanism of autophagy

Together with other ATG proteins such as beclin-1, ATG5-ATG12 contribute to the formation of the autophagosome, which sequesters cytoplasmic material before lysosomal delivery. The ubiquitin-like attachment of Atg12 and Atg5 requires the activity of Atg7, which function in a similar manner to E1 and E2 enzymes in the ubiquitin system. LC3-I is converted to LC3-II through lipidation by a ubiquitin-like system involving Atg7 and Atg3 that allows for LC3 to become associated with autophagic vesicles for efficient autophagy. (Modified from source: Cell signaling technology)

Thus, the Atg12-Atg5 complex formation followed by a unique lipidation modification of LC3 plays an indispensable role for the formation of autophagosome [83, 99, 110, 112, 115-120]. The mammalian homologue of Atg6/ Beclin-1, is a tumor suppressor and a part of the PI(3)KC3 lipid kinase complex that induces autophagy. Whilst the autophagic ability of this complex (beclin1- PI(3)KC3) is suppressed by the antiapoptotic BCL-2 protein [124], several pro apoptotic signals (TNF, TRAIL and FADD) induce autophagy [121-123] providing proof for an extensive cross talk between apoptosis and autophagy.

## 1.4 HAX1

HAX1 (HS-1 associated protein X1) was primarily identified as a HS1 (Hematopoietic cell lineage specific-1) interacting protein controlling the nuclear localization of HS1 [125]. HAX-1, a 35 KDa intracellular protein is ubiquitously expressed and possess similarity to the BH1 and BH2 domains of the Bcl-2 family proteins [125]. The HAX1 protein majorly localizes to the mitochondria and to a smaller extent to the endoplasmic reticulum as well as the nuclear envelope [125]. HAX1 protein is antiapoptotic in function as it serves as an inhibitor of the mitochondrial initiator caspase, caspase-9 [126] and protects cell death during hypoxia reoxygenation [127]. HAX1 is up regulated during various apoptotic stimuli, showing its involvement in both receptor and mitochondria mediated apoptosis pathways [126]. Interestingly, the biological role of HAX1 may not be confined to apoptosis. HAX1 interacts with numerous other cellular proteins such as PKD2 [128], cortactin [128], IL-1 alpha [129], BSEP [130], Galpha 13 [131], Omi/HtrA2 [132], PHB2, Phospholamban [133], Caspase-9 [126] and SERCA2 [134]. HAX1 also interacts with viral proteins such as EBNA-LP [135], EBNA5 [136], k15 protein of Kaposi-sarcoma virus [137] and HIV-1Vpr [42] whereby its antiapoptotic effects may be used by the virus to allow infected cells to survive. HAX1 is also an RNA binding protein, as it has been reported to interact with the 3'UTR of vimentin mRNA [138] and 3' UTR of DNA polymerase  $\beta$  mRNA [139]. The implications of these interactions remain obscure. Since HAX1 controls the nuclear localization of HS-1, the interaction of HAX1 with HS1 could be important for signal transduction to the mitochondria [125]. HAX1 potentially regulates the ion fluxes originating from the endoplasmic reticulum through its interaction with PKD2 [128]. HAX1 also interacts with the HS1 related protein Cortactin [128], a major substrate for tyrosine kinase such as Src, Fer and Syk, and is usually present in the cytosol [131] But in contrast to HS1, which is specifically expressed in hematopoietic cells, Cortactin is ubiquitously expressed [128] similar to HAX1 [125]. HAX1 thus may represent also a cytoskeletal associated protein, in line with the observation that it participates in cell migration potentiating Galpha 13 mediated Rac activation [131].

## **2. Focus of the current study**

Severe congenital neutropenia (SCN) is a rare, inborn hematological disorder associated with life threatening bacterial infections. Although previous studies have shown that mutations in the gene encoding neutrophil elastase (*ELA2*) [140], Wiskott-Aldrich syndrome (*WAS*) gene [13, 14], Growth factor independent 1 (*GFI1*) [15] and the endosomal adapter protein (*P14*) [16] result in neutropenia, the genetic defect underlying Kostmann syndrome caused by autosomal recessive mode of inheritance remained largely unknown and the molecular mechanism thus less understood.

The primary objectives of the current study were to identify the genetic defect causing Kostmann syndrome and understand the molecular etiology underlying the disease.

### **Specific aims**

- 1) To perform genome wide linkage analysis on families affected by SCN**
- 2) To perform sequencing based screening of candidate genes to identify the genetic defect underlying SCN**
- 3) To study and analyze the biological functions underlying the identified genetic defect in a tissue specific manner.**

## 3. Materials

### 3.1 Antibodies

Actin  
Catalase  
HAX1  
Atg12  
Atg 5  
LC3B  
Beclin-1  
AMPK alpha P- (Thr 172)  
Annexin V (FITC/APC conjugated)  
CD34+ (PE/FITC conjugated)  
Murine CD24+ (FITC conjugated)  
Other CD marker antibodies

### Company

Santa Cruz  
Epitomics  
BD pharmingen  
Cell signaling  
Cell signaling  
Cell signaling  
Cell signaling  
Cell signaling  
Molecular probes  
BD pharmingen  
BD pharmingen  
BD pharmingen

### 3.2 Cytokines

IL-3  
Il-6  
FLT-3 ligand  
Thrombopoietin  
Stem cell factor  
G-CSF  
GM-CSF

### Company

Peprtech  
Peprtech  
Peprtech  
Peprtech  
Peprtech  
Peprtech  
Peprtech

### 3.3 Cell culture reagents

Advanced DMEM medium  
RPMI 1640 medium  
Collagen A  
Foetal bovine serum  
PBS (phosphate buffered saline)  
Pencillin/streptomycin  
Trypsin/EDTA solution

### Company

Gibco  
Gibco  
Biochrome  
TAA  
Gibco  
Gibco, Sigma  
TAA

### 3.4 Chemicals

Agarose (Electrophoresis grade)  
Ammonium chloride  
Ammonium per sulphate  
Ampicillin  
Bromophenol blue  
BSA (bovine serum albumin)

### Company

Invitrogen  
Sigma  
Fluka  
Sigma  
Sigma  
Sigma



Chemiluminescence reagents	PIERCE
CM-H <sub>2</sub> DCFDA	Molecular probes
dNTP's	Invitrogen
DTT (Di Thi Tritol)	Roche
EDTA (N, N, N', N'-Ethylenediaminetetraacetate)	Sigma
Ethanol	J.T.Baker
Ethidium bromide	Sigma
Etoposide	Sigma
Ficol plaque	Amersham biosciences
HEPES buffer	Sigma
Hydrochloric acid	Merck
Hydrogen peroxide	Sigma
Isopropanol	J.T.Baker
JC-1	Molecular probes
KCl	Merck
LB agar	Merck
Meropenem	Pharmacy
Methanol	J.T.Baker
Mitotracker red 580	Molecular probes
Mounting medium with DAPI	Vectashield
NA orthovanadate	Cell signal technology
NNN'N' tetramethylethylenediamine (TEMED)	Sigma
PMA	Sigma
PMSF	Sigma
Polybrene	Sigma
Rapamycin	Cell signaling
Retronectin	TaKaRa
Sodium chloride	Merck
Sodium dodecyl sulphate (SDS)	Sigma
Sodium hydroxide	Merck
Staurosporine	Sigma
Stemspan	Stem cell technologies
Tetracyclin	Sigma
TNF $\alpha$	Sigma
Tunicamycin	Sigma
Tris	Invitrogen
Triton X 100	Sigma
Tween 20	Sigma
Valinomycin	Sigma

### 3.5 Enzymes, DNA and protein ladder

	Company
Antartic phosphatase	NEB
Taq DNA polymerase	Roche
Restriction enzymes	Fermentas
Precision plus protein ladder (Dual color)	BioRad

T4DNA ligase

NEB

### 3.6 Laboratory equipment

100 µm filter  
Centrifuge  
Electrophoresis apparatus for PAGE  
Fluorescence microscope  
Gel doc  
Chemi doc  
Thermo mixer  
Neubauer chamber  
PCR master cyclor  
PVDF membrane  
Spectrophotometer  
FACS Canto  
FACS can  
Cell sorter Moflow  
Auto MACS  
Chemiluminescent imaging station  
Light Microscope  
Light cyclor

### Company

Nalgene  
Sorval, Eppendorf  
BioRad  
Carl Zeiss  
Syngene  
BioRad  
Eppendorf  
Marienfeld  
Eppendorf  
ROTH  
Eppendorf  
BD Pharmingen  
BD Pharmingen  
DAKO Cytomation  
Miltenyi-Biotec  
BioRad  
Zeiss  
Roche

### 3.7 Kits

10X cell lysis buffer (protein isolation)  
Absolute RNA preparation kit  
Caspase-3/7 assay kit  
Genomic DNA preparation kit  
High fidelity cDNA synthesis kit  
Mounting medium  
Master SYBR Green kit  
pGEM-T cloning kit  
Plasmid DNA isolation kit

### Company

Cell signaling  
Stratagene  
Molecular probes  
Qiagen  
Roche  
Vectashield  
Roche  
Promega  
Qiagen

### 3.8 Preparation of buffers and media

**Agarose gel buffer (10X TBE):** 89 mM Tris base, 89 mM boric acid, 2 mM EDTA

**Blocking buffers (Western):** PBS-Tween (0.1%), 5 % non-fat milk

**DMEM-medium:** DMEM containing 10 % FCS, 100 U/ml penicillin, 0.1 mg/ml streptomycin, 0.3 mg/ml glutamine

**Laemmli electrophoresis buffer:** 50 mM Tris-HCl, 0.196 M glycine (pH 8.3), 20 % methanol

**Protease inhibitor cocktail (PIC):** 104 mM AEBSF, 0.08 mM Aprotinin, 2 mM leupeptin, 4 mM Bestatin, 1.5 mM Pepstatin A, 1.4 mM E-64

**RIPA buffer:** 10 mM Tris (pH 7.5), 150 mM NaCl, 1 mM EDTA, 1% NIP-40, 0.5 % Sodium Deoxycholate, 0.1 % SDS, PIC

**RPMI-medium:** RPMI containing 10% FCS, 100 U/ml penicillin, 0.1mg/ml streptomycin, 0.3 mg/ml glutamine and 10 mM  $\beta$ - Mercaptoethanol

**SDS PAGE buffer:** 25 mM Tris, 192 mM glycine, 0.1% SDS

**Transient transfection medium:** DMEM containing 100 U/ml penicillin, 0.1 mg/ml streptomycin, 0.3 mg/ml glutamine

**Transfer buffer (Western):** 192 mM glycine, 25 mM Tris

**Wash buffer (Western):** PBS, 0.1 % Tween-20

**FACS staining buffer:** 1X PBS containing 2 % foetal calf serum and 0.05 % sodium azide

**FACS blocking buffer:** 1X PBS containing 5 % foetal calf serum

## 4. Methods

### 4.1 Sequence analysis of *HAX1*

Total genomic DNA was prepared from peripheral blood by genomic DNA isolation kit (Qiagen) as per manufacturers instructions. The isolated genomic DNA was checked for its purity and the exons were subjected to PCR amplification with gene specific primers and the products obtained were further sequenced

#### HAX1 genomic PCR primers and conditions

Exon number	Primer sequence (5'--- 3')	Annealing temperature
Exon 1	Forward TCG AAA TCG CTT TTC GTA C Reverse GCG ACT TCT GTC CTC TCT G	55°C
Exon 2	Forward CTC CGA CCC TCT CCC TAG C Reverse ATG GGA AAG GAC TTG GGC	55°C
Exon 3	Forward GGG TTG GTG GGT GAA ATA AA Reverse CTC TGG TGA TCT GCC CAC	55°C
Exon 4 and 5	Forward CAG GAA GGA GTG TGT AAA T Reverse AGT CCC CAC CAT ATT CCG	50°C
Exon 6 and 7	Forward TGG GGT GAG TTG AAA GAA A Reverse TGA AAT CAG GTT TTA GAT G	50°C

#### PCR cycle program

##### (1 cycle)

**DNA denaturation** : 95°C (2 minutes)

##### (30 cycles)

**DNA denaturation** : 95°C (45 seconds)

**Primer annealing** : (x)°C (45seconds)

**DNA synthesis** : 72°C (45 seconds)

##### (1 cycle)

**DNA synthesis** : 72°C (10 minutes)

## **4.2 Cells and cell culture**

### **4.2.1 Isolation of neutrophil and PBMCs**

Heparinized peripheral venous blood was collected from healthy human donors and SCN patients as a source of neutrophils. The neutrophils were isolated by a density gradient based ficoll technique.

The heparinized blood was mixed with an equal volume of PBS and further layered on to 10 ml of ficoll plaque (Amersham biosciences). The samples were then spun at 1600 rpm for 30 minutes without brake. After centrifugation, the PBMCs appear in the buffy layer and the neutrophils appear in the lower fraction along with the erythrocytes. For PBMC isolation the buffy layer containing the PBMCs was carefully isolated and washed with PBS followed by a spin at 1300 rpm for 8 minutes. For the isolation of neutrophils, the neutrophil erythrocyte fraction was subjected to a hypotonic lysis by resuspending in 12 ml of ice cold ddH<sub>2</sub>O for 10 seconds, followed by addition of 4 ml of 0.6 M KCl and adding ice cold PBS to make up the volume to 50 ml in a falcon tube. The tube was then spun at 1300 rpm for 5 minutes at 4°C. The RBC lysis was repeated until a pale white neutrophil pellet was obtained. The purified neutrophils and PBMCs were resuspended to obtain 1x10<sup>7</sup> cells per ml in RPMI 1640 medium containing 10% FCS, L-glutamine, penicillin, streptomycin. The purity of the neutrophil preparation was assessed by microscopical visualization of Giemsa stained cytopsin preparation.

### **4.2.2 Isolation of CD34+ cells from the bone marrow**

Mononuclear cells from the total bone marrow (BM) cells were separated by density gradient based ficoll technique as described earlier. The mononuclear cell (MNC) fraction of the ficoll layer from bone marrow of healthy donors and patients was isolated. The isolated BM derived MNCs were briefly washed in ice cold PBS and further stained for the CD34+ surface marker to obtain hematopoietic stem cells. The isolated mononuclear cell fraction was briefly spun at 1200 rpm for 10 minutes and resuspended in FACS blocking solution. The cells were further incubated in the blocking buffer for 10 minutes on ice. The FITC or PE fluorochrome conjugated anti CD34 antibody was then added to the cells and further incubated for 30 minutes on ice in the

dark. The cells were then briefly washed in ice cold PBS and the cells stained for CD34+ were sorted by a flow cytometer (Moflow).

#### **4.2.3 Culturing of BM derived CD34+ cells**

The isolated CD34+ cells were then prestimulated for 48 hours in stemspan medium supplemented with 20 ng IL-3, 20 ng Stem cell factor, 10 ng FLT-3 ligand, 25 ng Thrombopoietin, 10 ng IL-6 and 0.1 % Meropenem at 37°C in an atmosphere of 5 % CO<sub>2</sub>. The prestimulated bone marrow CD34+ cells were transduced with a bicistronic retroviral vector expressing the human HAX1 cDNA and GFP (or) murine CD24 marker. The cells were then cultured for 48-56 hours in stemspan medium supplemented with a cytokine cocktail of 20 ng IL-3, 20 ng Stem cell factor, 10 ng FLT-3 ligand, 25 ng Thrombopoietin and 10 ng IL-6 at 37°C in an atmosphere of 5 % CO<sub>2</sub> in the presence of 0.1 % meropenem. The transduced cells were sorted based on the marker gene encoded in the retroviral vector by a moflow cell sorter (FACS). The sorted cells were further expanded in stem cell growth media for 6 days with fresh supplement of the cytokines in growth medium, for every 48 hours. The cells were then subjected to granulocytic differentiation in the presence of 10 ng/ml G-CSF and 10 ng/ml GM-CSF in RPMI 1640 medium supplemented with 10% FCS, L-glutamine, 0.1% Meropenem.

#### **4.2.4 *In vitro* differentiation of BM derived CD34+ cells to neutrophils**

The bone marrow derived CD34+ cells were further differentiated to myeloid lineage by culturing in the presence of 10 ng/ml IL-3, 10 ng/ml G-CSF, 15 ng/ml GM-CSF (Peprotech, Rocky Hill, NJ) in RPMI medium supplemented with 10 % FCS, 2 mM L-Glutamine, 1 % Penicillin-Streptomycin (Sigma, Munich, Germany), for 4 days.

#### **4.2.5 Culturing of fibroblasts and HEK293T cells**

The fibroblast and HEK 293T cells were grown as adherent culture in DMEM growth medium supplemented with 10% FCS and 2 mM L-glutamine in the presence of the antibiotics, penicillin and streptomycin.

#### **4.3 Apoptosis assay**

Progression of apoptosis in various tissues was analyzed upon induction with different apoptosis inducing agents. Apoptosis in neutrophils was induced by treating the cells with TNF  $\alpha$  (50 ng/ml), staurosporine (5  $\mu$ M), valinomycin (100 nM) or H<sub>2</sub>O<sub>2</sub> (2  $\mu$ M) in RPMI 1640 medium (for suspension cells) or DMEM (for adherent cells) in the presence of 10 % FCS as indicated in respective experimental condition. The cells were maintained at 37°C in an atmosphere of 5% CO<sub>2</sub> through induction. Apoptosis was assessed by a flow cytometry based technique. The cells were harvested at various time points and washed once with ice cold PBS followed by staining with 5  $\mu$ g/ml propidium iodide (SIGMA) along with FITC or APC conjugated Annexin V (Molecular probes) as per manufacturers instructions. The cells were then incubated on ice for 10 minutes in dark, before being analyzed by flow cytometry. Forward and sideward scatter were used to gate the cells and exclude cell debris. The cells positive for Annexin V were defined as cells undergoing apoptosis. The cells positive for Annexin V and propidium iodide were defined as apoptotic and those single positive for propidium iodide were defined dead.

#### **4.4 Mitochondria membrane potential assay**

The mitochondria membrane potential was analyzed by using JC-1, a cationic lipophilic dual emission dye (Molecular Probes), which selectively incorporates into the mitochondria.

The dye accumulates in the mitochondria with higher membrane potential to form J-aggregates, which emits red fluorescence at 590 nm and at regions with a reduced membrane potential the dye remains in its monomeric form, which in turn emits a green fluorescence at 527 nm. The ratio of the red to green fluorescence gives a measure of the mitochondria membrane potential. The cells were stained with 3.5  $\mu$ M

JC-1 dye for 15 minutes at 37°C, in prewarmed RPMI1640 medium supplemented with 10% FCS, L-glutamine, Penicillin and streptomycin. The cells were then washed twice with prewarmed PBS. The cells were then treated with Valinomycin (SIGMA), a K<sup>+</sup> selective ionophore at a concentration of 100 nM and the JC-1 emission was collected in FL-1 and FL-2 channels.

## **4.5 Assay of mitochondrial mass**

The mitochondria mass was analyzed by using mitotracker 580 (Molecular Probes), which selectively incorporates into the mitochondria, irrespective of the mitochondrial membrane potential. The accumulated dye in the mitochondria emits red fluorescence at 580 nm and is visualized by flow cytometry or by microscopy. The cells were stained with 10 nM mitotracker red 580 for 30 minutes at 37°C in pre warmed RPMI1640 medium supplemented with with 10% FCS, L-glutamine, Penicillin and streptomycin. The cells were then washed twice with pre warmed PBS. The cells were then treated with valinomycin (SIGMA), a K<sup>+</sup> selective ionophore at a concentration of 50 nM for indicated timepoints. The red fluorescence was collected in FL-2 channel and the fluorescence intensity was analyzed by flowjo software.

## **4.6 Cytosolic ROS assay**

The cells were prestained with freshly prepared 5-(and-6)- Chloromethyl-2'7'-dichlorodihydroxyfluorescein diacetate acetyl ester (CM-H<sub>2</sub>DCFDA) as per manufacturers instruction. The cell permeant indicator is nonfluorescent until removal of the acetate groups by intracellular esterases and oxidation occurring within the cell. ROS production was induced for varied time points with 2 μM PMA or 25 nM valinomycin. The production of ROS was analyzed by measuring the fluorescence intensity of the dye by flow cytometry.



## **4.7 Protein isolation and western blot analysis**

To prepare whole cellular protein extracts,  $1 \times 10^7$  cells were resuspended in 250  $\mu$ l of ice cold lysis buffer (20 mM HEPES, 10 mM KCl, 1 mM MgCl<sub>2</sub>, 20% glycerin, 0.1% Triton X 100, 0.5 mM DTT, 0.2 mM PMSF, 1 mM Na Orthovanadate) and incubated on ice for 30 minutes. The lysate was centrifuged at 12,000 g for 5 minutes at 4° C to clear cell debris. The protein lysate was then carefully transferred to a new container without disturbing the cell debris was then quantified and immediately used or stored at -80°C. The samples were incubated for 5 minutes at 95°C in loading buffer (250 mM Tris-HCl, pH 6.8, with 4% SDS, 20% glycerol, 0.01% bromophenol blue) along with 3%  $\beta$ -mercaptoethanol. 20-30  $\mu$ g of the total protein was loaded per lane on a 10% SDS Polyacrylamide gel and electrophoresed. The electrophoresed proteins were then transferred to Poly Vinylidene DiFluoride membrane (Roti-PVDF, ROTH) by wet electroblotting as per manufacturers instructions. The efficiency of transfer was estimated by monitoring the transfer of the pre stained ladder from the SDS polyacrylamide gel to the PVDF membrane. The membrane was then blocked (5 % skim milk, 0.1 % Tween 20 in PBS) at room temperature for 1 hour or overnight at 4°C, as per the primary antibody manufacturers directions.

Monoclonal or polyclonal primary antibody were used as per manufacturer's directions and detected with a respective HRP conjugated secondary Ab. The blot was developed by incubation in a chemiluminescence reagent (PIERCE, Amersham Biosciences, Freiburg, Germany) and imaged by Bio-Rad imaging system.

## **4.8 Flow cytometry analysis**

Single cell suspensions were analyzed by flow cytometry using a FACS can or FACS-Canto, employing CELL Quest or FACS Diva software (BD Biosciences, CA). Sorting of cells was performed using a Moflo cell sorter (DAKO Cytomation, Glostrup, Denmark).

The following monoclonal antibodies (all from BD Pharmingen, San Diego, CA except stated otherwise) were used: CD3-FITC & -biotin, CD4-FITC & -PE, CD8-FITC, -PE & -PerCP, CD11b-FITC & -biotin, CD11c-PE & -APC, CD34-FITC, PE, CD19 or B220-FITC, -PE

& -biotin, CD45RA-FITC or PE, CD45RO-PE or -FITC, CD62L-APC. IgM-FITC, IgG-PE, IgD-APC, IgA-FITC, CD21-APC, CD38-PE. In all experiments, cells were also stained with corresponding isotype matched monoclonal antibodies. Cells reacted with biotinylated monoclonal antibodies were incubated with fluorochrome conjugated streptavidin-PerCP or streptavidin-APC (BD Pharmingen). All fluorescence intensity plots are shown in log scales.

## 4.9 Immunofluorescence and light microscopy

Phase contrast images were taken using a Zeiss Axiovert 200M microscope at an original magnification of x 63. Photo documentation was performed using Open lab software. Giemsa stained neutrophils were observed using a Zeiss Axioplan 2 microscope (original magnification x 100).

## 4.10 RNA isolation, CDNA synthesis and Real Time PCR

Total RNA was isolated with “Absolutely RNA miniprep kit” (Stratagene, La Jolla, CA). cDNA was synthesized by using oligo dT primer and expand reverse transcriptase (Roche). Gene expression was determined by Real Time PCR based analysis of the cDNA, employing sequence specific forward and reverse primers. GAPDH specific primers were used as internal controls

Gene	Primer sequence (5' - 3')	Annealing temperature
GAPDH	Forward: GTCAGTGGTGGACCTGACC Reverse: TGAGCTTGACAAAGTGGTCG	56°C
HAX1	Forward: AGACTACGGGAGGGACAGACTT Reverse: CCATAGGCCATACATCAAACC	56°C

The PCR reaction was performed in duplicates using a LightCycler–FastStart DNA Master SYBR Green I kit (Roche) according to the manufacturer’s instructions.

## 4.11 Molecular cloning

### 4.11.1 Generation of *HAX1* expression constructs

Desired full length cDNA of HAX1 or GFP was amplified by Polymerase Chain Reaction (PCR), with sequence specific primers, containing modulated 5' and 3' ends facilitating site directed cloning. The obtained PCR product was checked on agarose gel. The PCR product was then eluted and ligated with pGEM-T, an intermediate cloning vector, as per the manufacturers instructions (Promega).

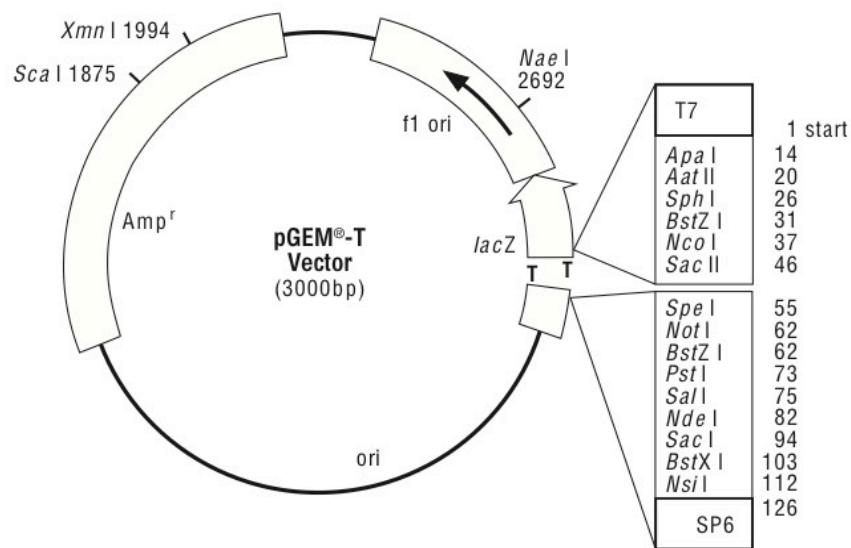


**Fig 10. pGEM-T vector map**

The pGEM-T vector system with single 3'-T overhangs at the insertion site provides a compatible end for the PCR products and greatly improves the efficacy of ligation.

The ligation mix was then transformed into competent bacterial cells (*E.coli* DH5 $\alpha$ ) and plated on to LB agar plate containing a selection medium (LB/ampicillin/IPTG/X-gal). The plates were then incubated overnight at 37°C facilitating growth of the bacteria. Single white colonies, which now contain the desired cDNA insert was further inoculated into LB medium with the desired antibiotic and shaken vigorously in an orbital shaker at 37°C overnight. Plasmid DNA was prepared from these individual clones in culture, by a commercially available kit (QIAGEN). The isolated plasmid DNA was further confirmed for the presence of insert by restriction digestion as per manufacturers protocol (Promega). The positive clone was identified by further

sequence confirmation to eliminate any mutations resulting from PCR amplification. The resulting positive clones were released from pGEM-T by performing a restriction digestion at their respective cloning sites to obtain the cDNA fragments ready for ligation and directionally cloned to an pMMP plasmid [141], transformed, selected and the plasmid DNA was purified and sequence confirmed before further use.

**pMMP-*GFP* construct oligonucleotides.**

Gene	Primer sequence (5' - 3')	Annealing temperature
<i>GFP</i>	Forward: TAT GCC ATG GTG AGC AAG GG Reverse: GGA TCC TCA GGT AGT GGT TGT C	56°C

**pMMP- *GFP HAX1* fusion construct oligonucleotides.**

Gene	Primer sequence (5' - 3')	Annealing temperature
<i>GFP</i>	Forward: TAT GCC ATG GTG AGC AAG GG Reverse: CGG CCG GGT AGT GGT TGT C	56°C
<i>HAX1</i>	Forward: CGG CCG AGC CTC TTT GAT CT Reverse: GGA TCC CTA CCG GGA CCG G	55°C

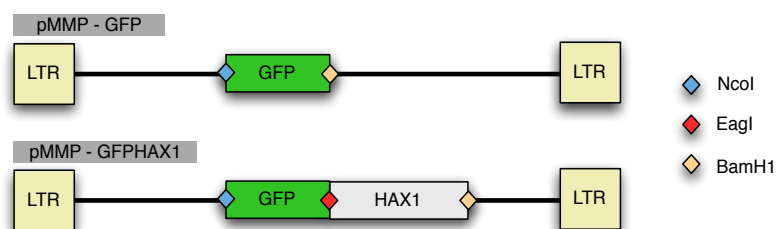


**Fig 11. Cloning of *HAX1 GFP* fusion in pMMP.**

cDNA encoding either *GFP* or *GFP HAX1* fusion complex were cloned into the pMMP retroviral backbone

### pMMP-*HAX1*-IRES-mCD24+

Gene	Primer sequence (5' 3')	Annealing temperature
HAX1	Forward: TCA TGA GCC TCT TTG ATC TCT T Reverse: GGA TCC CTA CCG GGA CCG G	56°C

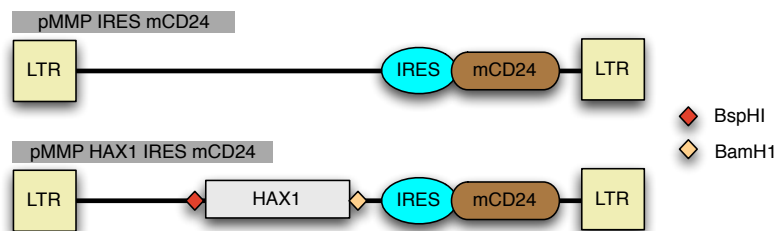


**Fig 12. Cloning of *HAX1* in pMMP-IRES-mCD24+**

cDNA encoding *HAX1* was cloned into retroviral backbone having murine *CD24* as a marker gene.

### 4.11.2 Generataion of shRNA constructs targeting *HAX1*.

#### shRNA I oligonucleotide for *HAX1*

Top strand	5' <b>GATCGGACTCAATGCTTAAGTATCCTTCAAGAGAGGATACTTAAGCATTGAGTCC</b> TTTTT3'
Bottom strand	5'AGCTAAAA <b>AGGACTCAATGCTTAAGTATCCTCTCTTGAAGGATACTTAAGCATTGAGTCC</b> 3'

#### shRNA II oligonucleotide for *HAX1*

Top strand	5' <b>GATCGCTTAAGTATCCAGATAGTCAT</b> TCAAGAGAT <b>GACTATCTGGATACTTAAGCTTT</b> TTT3'
Bottom strand	5'AGCTAAAA <b>AGCTTAAGTATCCAGATAGTCAT</b> TCTCTTGAAT <b>GACTATCTGGATACTTAAGC</b> 3'

The nucleotides in purple represent the restriction sites for directional cloning.

The nucleotides in blue represent the termination sequence.

The nucleotides in green, and red represent the *HAX1* siRNA sequence

The highlighted nucleotides represent the loop sequence

The top and bottom strands of shRNAI and shRNAII were self annealed at 55°C, respectively and directionally cloned as a BglII/HindIII fragment into pSuper plasmid (Oligoengine, Seattle, WA). The nucleotide sequence was confirmed in the plasmid. The cloned shRNA oligonucleotides were then released from the pSUPER plasmid along with the H1 (polymerase III) promoter as a SmaI/HincII fragment and

were directionally cloned into the compatible *Sna*BI site of the lentiviral vector pRRL.PPT.SF.DsRedEx.Pre *Sna*B1.

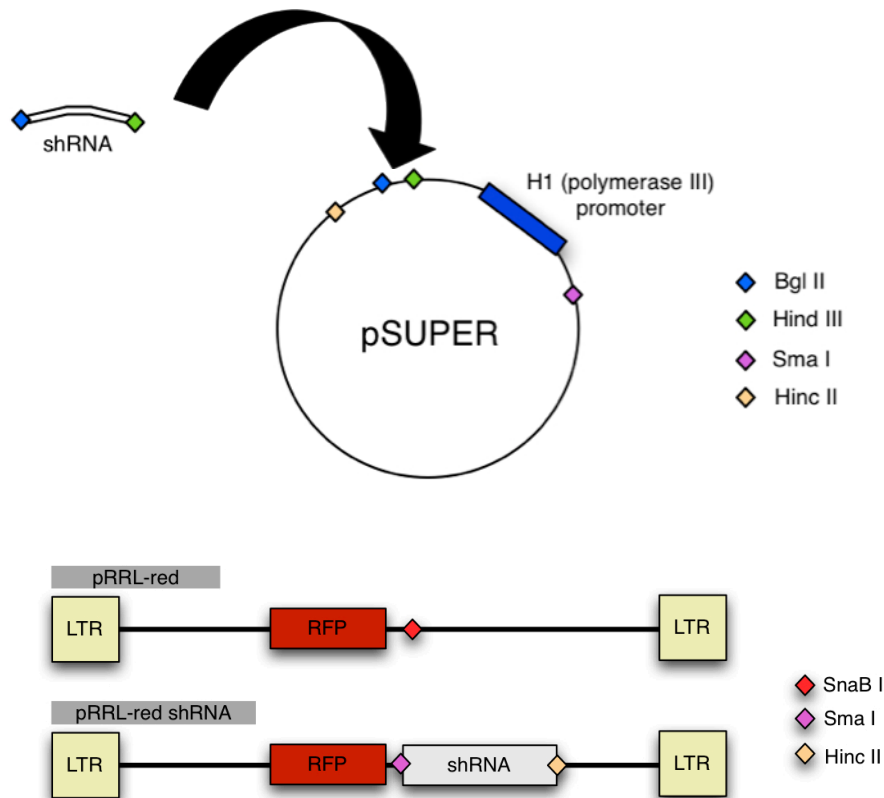


**Fig 13. Cloning of HAX1 shRNA in pRRL.PPT.SF.DsRedEx.Pre *Sna*B1.**

The designed DNA oligonucleotides corresponding to siRNA sequence were self annealed and directionally cloned in to the pSUPER plasmid containing the H1 promoter. The shRNA coding nucleotides along with the H1 promoter were further restriction digested, purified and cloned into the pRRL.PPT.SF.DsRedEx.Pre *Sna*B1 lentiviral plasmid

## 4.12 Retroviral gene transfer

The human HAX1 cDNA was cloned into the retroviral vector pMMP-IRES-mCD24. Recombinant VSV-G pseudotyped retrovirus was generated by transient transfection into the packaging cell line 293GPG [141].

BM derived CD34<sup>+</sup> cells were stimulated for 48 hours in the presence of a stem cell cytokine cocktail, as described earlier and transduced at a multiplicity of infection (MOI) of 10 in the presence of viral immobilizing retronectin. In brief, the cells were exposed to recombinant retrovirus for 1 hour at 37 °C, followed by spinoculation for 2

hours at x 700 g and further incubation at 37 °C in 5% CO<sub>2</sub>. Subsequently, cells were washed and cultured for additional 48 hours in the presence of the stem cell cytokine cocktail. The transduced cells were selected using a reporter gene. The cells were then subjected to granulocytic differentiation and used for further *in vitro* experiments.

Adherent cells such as fibroblast from patients and healthy donors, as well as HeLa and HEK293T were grown to 70-80% confluency in the presence of 10% FCS supplemented growth medium.

The generated retrovirus or lentivirus was concentrated by spinning at 12000 rpm for 30 minutes at 4 °C. The concentrated virus was transduced at a MOI of 10 in the presence of 1X polybrene. The cells were incubated with the virus for 24 to 36 hours at 37 °C in 5% CO<sub>2</sub>. After 24 hours the cells were supplemented with fresh medium and cultured further for 24 hours, before they were assessed for the viral transduction. In case of fibroblasts, the transduction procedure was repeated twice before the cells were finally sorted and cultured further. In every experimental procedure, the control backbone virus was transduced to cell types at the same time point and treated similarly.

## **4.13 Electron microscopy**

Bone marrow samples from patients and healthy donor controls were subject to hypotonic lysis. Pelleted cells were fixed in 2.5% glutaraldehyde in 0.1 M sodium cacodylate (pH 7.3) (Merck Schuchardt, Hohenbrunn, Germany), followed by 2% osmium tetroxide (Polysciences, Warrington, P.A.) in the same buffer. After embedding in Epon (Serva, Heidelberg, Germany), thin sections were produced and stained with uranyl acetate (Merck) and lead citrate (Merck). Samples were analyzed using a Philips electron microscope 301.

## 5. Results

### 5.1 Identification of mutations in *HAX1* genomic DNA

The use of genome wide genotyping array has potentiated the assessment of genetic disorders and has emerged as an aid for clinical diagnosis [142]. To define the molecular etiology of autosomal recessive SCN, we initiated a genome wide screen in three unrelated families with members suffering from recurrent infections due to neutropenia, as characterized by reduced number of neutrophils in the peripheral blood. In this approach, we performed high throughput homozygosity mapping to help us identify homozygosity tracks in these recessive families. The analysis revealed a critical linkage region in chromosome 1q comprising 275 candidate genes with a significant LOD score. Genomic DNA sequence analysis of the several functional candidate genes including *MAPBIP*, *RAB25* and *IL6R* showed wild type sequences in case of the affected individuals. We considered *HAX1*, as a candidate gene for SCN because of its potential role in the regulation of actin cytoskeleton and reported role as an antiapoptotic protein.

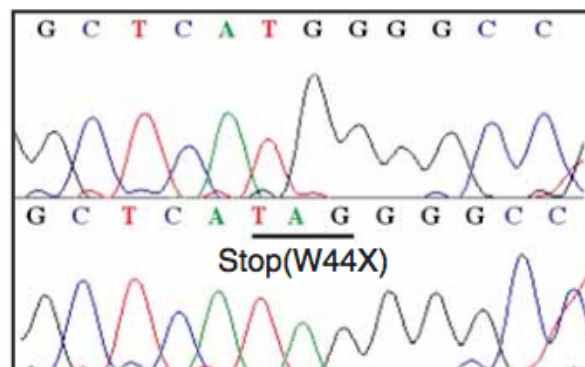


#### Fig 5.1.1. Sequencing of *HAX1* shows mutated sequence in exon 2

The exon region of *HAX1* was PCR amplified from total genomic DNA and the nucleotides were further sequenced. The obtained nucleotide sequence was analyzed in comparison to a wildtype sequence obtained from the NCBI database.



Sequencing of the *HAX1* genomic DNA identified a homozygous single nucleotide insertion leading to a premature stop codon (W44X) in all affected individuals, while the parents and the unaffected siblings had at least one allele with the wildtype sequence. Subsequent sequencing of additional SCN patients, including patients belonging to the family, originally described by Kostmann revealed novel mutations in *HAX1* in addition to our previously identified mutation.

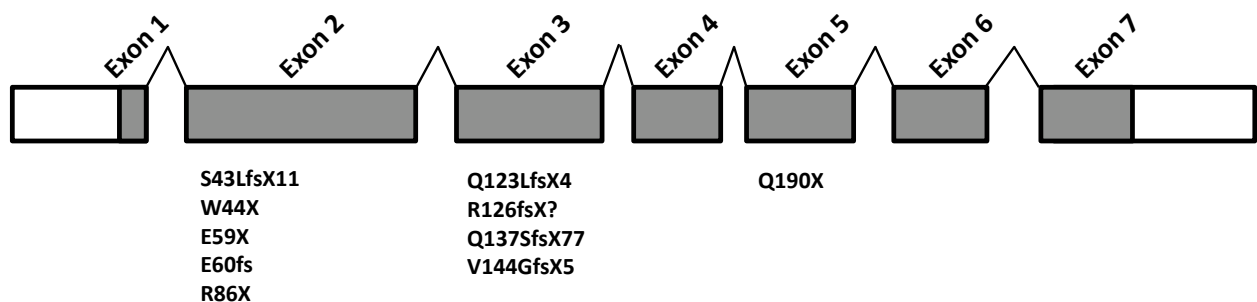
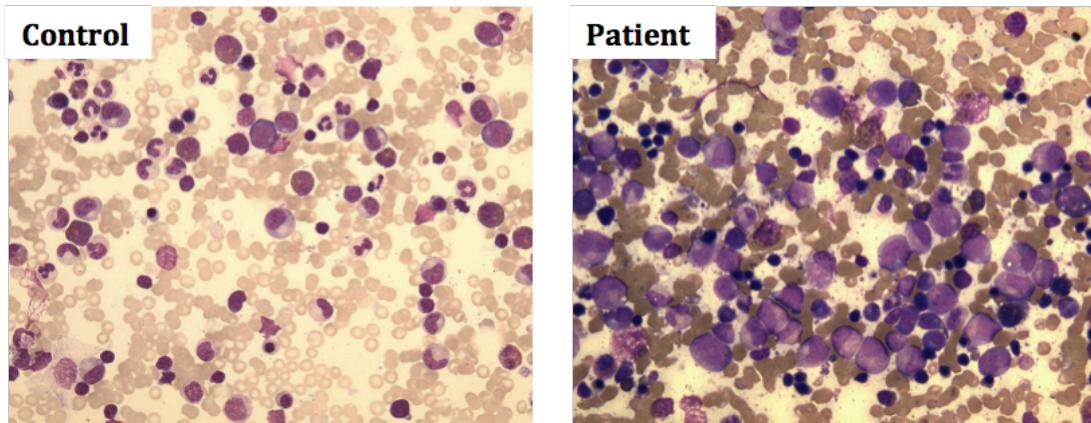


**Fig 5.1.2. Identification of different mutations in *HAX1* causing SCN**

Sequence analysis of various SCN patients identified a number of different mutations in *HAX1* as the cause of neutropenia. These identified mutations result in a premature stop codon or a frameshift leading to absence of the protein.

**5.2 BM of *HAX1* mutated patients show a phenotype of SCN**

The condition of SCN as described by Rolf Kostmann is characterized by an arrest in the maturation of myeloid cell lineage at the promyelocyte-myelocyte stage of differentiation accompanied by increased apoptosis of the myeloid cells, leading to a reduced number of circulating mature neutrophils. With the identification of different kinds of mutations in *HAX1*, we analyzed the bone marrow from the affected individuals compared to healthy donor as control samples. Bone marrow tissue smears were prepared and microscopically examined following a Giemsa staining.



Original magnification x 600

### **Fig 5.2.1. Microscopical examination of Giemsa stained bone marrow smear**

Bone marrow tissues were smeared on glass slides and further stained with Giemsa dye and examined microscopically.

Bone marrow smears from patients with mutation in *HAX1* showed the characteristic paucity of mature neutrophils as originally described by Kostmann [8]. The *HAX1* deficient bone marrow exhibits a “myeloid maturation arrest” at the level of promyelocyte-myelocyte. Of note, heterozygote carriers had a normal bone marrow.

### **5.3 Mutations identified in *HAX1* results in complete absence of the protein.**

Computational analysis of the mutations in *HAX1* revealed that the varied mutations identified in *HAX1* would result in the generation of a truncated protein or a complete absence of the protein due to the resulting premature stop codon or frame shift mutations in these affected SCN patients. Our primary aim was then set to examine the *HAX1* protein in these affected individuals. Whole cell protein extracts of EBV immortalized B-lymphocytes from patients and healthy donors were analyzed by western blot for presence of *HAX1*. 20  $\mu$ g of whole cell protein lysate was stacked and separated in 8 and 10% poly acrylamide gel (PAGE) respectively. The proteins were then transferred on to PVDF membrane and blotted with a *HAX1* MAbs. The presence of *HAX1* protein in whole cellular extracts was further analyzed by western blot, as described earlier.

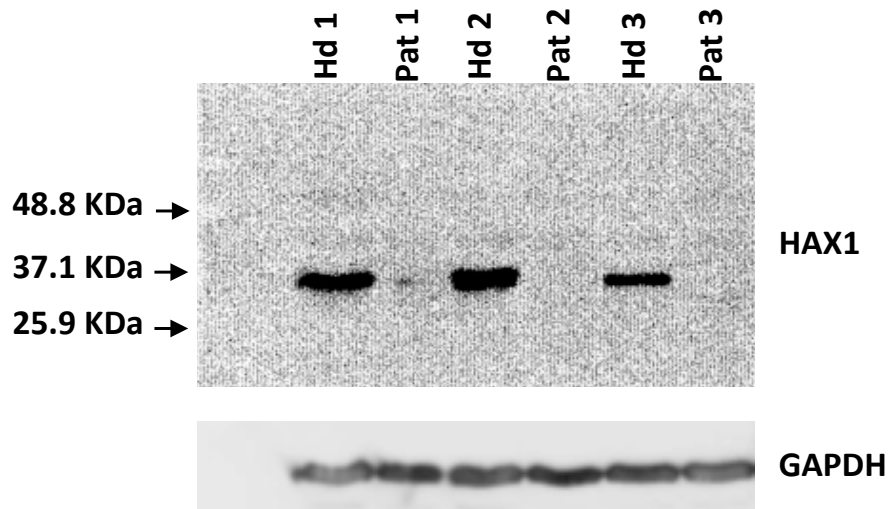


**Fig 5.3.1. Western blot analysis of EBV immortalized B-lymphocytes**

Total cellular protein extract was isolated from EBV immortalized B cells of patients with mutations in *HAX1* and healthy donors. The expression level of HAX1 was detected by western blot, using a HAX1 specific monoclonal antibody.

HAX1 a ubiquitously expressed protein has a molecular weight of 32-35 KDa. We analyzed for the whole cell protein extracts for presence of the full length and truncated HAX1 protein in these affected individuals as compared to healthy donors. HAX1 protein was completely absent in these SCN patients with a homozygous germline mutation in *HAX1*, as determined by western blot analysis. Whereas the unaffected healthy donors (including heterozygous carriers) expressed detectable levels of HAX1, identified as a 35 KDa band by western blot analysis.

## 5.4 Intracytoplasmic localization of HAX1

Knowledge on the cellular compartmentalization is of utmost necessity to study the biological role of a protein. In view of the conflicting data reported in the literature, we wanted to unambiguously determine whether HAX1 is localized in mitochondria, nucleus, or cytoplasm. This would further facilitate us to understand the various role of HAX1. As an approach to identify the intracellular localization of HAX1, we generated amino terminal GFP fusion construct of HAX1 in a CMMP retroviral backbone and transfected HeLa cells with plasmid backbone encoding GFP as control or the HAX1-GFP fusion as test. After 36 hours of transfection, the cells were processed and analyzed microscopically.

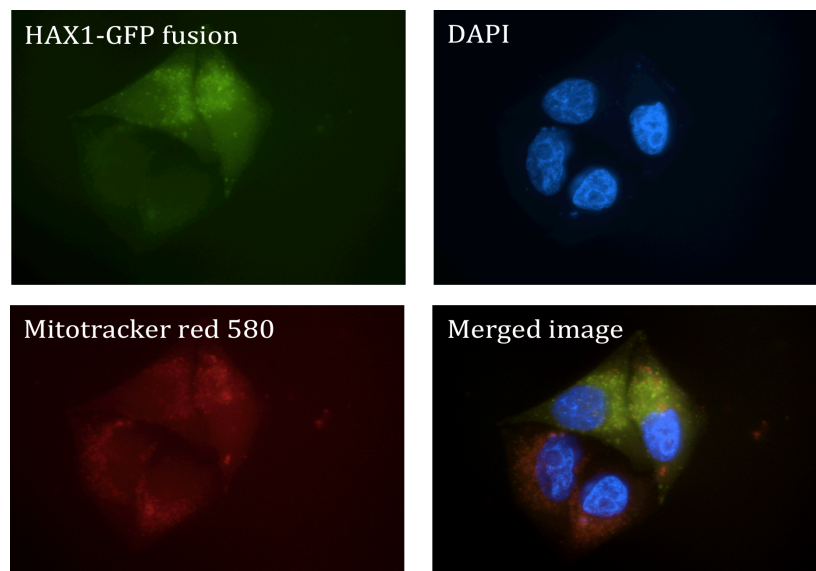


### Fig 5.4.1. Localization of HAX1

HeLa cells were transfected with HAX1 fused to a GFP reporter and stained with DAPI and mitotracker red. The cells were further processed and visualized under a fluorescence microscope.

The mitochondrion was stained red using mitotracker red, the nucleus was stained with DAPI and HAX1-GFP fusion protein had green fluorescence. HAX1 localizes to the mitochondria, as observed by overlapping yellow signals in the transfected cell (fig 5.4.1). The HAX1-GFP fusion protein was not detected in nucleus, golgi bodies,

endoplasmic reticulum or the lysosome (data not shown). This result is in line with the previously reported observations that HAX1 localizes majorly to the mitochondria.

### 5.5 HAX1 deficient cells have an increased rate of apoptosis

We reasoned that HAX1 deficiency would result in a state facilitating cellular apoptosis and analyzed the survival of neutrophils and peripheral blood mononuclear cells upon exposure to stress. Peripheral blood neutrophils were exposed to TNF  $\alpha$  or H<sub>2</sub>O<sub>2</sub> and the PBMCs were exposed to TNF  $\alpha$  or staurosporine or H<sub>2</sub>O<sub>2</sub> in a 5% CO<sub>2</sub> incubator. Annexin V staining and propidium iodide uptake was used to assess the percentage of apoptotic cells. The cells were collected at indicated time points, washed and analyzed for apoptosis by flow cytometry. The binding of annexin V to phosphatidyl serine marks an early apoptotic event and the uptake of propidium iodide due to a disintegrating nucleus marks an apoptotic cell. Hence cells positive for annexin V, PI or both, were accounted apoptotic.

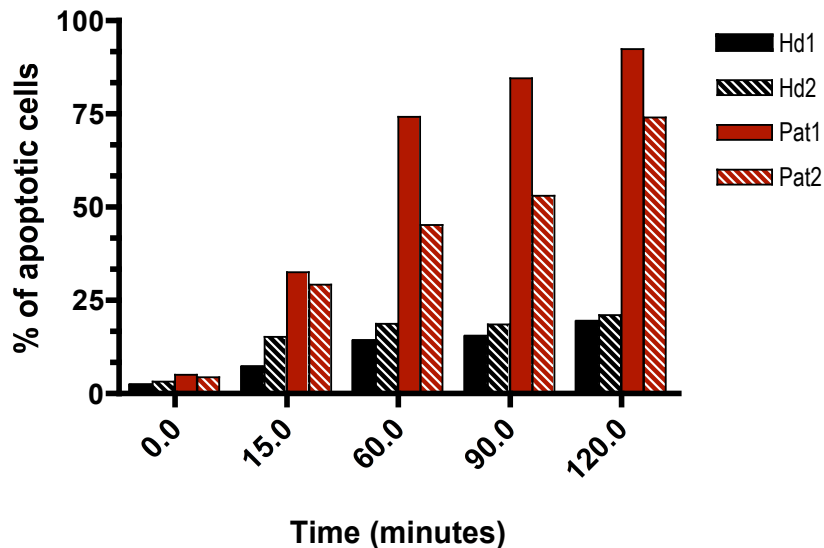


**Fig 5.5.1. FACS analysis of neutrophil apoptosis upon exposure to H<sub>2</sub>O<sub>2</sub>**

Neutrophils isolated from the peripheral blood of two healthy donors (Hd 1&2.) and HAX1 deficient patient (Pat 1&2) were treated with H<sub>2</sub>O<sub>2</sub>. Accounting the annexin V and propidium iodide positive cells by flow cytometry at indicated time points monitored the percentage of apoptosis.

### Fig 5.5.2. FACS analysis of neutrophil apoptosis upon exposure to TNF $\alpha$

Neutrophils isolated from the peripheral blood of healthy donor administered with G-CSF (Hd1 G-CSF.), healthy donor without G-CSF dose (Hd2) and HAX1 deficient patient (HAX1 pat) were treated with TNF $\alpha$  and stained with annexin V positive and propidium iodide at indicated time points to measure the percentage of apoptotic cells

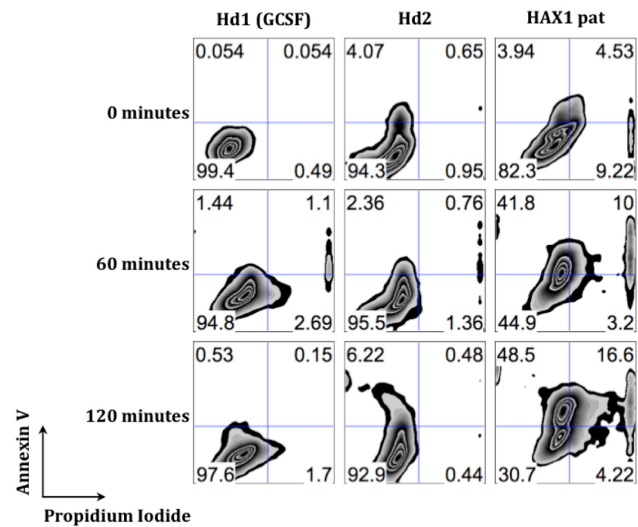
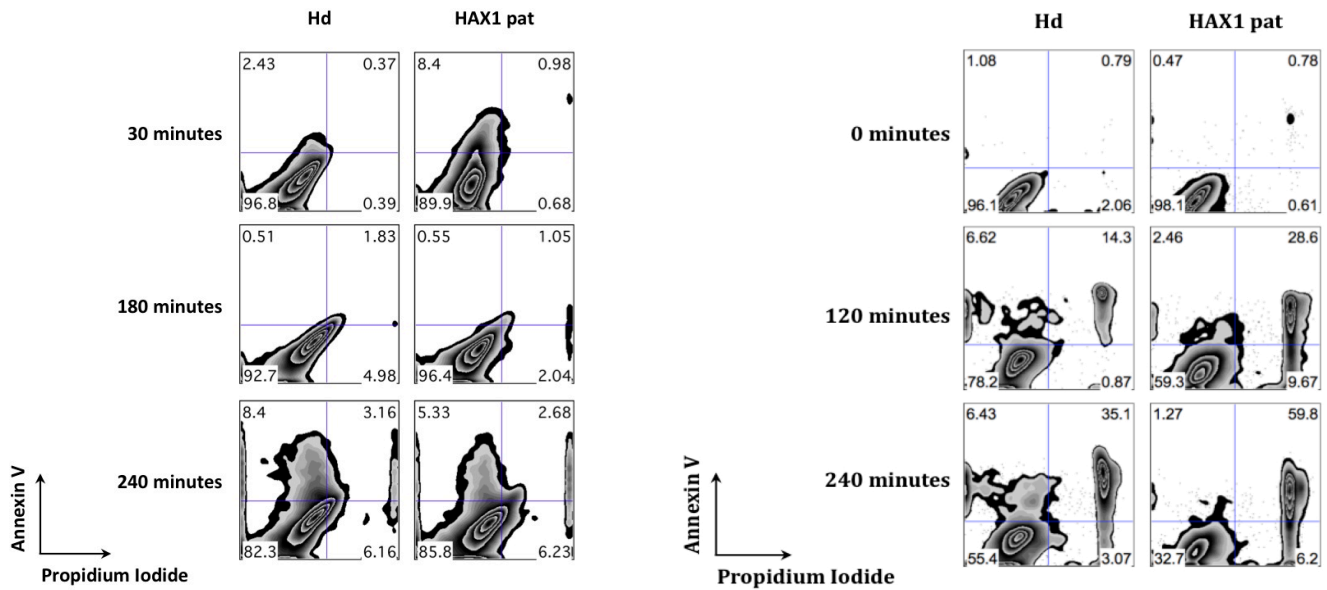


Fig (5.5.2) indicates representative FACS plots comparing the rate of apoptosis in HAX1 deficient patient neutrophils compared to healthy donor controls. The percentage of apoptosis was assessed on the basis of annexin V binding and PI uptake in the subjected neutrophils. HAX1 deficient neutrophils showed an increased rate of apoptosis, in contrast to neutrophils from healthy donor controls when challenged with different apoptotic stimuli such as TNF  $\alpha$  (fig 5.5.2), H<sub>2</sub>O<sub>2</sub> (fig 5.5.1) and staurosporine (data not shown)

Since HAX1 is ubiquitously expressed, we were interested to learn whether nonhematopoietic cells also had an increased susceptibility to apoptosis. We therefore assessed apoptosis in PBMCs and fibroblast of HAX1 deficient patients compared to healthy donors. Fig (5.5.3) indicates experimental results on measurement of apoptosis in HAX1 deficient total PBMCs as compared to healthy donor controls upon exposure to staurosporine. The PBMCs of the patients undergo a normal rate of apoptosis, similar to healthy donor samples. Further studies on EBV immortalized B cells of HAX1 deficient donors compared to health control donors also showed no significant difference in the rate of apoptosis (data not shown).



### Fig 5.5.3. Apoptosis in PBMCs and fibroblast

Total peripheral blood mononuclear cells (left) isolated from healthy donor (Hd) and HAX1 deficient patient (HAX1 pat) were exposed to staurosporine and *in vitro* cultured fibroblast (right) isolated from healthy donor (Hd) and HAX1 deficient patient (HAX1 pat) were exposed to H<sub>2</sub>O<sub>2</sub>. The cells were stained with annexin V and propidium iodide at indicated time points to measure the percentage of apoptotic cells

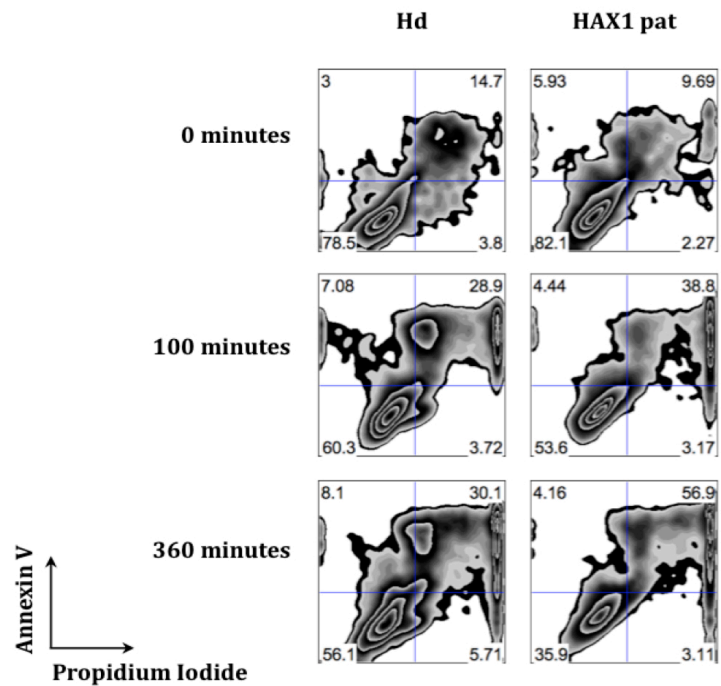
Fig (5.5.3) shows representative FACS plot analysis of apoptosis in fibroblast tissues of HAX1 deficient patients compared to healthy donor controls upon exposure to H<sub>2</sub>O<sub>2</sub>. Interestingly, the fibroblast cells of HAX1 deficient patient show an increase in the rate of apoptosis as compared to healthy donors. The results obtained, were further confirmed in multiple HAX1 deficient patients (data not shown). It is unclear though why the ubiquitously expressed HAX1 exhibits a myeloid specific clinical phenotype.

Results from our earlier experiments indicate that HAX1 deficiency causes SCN by lowering the threshold for apoptosis in cells of myeloid lineage. In order to further validate our finding, we *in vitro* differentiated bone marrow derived hematopoietic CD34+ stem cells from health donor controls and HAX1 patients to myeloid lineage in the presence of IL3, G-CSF and GM-CSF. Monitoring the rate of apoptosis upon exposure to apoptotic stimuli further assessed the control of HAX1 over apoptosis in these *in vitro* differentiated myeloid progenitors.



### Fig 5.5.4. Apoptosis in *in vitro* differentiated neutrophil granulocytes

CD34+ cells from total bone marrow of healthy donor (Hd) and HAX1 deficient patient (HAX1 pat) was isolated and differentiated *in vitro* to granulocytic lineage in the presence of G-CSF and GM-CSF as described earlier. The differentiated cells were treated with H<sub>2</sub>O<sub>2</sub> and the percentage of apoptotic cells were quantified by FACS based identification of the annexin V and propidium iodide positive cells.



BM derived CD34+ cells were purified, cultured and induced for granulocytic differentiation in the presence of IL3, G-CSF and GM-CSF as described earlier. The myeloid progenitors thus obtained from HAX1 deficient patients and healthy donors were subjected to apoptosis by treatment with a variety of apoptotic stimuli such as H<sub>2</sub>O<sub>2</sub> and staurosporine (data not shown) in the absence of cytokines IL3, G-CSF and GM-CSF. *In vitro* differentiated HAX1 deficient myeloid progenitors showed an increased susceptibility to apoptosis upon exposure to H<sub>2</sub>O<sub>2</sub>. These results further strengthen our previous findings that HAX1 deficient neutrophils are susceptible to an increased rate of apoptosis.

### 5.6 HAX1 deficient cells show a rapid loss of MMP ( $\Delta\Psi_m$ )

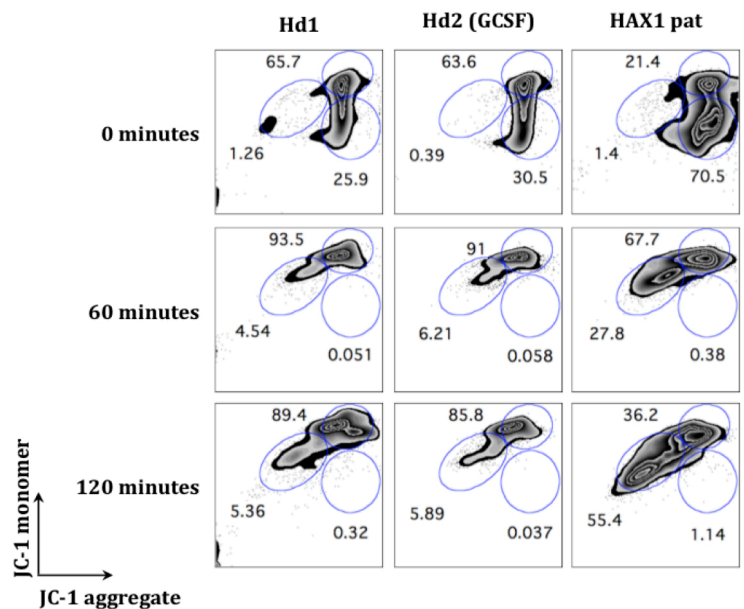
In line with our finding that deficiency of HAX1 results in increased rate of apoptosis in neutrophils, we set our further goals in understanding how HAX1 extends its control over apoptosis. Antiapoptotic BCL-2 family proteins have been largely renowned for their role in maintaining cellular homeostasis by extending a control over mitochondrial membrane potential (MMP/ $\Delta\Psi_m$ ). Since HAX1 may possess BH1 and BH2 similarity domains and is localized majorly to the mitochondria, we reasoned that HAX1 possess



similar functions to antiapoptotic members of the BCL-2 family. To address this, we chose to analyze the reported and most definitive role of antiapoptotic BCL-2 members in control over mitochondrial pathway of apoptosis, the MMP ( $\Delta\Psi_m$ ). To test our hypothesis, we challenged the neutrophils from HAX1 deficient patients and healthy controls with a potassium selective ionophore, valinomycin that facilitates mitochondrial transport of  $K^+$ . This facilitated transport across membrane barrier results in excess accumulation of  $K^+$  and hence an increased consumption of  $O_2$  inside the mitochondria. This subsequently leads to a drop in the mitochondrial membrane potential. Prior to treatment with valinomycin, the cells were stained with JC-1, a dual emission dye. The monomeric form of the dye, fluoresces green and accumulates in the mitochondria irrespective of the membrane potential of a mitochondrion. But the aggregation of the monomer leading to formation of J-aggregates and fluoresces red, requires a mitochondria with higher mitochondrial membrane potential ( $\Delta\Psi_m$ ).

**Fig 5.6.1. FACS analysis of  $\Delta\Psi_m$  in neutrophils upon exposure to valinomycin**

Neutrophils isolated from the peripheral blood of healthy donor (Hd1), healthy donor administered with G-CSF dose (Hd2 G-CSF) and HAX1 deficient patient (HAX1 pat) were stained with JC-1 a double emission dye. The percentage of cells with JC-1 aggregate and JC-1 monomer were further quantified upon exposure to valinomycin, at indicated time points.



Loss of mitochondrial membrane potential is an early event of mitochondrial pathway of apoptosis. HAX1 deficient granulocytes, though possess a higher mitochondrial membrane potential as compared to healthy donor controls in the uninduced state, show a rapid dissipation of  $\Delta\Psi_m$  upon exposure to valinomycin, whereas neutrophils from healthy donor controls show a strict maintenance of inner mitochondrial membrane potential. Hence it was inferred from these results that HAX1 deficiency leads to increased apoptosis through loss of control over maintenance of mitochondrial membrane potential in neutrophil granulocytes.

Results from our previous experimental observations indicate that the phenotype of increased apoptosis in case of HAX1 deficiency is not limited to neutrophils but also fibroblast. To further validate these results we analyzed the mitochondrial membrane potential in HAX1 deficient fibroblast and total PBMCs as compared to healthy donors.

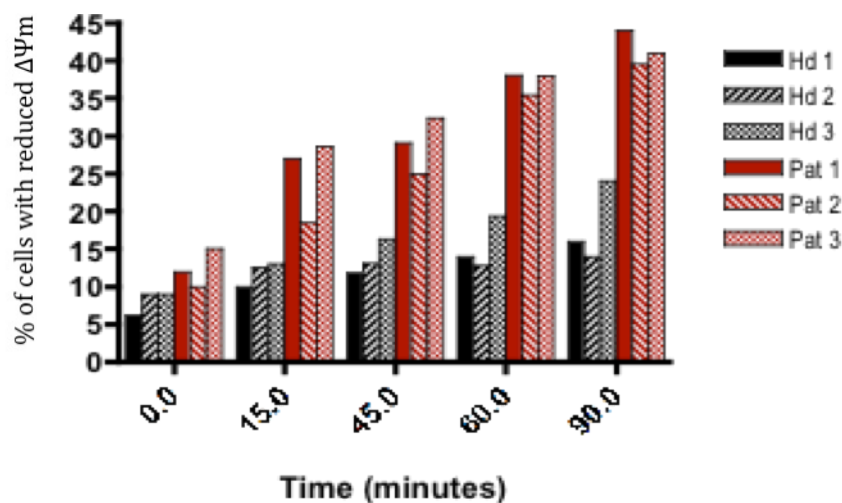


**Fig 5.6.2. FACS analysis of  $\Delta\Psi_m$  in fibroblast upon induction with valinomycin**

*In vitro* cultured fibroblast isolated from healthy donors (Hd 1,2&3) and HAX1 deficient patient (Pat1,2&3) were prestained with JC-1 a double emission dye. The percentage of cells with JC-1 aggregate and JC-1 monomer was further quantified by flow cytometry upon exposure to valinomycin, at indicated time points.

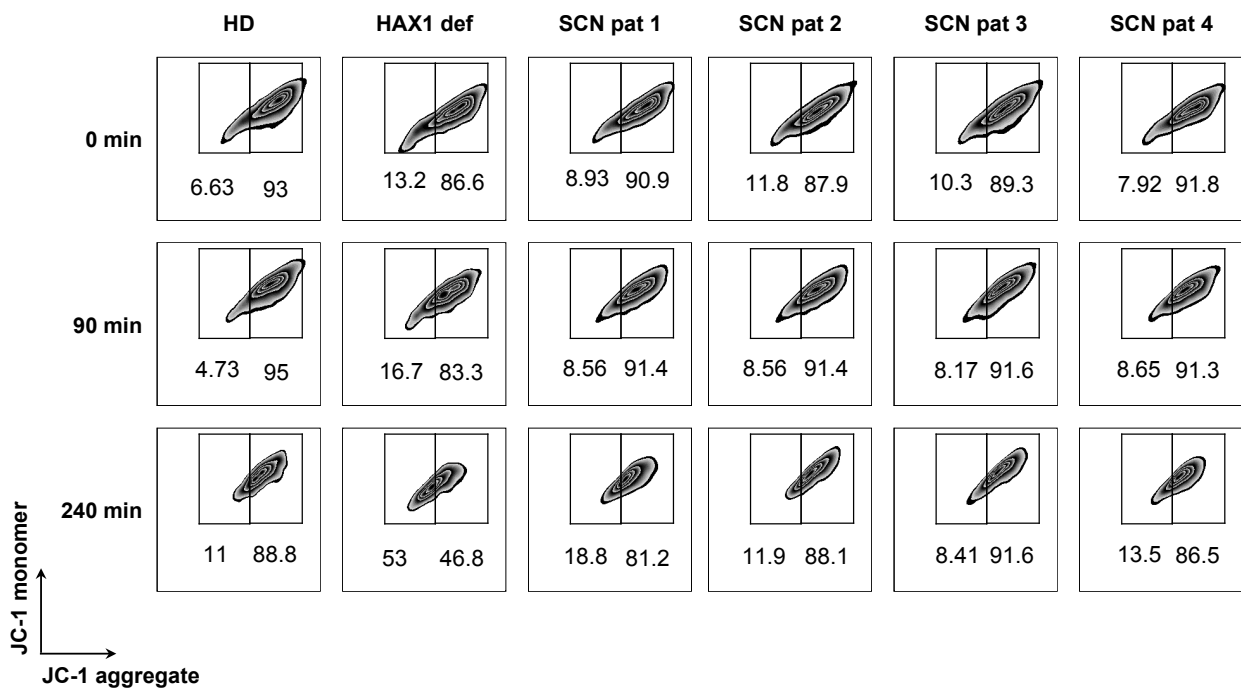


**Fig 5.6.3. Analysis of  $\Delta\Psi_m$  in fibroblast upon induction with valinomycin**

*In vitro* cultured fibroblast isolated from healthy donor (HD), HAX1 deficient patient (HAX1 def) and SCN patients with no mutations in *HAX1* (Pat 1,2,3&4) were prestained with JC-1 a double emission dye. The percentage of cells with JC-1 aggregate and JC-1 monomer were further quantified upon exposure to valinomycin, at indicated time points by FACS.

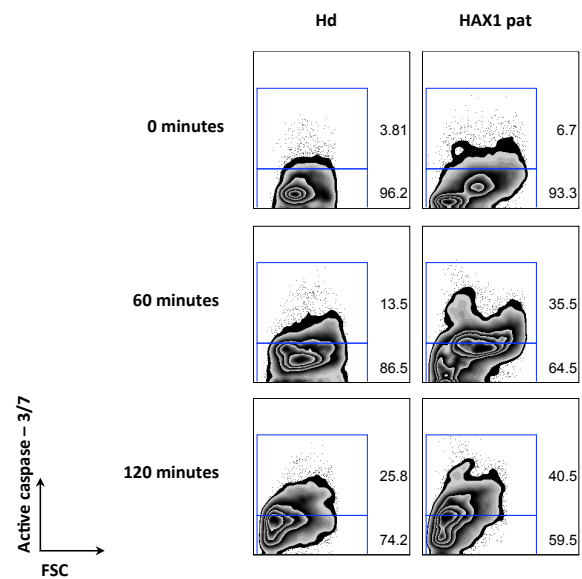
Similar to the HAX1 deficient neutrophils, HAX1 deficient fibroblasts also show a rapid dissipation of mitochondrial membrane potential, compared to healthy donor control cells (fig 5.6.3). In contrast, the PBMCs and EBV immortalized B lymphocytes from HAX1 deficient patients however did not show the phenotype of altered mitochondrial membrane potential (data not shown)

### 5.7 HAX1 deficient cells show increased caspase activation

Because of the reported interaction of HAX1 with the mitochondrial serine protease Omi/HtrA2, and its involvement in caspase independent cell death in neutrophil granulocytes, we analyzed the activation of effector caspases in neutrophil granulocytes and fibroblast of HAX1 deficient patients as compared to healthy donors.

### Fig 5.7.1. Analysis of caspase3/7 activation in neutrophils

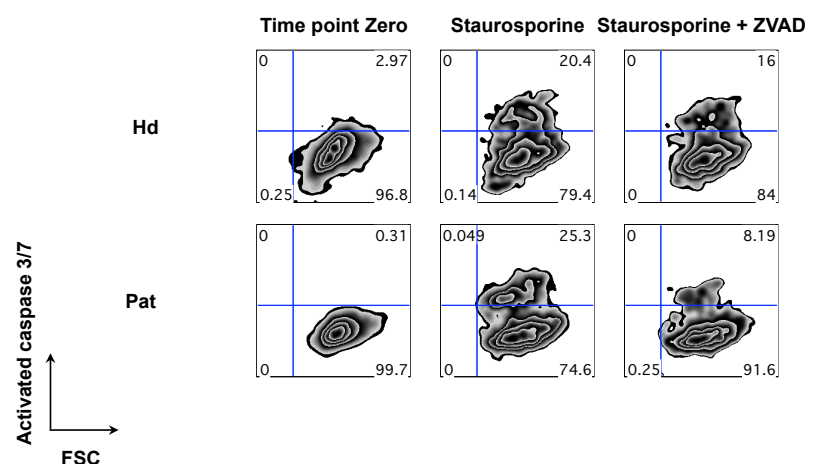
Neutrophils isolated from the peripheral blood of healthy donor (Hd) and HAX1 deficient patient (HAX1 pat) were exposed to staurosporine and the percentage of cells with increase in levels of active effector caspase (effector caspase 3/7) was assayed by FLICA based technology using flow cytometry.



HAX1 deficient granulocytes exhibit a higher degree of activation of the effector caspases-3/7 when exposed to staurosporine (fig 5.7.1) and TNF  $\alpha$  (data not shown). Similarly, HAX1 deficient fibroblasts show accelerated activation of caspases-3/7 when exposed to staurosporine. But the general caspase inhibitor Z-VAD could block the activation of these effector caspases 3&7.

### Fig 5.7.2. Effect of Z-VAD on caspase3/7 activation in fibroblast

*In vitro* cultured fibroblast isolated from healthy donor (Hd) and HAX1 deficient patient (Pat) were exposed to staurosporine in the presence or absence of a general caspase inhibitor (Z-VAD). The percentage of cells with increased levels of active effector caspase (effector caspase 3/7) was assayed by FLICA based technique using flow cytometry.



Taken together these results suggest that increased apoptosis observed in case HAX1 deficiency is a caspase dependent process.

## 5.8 Silencing of *HAX1* mRNA is inadequate.

To further demonstrate that deficiency of *HAX1* causes increased apoptosis, we tried to knock down the mRNA encoding *HAX1*, by a RNA silencing technique. A shRNA-based approach was adapted to down regulate the mRNA of *HAX1*. Double stranded short interfering RNA oligos corresponding to *HAX1* mRNA sequence were designed and directionally cloned into a lentiviral backbone pRRL.PPT.SF.DsRedEx.Pre *SnaB1*. The shRNA cloned lentiviral plasmids were transiently transfected into HEK 293T cell lines and the levels of endogenous *HAX1* mRNA was further quantified to assess the ability of these siRNA to silence *HAX1* mRNA.

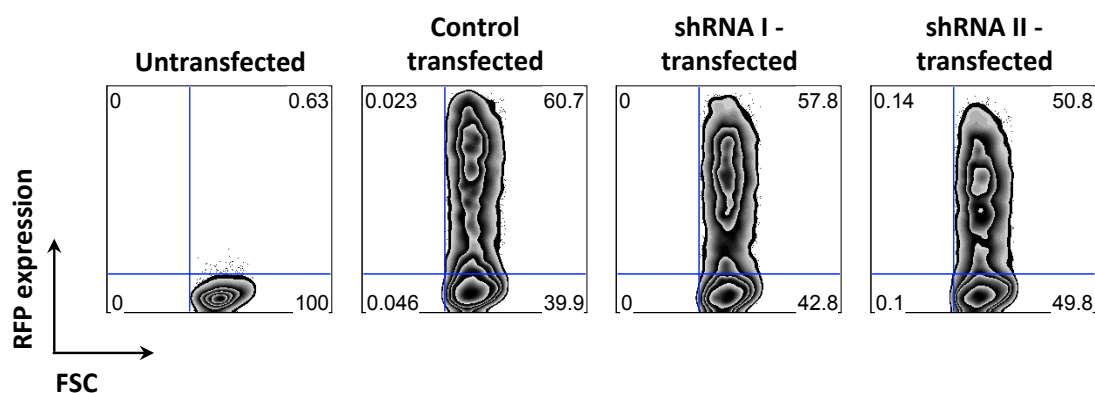


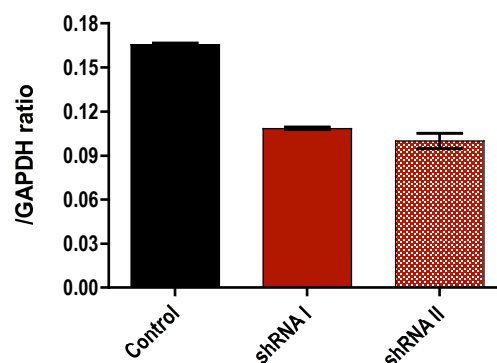
**Fig 5.8.1. Analysis of transfection efficiency of *HAX1* shRNA**

HEK 293T cells were transiently transfected with shRNA encoding plasmids targeting *HAX1* mRNA or control vector. The cells were collected by trypsination after 36-48 hours and the percentage of RFP positive cells were analyzed using flow cytometry.

The figure (5.8.1) represents FACS plots indicating the transfection efficiency obtained with the lentiviral control and shRNA plasmids. Approximately 50% of the cells were transfected in case of the control as well as the shRNA constructs, as estimated by the FACS analysis. The cells were then further harvested and the *HAX1* mRNA expression level was analyzed by real time RT PCR employing *HAX1* gene specific primers as described earlier.

**Fig 5.8.2. Analysis of *HAX1* expression**

cDNA synthesised from HEK 293T cells transfected with shRNA encoding plasmids targeting *HAX1* mRNA or control vector was subjected to realtime PCR analysis to evaluate the knockdown of *HAX1*.



Analysis of *HAX1* mRNA levels indicates that both shRNAI and shRNAII are efficient in silencing the *HAX1* mRNA. Nevertheless, the knockdown of *HAX1* mRNA by shRNA1 or shRNA2 is inadequate. Thus, the RNA silencing technique could not be further employed for assaying the antiapoptotic functions of HAX1.

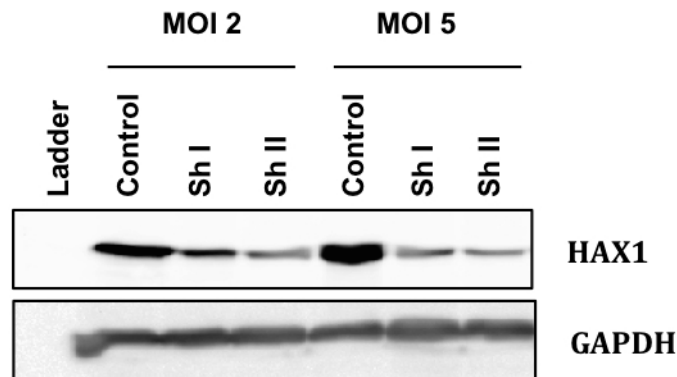


**Fig 5.8.2. Western blot analysis of knock down of HAX1**

HEK 293T cells were stably transduced with shRNA encoding lentivirus targeting *HAX1* mRNA (Sh I&II) or control vector (control) at different MOI and sorted by flow cytometry to obtain a purity of >96%. Total cellular protein extract was isolated from these cells and the expression level of HAX1 in these cells was detected by western blot using a HAX1 specific monoclonal antibody.

## 5.9 Reconstitution of $\Delta\Psi_m$ by retroviral gene transfer of *HAX1*.

To prove the notion, that deficiency of HAX1 results in increased susceptibility towards loss of mitochondrial membrane potential and thus apoptosis, complementation experiments were performed using *HAX1* encoding retroviruses. In this regard, we purified BM derived CD34+ cells from HAX1 deficient and healthy control individuals and transduced them with bicistronic retroviral vectors encoding *HAX1* and a marker gene. The retroviral plasmids encoding *HAX1* cDNA was constructed by amplifying the cDNA generated from total mRNA of healthy donor control individuals by PCR and directionally cloned in to pMMP-IRES-mCD24+ retroviral plasmid, as described previously. The control and *HAX1* encoding retroviral particles were generated and healthy donors and patient cells were transduced with an MOI of 2 as described earlier. A FACS based sorting of cells expressing the marker gene further purified these transduced cells. These sorted cells accounting >98% purity were briefly cultured followed by induction for myeloid differentiation in the presence of G-CSF, GM-CSF and IL3. The mitochondrial membrane potential of these differentiated myeloid progenitors were further analyzed upon exposure to valinomycin.

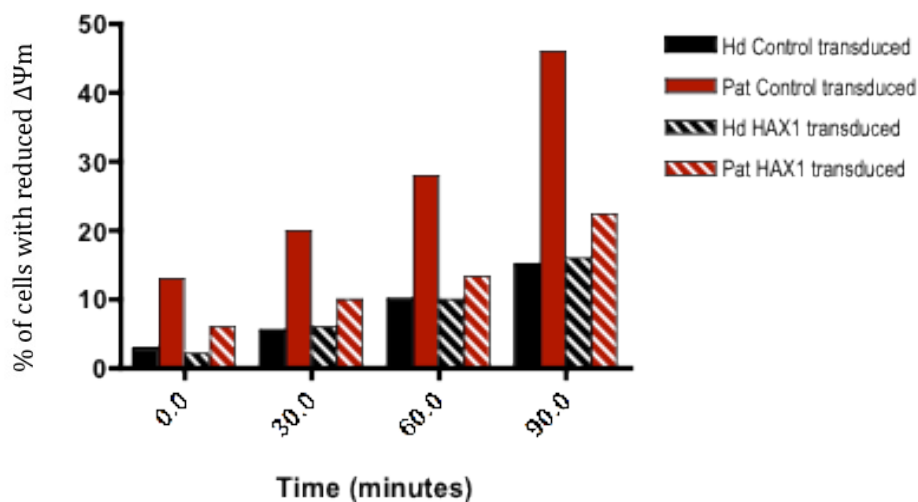


**Fig 5.9.1. Reconstitution of  $\Delta\Psi_m$  in *in vitro* differentiated myeloid progenitors**

*In vitro* differentiated neutrophils from healthy donor (Hd) and HAX1 deficient patient (Pat) were transduced with a retroviral construct expressing HAX1 or control vector. The cells were further stained with JC-1 a double emission dye, prior to treatment with valinomycin. The percentage of cells with JC-1 aggregate and JC-1 monomer were further quantified at indicated time points by flow cytometry.

In line with our previous observation that HAX1 deficient SCN patient neutrophils and fibroblast show reduced control over loss of mitochondrial membrane potential, *in vitro* differentiated myeloid progenitors from the SCN patients also exhibited a reduced maintenance of mitochondrial membrane potential upon exposure to the potassium ionophore, valinomycin.

As expected, the myeloid progenitors of SCN patients transduced with *HAX1* exhibits a phenotype similar to the healthy donor controls. The loss of mitochondrial membrane potential in SCN patients was significantly delayed in *HAX1* transduced cells as compared to cells transduced with the reporter gene. The phenotype of increased apoptosis and reduced mitochondrial membrane potential is also identified in case of HAX1 deficient fibroblast.

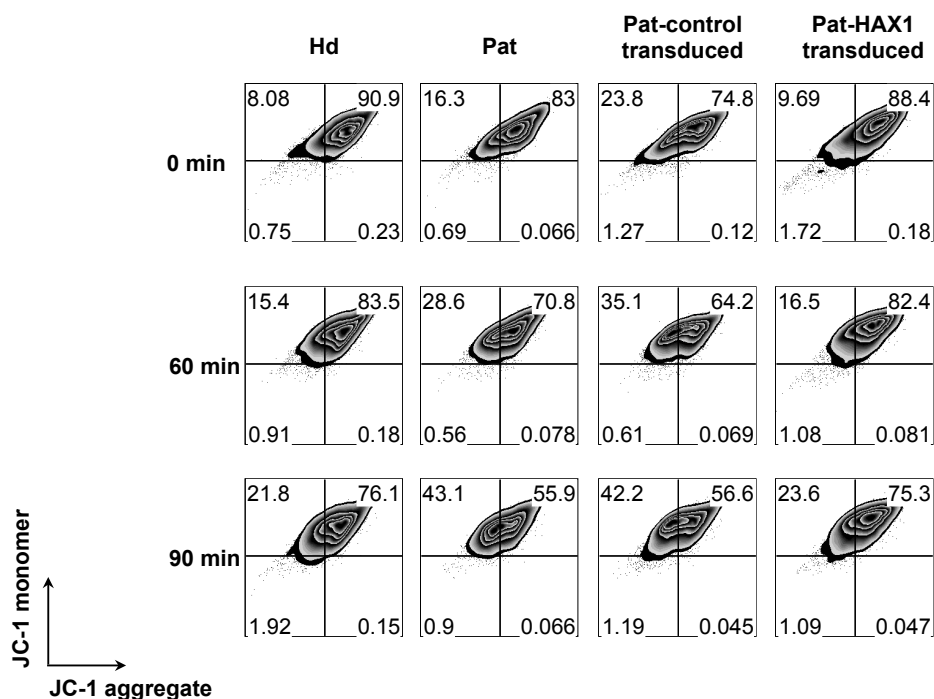


### Fig 5.9.2. FACS analysis demonstrating reconstitution of $\Delta\Psi_m$ in fibroblast

*In vitro* cultured fibroblast from healthy donor (Hd), HAX1 deficient patient (Pat) cells and HAX1 deficient patient transduced with a retroviral construct expressing HAX1 (Pat-HAX1 transduced) or control vector (Pat-control transduced) were stained with JC-1 a double emission dye. The percentage of cells with cells with high  $\Delta\Psi_m$  was calculated by flow cytometry based technique.

To confirm the observed results, we performed reconstitution assay of mitochondrial membrane potential in fibroblast cells. Similar to the myeloid progenitors, fibroblasts transduced with *HAX1* also showed a reconstituted phenotype, exhibiting strict control over loss of mitochondrial membrane potential indicating a controlled apoptotic program upon HAX1 expression.

Henceforth, we concluded that HAX1 is a critical regulator of apoptosis. Similar to the antiapoptotic BCL-2 proteins, HAX1 exhibits its antiapoptotic function by extending control over loss of mitochondrial membrane potential.



## 5.10 HAX1 deficient neutrophils show reduced mitochondrial mass

A comprehensive study on HAX1 deficient tissues indicates that apoptosis in HAX1 deficient cells occurs through the mitochondrial pathway and in a caspase dependent manner. To further elucidate the biological functions of HAX1 in neutrophil granulocytes and to delineate the biochemical events underlying the clinical phenotype of SCN, we analyzed further downstream events of the mitochondrial pathway of apoptosis. Mitochondrial mass, a sequestered event is significantly altered during the course of cell death. We stained the HAX1 deficient neutrophil granulocytes and PBMCs with mitotracker red, a mitochondrion selective probe. The changes in mitochondrial mass was then assessed over time upon exposure to valinomycin.

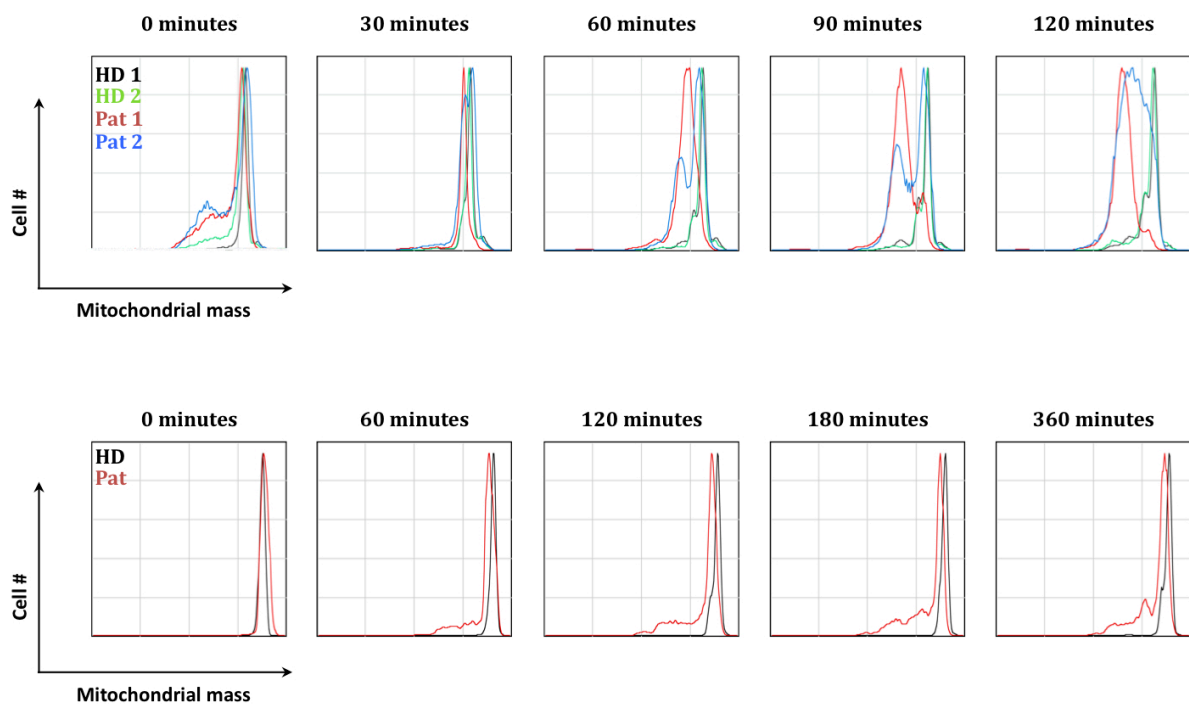


**Fig. 5.10.1. Analysis of mitochondrial mass in neutrophils**

Neutrophils isolated from the peripheral blood of healthy donor (HD 1&2) and HAX1 deficient patient (Pat 1&2) (**Above**) or neutrophils isolated from the peripheral blood of healthy donor (HD) and *ELA2* mutated patient (Pat) (**Below**) were stained with a mitochondrion selective probe (mitotracker 580) prior to treatment with valinomycin. The loss of mitochondrial mass was monitored at indicated time points by flow cytometry.

HAX1 deficient granulocytes showed a rapid loss of mitochondrial mass upon exposure to valinomycin (fig 5.10.1). Mitochondrial mass, a measure of the amount of intact mitochondria within a cell, decreased rapidly in these HAX1 deficient cells indicating a

phenotype of increased apoptosis. This phenotype however was not observed in case of PBMCs or B-lymphocytes (data not shown).

### 5.11 HAX1 deficient neutrophils have decreased cellular ATP

Maintenance of mitochondrial inner membrane potential is an ATP requiring process and a critical regulator of mitochondrial functions such as oxidative phosphorylation. Mitochondrial oxidative phosphorylation coupled ATP synthesis contributes a major percentage of the cellular ATP. With our previous identification that HAX1 deficiency results in mitochondrial dysfunction, we hypothesized that HAX1 deficiency could result in the decrease of cellular ATP. We monitored the AMP/ATP ratio in the cell by monitoring the levels of cellular AMPK $\alpha$ . We induced the neutrophils with valinomycin, promoting loss of mitochondrial membrane potential.

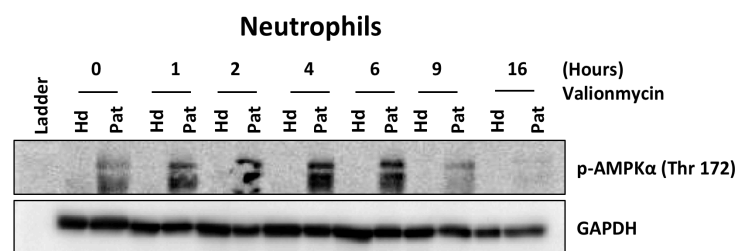


#### Fig 5.11.1. Analysis of AMP/ATP ratio in neutrophil granulocytes

Neutrophils isolated from the peripheral blood of healthy donor (Hd) and HAX1 deficient patient (Pat) were treated with valinomycin. Total cellular protein extract was isolated from these cells at indicated time points and the phosphorylation status of AMPK $\alpha$  in these cells was quantified by western blot analysis.

HAX1 deficient neutrophils showed an increased level of phosphorylation of the AMPK $\alpha$  protein at Thr 172, indicating an elevated level of cellular AMP and a drop in cellular ATP.

### 5.12 HAX1 deficient neutrophils show increased ROS production

Reactive oxygen species (ROS) are byproducts of oxidative phosphorylation. Hampered mitochondrial membrane potential leads to mitochondrial dysfunction resulting in insufficient ATP production and inefficient control over ROS production. The ROS thus produced are released from the mitochondrion to the cytosol. Hence a reduction in mitochondrial membrane potential leads to changes in levels of cytosolic reactive

oxygen species (ROS) resulting in a state of oxidative stress. Since HAX1 deficiency results in decreased mitochondrial membrane potential, we hypothesized that HAX1 deficiency results in increased ROS production and thus hampering the antioxidative defense. We analyzed the rate of cytosolic ROS production in neutrophil granulocytes. Healthy donor and HAX1 deficient peripheral blood neutrophil granulocytes were isolated and analyzed for ROS production upon exposure to valinomycin or PMA by a flow cytometry based technique.

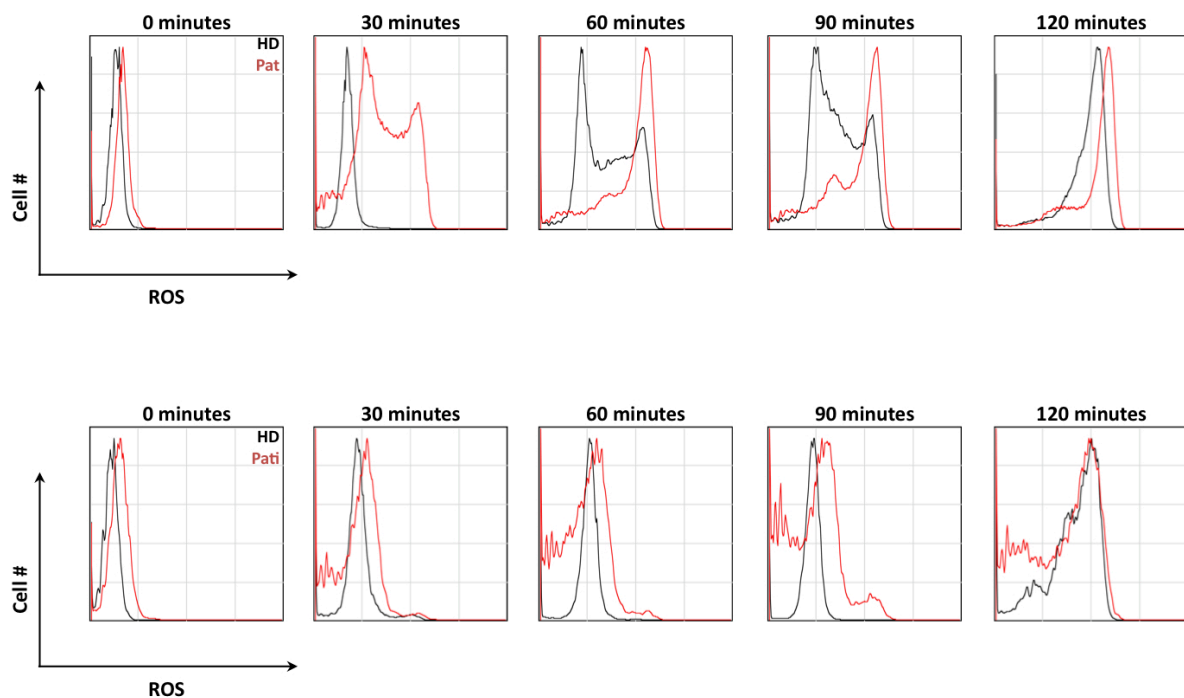


**Fig. 5.12.1. FACS analysis of ROS production in neutrophil granulocytes**

Neutrophils isolated from the peripheral blood of healthy donor (HD) and HAX1 deficient patient (Pat) **(Above)** or neutrophils isolated from the peripheral blood of healthy donor (HD) and *ELA2* mutated patient (Pati) **(Below)** were stained with CM-H<sub>2</sub>DCFDA prior to induction for ROS production. The rate of ROS production was further monitored at indicated time points by flow cytometry upon exposure to PMA.

The rate of ROS production in neutrophils was enhanced in case of HAX1 deficiency upon treatment with valinomycin and PMA. HAX1 deficient neutrophils showed an increased rate of ROS production.

This phenotype is specific to HAX1 deficiency as the accelerated ROS production was not observed in neutrophils of SCN patients with mutation in *ELA2* and SCN patients without any mutations in *HAX1* (data not shown).

### 5.13 HAX1 deficient neutrophils show hampered antioxidant defense

ROS are continuous byproducts of oxidative phosphorylation process and are toxic to the cell. Antioxidant defense enzymes such as catalase and mnSOD, degrade the ROS to protect cells. Increased ROS production and its release into the cytosol, further accumulates and targets degradation of these antioxidant defense proteins such as catalase leading to oxidative stress in a cell. Hence an accumulation in ROS would subsequently lead to reduction in levels of the antioxidant defense proteins such as catalase. Since HAX1 deficiency leads to increased ROS production we hypothesized that the antioxidative degradation of catalase must be accelerated in HAX1 deficient cells upon induction for loss of mitochondrial membrane potential. We analyzed the rate of catalase degradation in neutrophil granulocytes upon exposure to the potassium ionophore, valinomycin. Neutrophils from healthy donor controls and HAX1 deficient patients were purified as described earlier. Whole cell protein extracts were prepared from these neutrophils at indicated time points and analyzed by western blot. Catalase degradation was accelerated in HAX1 deficient granulocytes upon treatment with valinomycin suggesting that HAX1 deficiency is associated with increased exposure to ROS.

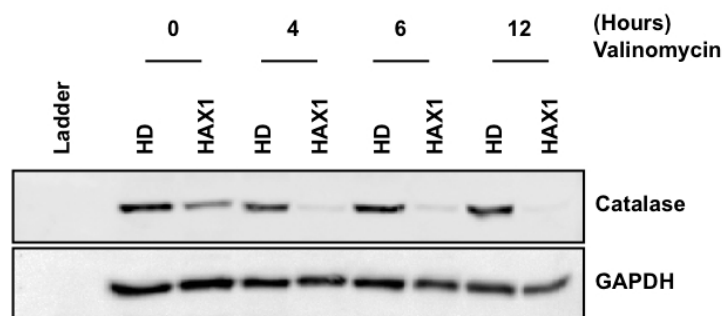


**Fig 5.13.1. Antioxidant defense in neutrophil granulocytes**

Neutrophils isolated from the peripheral blood of healthy donor (Hd) and HAX1 deficient patient (Pat) were treated with valinomycin. Total cellular protein extract was isolated from these cells at indicated time points and the expression levels of catalase in these cells was quantified by western blot analysis.

## 5.14 HAX1 deficient granulocytes exhibit enhanced autophagy

Defective antioxidant defense resulting from increased cytosolic ROS hampers intracellular organelles leading to apoptosis. Mitochondrial dysfunction results in increased ROS generation. We hypothesized that the cell would exert an increased rate of autophagy as an adaptive mode of survival. We analyzed the rate of autophagy in HAX1 deficient neutrophils, fibroblasts and PBMCs. To induce autophagy, we exposed healthy donor and HAX1 deficient cells to rapamycin, an autophagy inducing drug. Whole cell extracts were prepared at various time points and analyzed for expression levels of proteins regulating autophagy. Interestingly, the HAX1 deficient neutrophils showed an increased level of the autophagy essential gene Beclin-1. However, the increase in Beclin-1 protein was observed only in HAX1 deficient neutrophils but not in case of HAX1 deficient mononuclear cells. HAX1 deficient neutrophils, but neither PBMCs nor *in vitro* cultured fibroblast (data not shown) showed this phenotype of increased levels of Beclin-1 protein as analyzed by western blot.

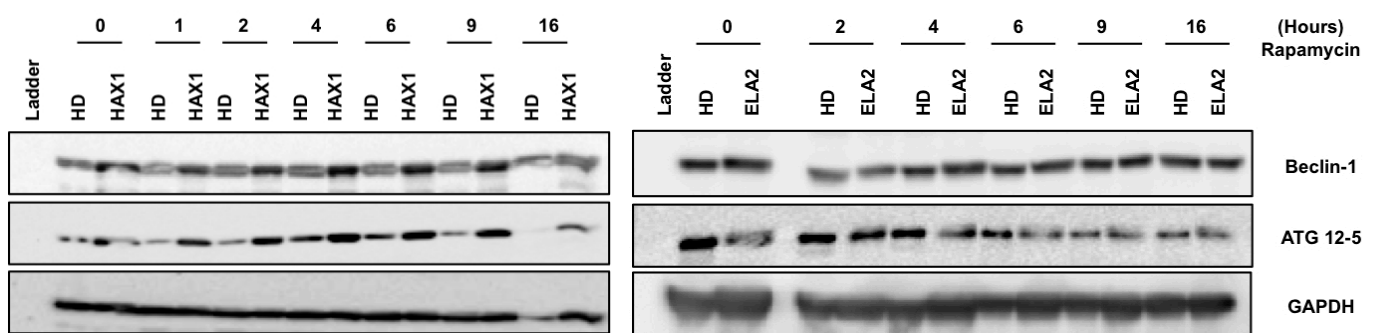


**Fig. 5.14.1. Analysis of beclin-1 and ATG 12-5 complex expression in neutrophils**

Neutrophils isolated from the peripheral blood of healthy donor (HD), HAX1 deficient patient (HAX1) (**left**) and neutrophils isolated from healthy donor (HD) and *ELA2* mutated patient (*ELA2*) (**right**) were treated with rapamycin. Cells were harvested at indicated time points and total cellular protein extract was analyzed for the expression levels of beclin-1 protein and ATG12-5 protein complex by western blot.

Increase in Beclin-1 marks the initiation of autophagy and leads to an avalanche of autophagic events such as ATG12-5 complex formation and LC3II sequestration leading to phagophore formation. We monitored the immediate key event, the formation of ATG12-5 complex in HAX1 deficient neutrophils upon induction with rapamycin.

The level of Beclin-1 protein and ATG 12-5 protein complex formation was increased in HAX1 deficient neutrophils but not mononuclear cells. This observed phenotype is specific to HAX1 deficiency, as SCN neutrophils expressing functional HAX1 (ELA2 patients) did not show increased levels of autophagy, as assessed by beclin-1 expression and ATG12-5 complex formation.

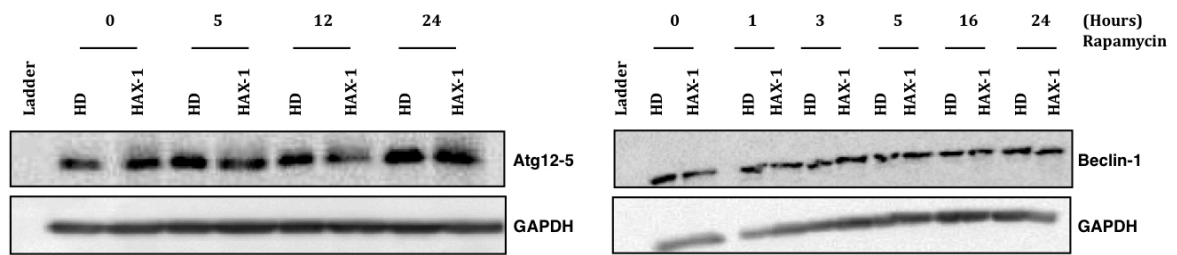


**Fig. 5.14.2. ATG12-5 complex formation and beclin-1 expression in PMBCs**

Peripheral blood mononuclear cells isolated from healthy donor (HD) and HAX1 deficient patient (HAX-1) were treated with rapamycin. Cells were harvested at indicated time points and total cellular protein extract was analyzed for the expression levels of beclin-1 protein and ATG12-5 protein complex by western blot.

This is in line with our previous observation that HAX1 deficient neutrophils, but not mononuclear cells have a decreased mitochondrial membrane potential, accompanied by increased levels of cytosolic ROS. Furthermore, we performed transmission electron microscopy (TEM) in HAX1-deficient bone marrow cells.

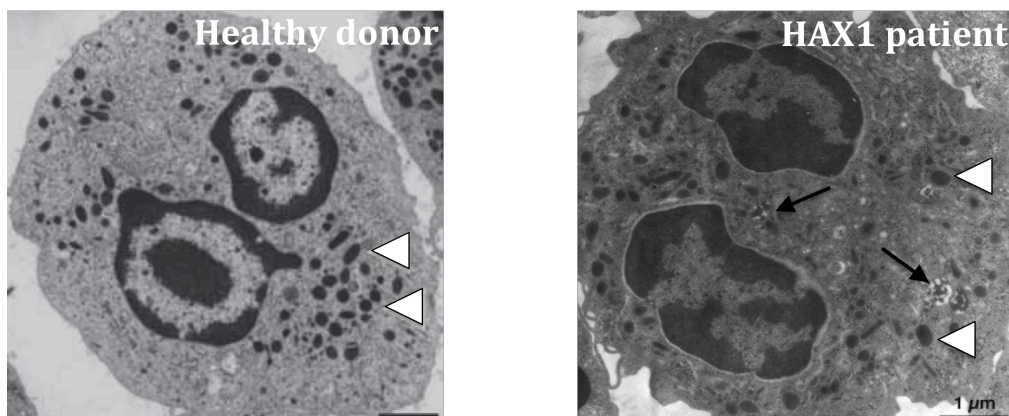


**Fig 5.14.3. Transmission electron microscopy analysis of neutrophils**

Mononuclear cells isolated from the bone marrow of healthy donor (left) and HAX1 deficient patient (right) were sectioned and analyzed by transmission electron microscopy. The phagophore formation, if any are indicated (black arrow).

Interestingly, we observed that HAX1 deficient neutrophils but not healthy donor controls showed increased phagophore formation, denoting increased levels of autophagy during neutrophil differentiation. This phenotype is specific to HAX1 deficient neutrophils and not mononuclear cells. Also, the phenotype of phagophore formation is not observed in neutrophils of SCN patients with functional HAX1 (data not shown), indicating its specificity to HAX1 deficiency

## 6. DISCUSSION

### 6.1 Individuals with autosomal recessive severe congenital neutropenia reveal mutations in *HAX1*

Neutropenia is a rare, inborn hematological disorder associated with life threatening bacterial infections. Previous studies have shown that mutations in the gene encoding neutrophil elastase (*ELA2*) [140], Wiskott-Aldrich syndrome (*WAS*) gene [13, 14], Growth factor independent 1 (*GFI1*) [15] and the endosomal adapter protein (*P14*) [16] result in neutropenia. Still the genetic defect underlying classical SCN, characterized by autosomal recessive mode of inheritance remained largely unknown and the molecular mechanism thus poorly understood.

The primary objectives of the current study were to identify the genetic defect causing Kostmann syndrome and understand the molecular etiology underlying the disease. In this view, we performed genome wide linkage analysis on three unrelated families with members suffering from recurrent infections due to neutropenia and identified a linkage interval on chromosome 1, spanning 275 genes. Although we identified many interesting candidate genes such as *MAPBIP*, *RAB25* and *IL6R*, sequence analysis showed wild type sequence for these genes.

Altered tissue homeostasis through increased apoptosis plays a major role in a variety of bone marrow disorders. Previous reports provide evidence of elevated apoptosis in the bone marrow of patients belonging to the original kindred described by Kostmann [8, 22]. Scientists have discovered that mutation in *ELA2* results in increased unfolded protein response (UPR) leading to the increased rate of apoptosis in differentiating neutrophils [12, 140, 143]. Also dominant negative mutations in the neutrophil elastase (NE) transcriptional repressor *GFI1* induce SCN through increased NE expression, inducing an UPR stress [15, 144]. A recent study also identified that specific mutation in the gene encoding Wiskott-Aldrich syndrome protein (WASp) leads to increased actin polymerization resulting in an X-linked form of neutropenia with an intrinsic failure of myelopoiesis [13, 14].



We prioritized the evaluation of *HAX1* as a primary candidate gene, in view of its previously reported anti apoptotic functions [125] and its role in the regulation of actin cytoskeleton [131]. We identified a homozygous single nucleotide insertion leading to a premature stop codon (W44X) in all affected individuals from these different families resulting in complete absence of the protein as assessed by western blot. Subsequent sequencing of additional SCN patients revealed numerous novel mutations in *HAX1*. Thus a reverse genetics based approach, identified different mutations in *HAX1* as causative of SCN. Interestingly individuals from the original Kostmann family also had homozygous mutations in *HAX1* (Q190X) providing proof that the disease originally described by Kostmann is caused by *HAX1* mutation.

## **6.2 HAX1 deficiency results in increased apoptosis through defective maintenance of mitochondrial membrane potential (MMP/ $\Delta\Psi_m$ )**

Although the majority of reports identify HAX1 to be localized in the mitochondrion [132-134], a few other studies have also indicated that HAX1 is also localized in the endoplasmic reticulum and the nuclear envelope [128, 137, 145]. In agreement with previous reports [132-134], we identified that HAX1 localizes to the mitochondrion and to a certain extent, to the cytoplasm. Mitochondria are key regulators of cellular homeostasis and potent integrators and coordinators of cell death [31, 146-148], targeting signaling pathways of other cellular organelles such as the endoplasmic reticulum and the nucleus towards apoptosis [149, 150]. HAX1 has also been reported to interact with proapoptotic proteins such as mitochondrial serine protease Omi/HtrA2 [132] and caspase [126, 151]. A recent study identified that HAX1 also interacts with SERCA2 and its inhibitor phospholamban [134], extending control over cellular calcium homeostasis.

In view of the subcellular localization of HAX1 and its interaction with various proapoptotic proteins, we analyzed the rate of apoptosis in tissues of affected individuals as compared to healthy donor controls. Our results indicate that HAX1 deficient neutrophils exhibit an accelerated rate of apoptosis. This observation is in

agreement with the previous studies that a majority of the SCN patients with unknown genetic defect or mutations in *ELA2* show increased apoptosis in the bone marrow [12, 22, 143]. But unlike *ELA2*, *HAX1* is ubiquitously expressed [125]. So we monitored apoptosis in other hematopoietic and nonhematopoietic tissues. Interestingly, *HAX1* deficient fibroblast and bone marrow derived CD34+ cells also exhibited an increased rate of apoptosis in comparison to unaffected individuals. But in contrast, peripheral blood mononuclear cells from the affected individual did not show a difference in the rate of apoptosis.

Studies in the past have identified that antiapoptotic members of the Bcl-2 gene family enhance cell viability under conditions that would otherwise produce cell death [18, 21, 43, 44, 47, 77, 146, 152, 153]. Proapoptotic members of the Bcl-2 family such as Bax and Bak extend their control over apoptosis by governing the mitochondrial outer membrane permeabilization (MOMP) [28]. Previous reports have identified that *HAX1* possess homology to the Bcl-2 proteins [125] and overexpression of *HAX1* positively regulates the maintenance of mitochondrial membrane potential [132]. Furthermore, loss of mitochondrial transmembrane potential results in the release proapoptotic factors such as cytochrome *c*, *omi/HtrA2* and AIF into the cytoplasm, leading to apoptosis of the cell in a caspase dependent manner [35, 132, 146, 152, 154, 155]. An interesting study also denotes that *HAX1* is degraded by mitochondrial associated *Omi/HtrA2* with the onset of apoptosis [156] suggesting its role as a mitochondrial antiapoptotic protein. Our study demonstrates that *HAX1* deficient neutrophils and fibroblast show a rapid loss of mitochondrial membrane potential and increased apoptosis in a caspase dependent manner.

To further prove that *HAX1* is inevitable for survival of neutrophils, we employed a shRNA based approach to knockdown *HAX1*. However, the approach was not feasible for functional experiments since the employed RNA interference was not sufficient to substantially decrease *HAX1* protein expression. We stably transduced tissues of affected and healthy donor control individuals with *HAX1* or control vector and studied the regulation of mitochondrial membrane potential. Patient fibroblast and myeloid progenitors transduced with *HAX1* showed an effective maintenance of mitochondrial

membrane potential as compared to cells transduced with control vector. Together, our data suggests that HAX1 is essential for maintenance of mitochondrial membrane potential, hence preventing mitochondrial dysfunction and cellular apoptosis.

### **6.3 Deficiency of HAX1 results in mitochondrial dysfunction and induces oxidative stress**

It has been well established that the antiapoptotic Bcl-2 proteins function at mitochondria to prevent the release of apoptogenic factors [78, 79, 157, 158] and a defective maintenance of mitochondrial membrane potential results in generation of reactive oxygen species (ROS) [31], which upon accumulation hampers the mitochondria and other cellular organelles causing cellular apoptosis [6, 39, 159-161]. Although it has been previously reported that over expression of HAX1 positively regulates the maintenance of MMP ( $\Delta\Psi_m$ ), the role of HAX1 in mitochondria is still unclear. We identified that HAX1 deficient neutrophils show an increased rate of ROS production, suggesting that HAX1 extends control over ROS production and thus potentiating a role in mitochondrial signaling. It has been shown that cells maintain ROS at a tolerable level by means of antioxidants such as the redox system, superoxide dismutase (SOD) and catalase [6, 162]. We observed that HAX1 deficient neutrophils show defective antioxidative defense as marked by increase in catalase degradation.

Loss of mitochondrial membrane potential associated alterations of the mitochondrial mass is a key event of cell death [162]. We identified that HAX1 deficient neutrophils show a loss of mitochondrial mass upon stimulating the dissipation of mitochondrial membrane potential. Previous reports have identified that dysfunction of the mitochondria due to qualitative or quantitative changes, results in the impairment of variety of biological process such as oxidative phosphorylation and ATP synthesis. Mitochondrial oxidative phosphorylation coupled ATP synthesis contributes a major percentage of the cellular ATP. HAX1 deficient cells show an increased level of AMPK $\alpha$  phosphorylation at residues threonine 172, indicating that HAX1 deficient neutrophils show a relatively high AMP/ATP content. Thus our results prove that HAX1 deficient

neutrophils show severe mitochondrial dysfunction, biogenesis, inefficient control over oxidative phosphorylation coupled ROS production and thus an increased susceptibility towards oxidative stress.

#### **6.4 Deficiency of HAX1 results in Beclin-1 dependent autophagy in neutrophil granulocytes**

A eukaryotic cell is a well integrated unit that consists of numerous subcellular organelles functioning in an organized fashion to maintain intracellular homeostasis [163]. Although transient low level ROS produced is utilized for signal transduction, defective antioxidant defense resulting from increased cytosolic ROS hampers intracellular organelles leading to apoptosis. Autophagy is a cellular process that causes degradation of cellular components to ensure survival [83, 84, 99, 110]. However, autophagy if accelerated or futile leads to a type of programmed cell death different from that of apoptosis. Previous studies have identified numerous protein involved in autophagic process and grouped them as autophagy related genes (ATG) [109, 164]. Recent studies have identified the onset of autophagy as marked by increase of Beclin-1 (a mammalian homologue of Atg6) [165] followed by an increase in the formation of a protein complex between ATG 12 and ATG 5 [114, 117]. The final steps of autophagy are characterized by the sequestration and formation of a light chain 3 beta (LC3B -II) phagophore complex, which is further sequestered and metabolized by the lysosomal machinery [76, 105]. Oxidative signaling has been implicated in a variety of experimental interventions that lead to the initiation of numerous adaptive responses. The cell regulates oxygen homeostasis by various regulatory genes such as *EPO*, *VEGF* and coordinates a series of events to inhibit mitochondrial biogenesis. It has been reported that induction of mitochondrial autophagy in concert with inhibition of mitochondrial biogenesis is a critical adaptive mechanism to maintain oxygen homeostasis. Our results indicate that HAX1 deficient neutrophils show increased expression of autophagy related gene beclin-1, accompanied by increased Atg 12-5 complex formation, which is the hallmark of autophagy. Moreover transmission electron microscopical analysis reveals formation of autophagic vacuoles in differentiating neutrophils in the bone marrow. Thus, in agreement with previous studies, a severe mitochondrial dysfunction observed in case of HAX1 deficiency

potentiates a disturbance in cellular homeostasis inducing an autophagic response by the cell.

In conclusion, the present study identifies a novel and key role for the ubiquitously expressed antiapoptotic protein HAX1 in maintenance of neutrophil homeostasis. And our study provides important insights into the role of HAX1 in apoptosis and autophagy.

## 7. Bibliography

1. Gabay, J.E., et al., *Antibiotic proteins of human polymorphonuclear leukocytes*. Proc Natl Acad Sci U S A, 1989. **86**(14): p. 5610-4.
2. Owen, C.A., et al., *Cell surface-bound elastase and cathepsin G on human neutrophils: a novel, non-oxidative mechanism by which neutrophils focus and preserve catalytic activity of serine proteinases*. J Cell Biol, 1995. **131**(3): p. 775-89.
3. Tkalcevic, J., et al., *Impaired immunity and enhanced resistance to endotoxin in the absence of neutrophil elastase and cathepsin G*. Immunity, 2000. **12**(2): p. 201-10.
4. Faurschou, M. and N. Borregaard, *Neutrophil granules and secretory vesicles in inflammation*. Microbes Infect, 2003. **5**(14): p. 1317-27.
5. Reeves, E.P., et al., *Killing activity of neutrophils is mediated through activation of proteases by K<sup>+</sup> flux*. Nature, 2002. **416**(6878): p. 291-7.
6. Fuchs, T.A., et al., *Novel cell death program leads to neutrophil extracellular traps*. J Cell Biol, 2007. **176**(2): p. 231-41.
7. Pham, C.T., *Neutrophil serine proteases: specific regulators of inflammation*. Nat Rev Immunol, 2006. **6**(7): p. 541-50.
8. Kostmann, R., *Infantile genetic agranulocytosis; agranulocytosis infantilis hereditaria*. Acta Paediatr Suppl, 1956. **45**(Suppl 105): p. 1-78.
9. Welte, K., C. Zeidler, and D.C. Dale, *Severe congenital neutropenia*. Semin Hematol, 2006. **43**(3): p. 189-95.
10. Shi, N.Y.a.Y., *MECHANISMS OF APOPTOSIS THROUGH STRUCTURAL BIOLOGY*. 2006.
11. Xia, J. and D.C. Link, *Severe congenital neutropenia and the unfolded protein response*. Curr Opin Hematol, 2008. **15**(1): p. 1-7.
12. Horwitz, M., et al., *Mutations in ELA2, encoding neutrophil elastase, define a 21-day biological clock in cyclic haematopoiesis*. Nat Genet, 1999. **23**(4): p. 433-6.
13. Moulding, D.A., et al., *Unregulated actin polymerization by WASp causes defects of mitosis and cytokinesis in X-linked neutropenia*. J Exp Med, 2007. **204**(9): p. 2213-24.
14. Devriendt, K., et al., *Constitutively activating mutation in WASP causes X-linked severe congenital neutropenia*. Nat Genet, 2001. **27**(3): p. 313-7.
15. Person, R.E., et al., *Mutations in proto-oncogene GFI1 cause human neutropenia and target ELA2*. Nat Genet, 2003. **34**(3): p. 308-12.
16. Bohn, G., et al., *A novel human primary immunodeficiency syndrome caused by deficiency of the endosomal adaptor protein p14*. Nat Med, 2007. **13**(1): p. 38-45.
17. Riedl, S.J. and Y. Shi, *Molecular mechanisms of caspase regulation during apoptosis*. Nat Rev Mol Cell Biol, 2004. **5**(11): p. 897-907.
18. Danial, N.N. and S.J. Korsmeyer, *Cell death: critical control points*. Cell, 2004. **116**(2): p. 205-19.
19. Lockshin, R.A. and C.M. Williams, *Programmed Cell Death--I. Cytology of Degeneration in the Intersegmental Muscles of the Pernyi Silkworm*. J Insect Physiol, 1965. **11**: p. 123-33.

20. Green, D.R. and G.I. Evan, *A matter of life and death*. *Cancer Cell*, 2002. **1**(1): p. 19-30.
21. Adams, J.M. and S. Cory, *The Bcl-2 protein family: arbiters of cell survival*. *Science*, 1998. **281**(5381): p. 1322-6.
22. Carlsson, G., et al., *Kostmann syndrome: severe congenital neutropenia associated with defective expression of Bcl-2, constitutive mitochondrial release of cytochrome c, and excessive apoptosis of myeloid progenitor cells*. *Blood*, 2004. **103**(9): p. 3355-61.
23. Schendel, S.L., M. Montal, and J.C. Reed, *Bcl-2 family proteins as ion-channels*. *Cell Death Differ*, 1998. **5**(5): p. 372-80.
24. Thornberry, N.A. and Y. Lazebnik, *Caspases: enemies within*. *Science*, 1998. **281**(5381): p. 1312-6.
25. Ashkenazi, A. and V.M. Dixit, *Death receptors: signaling and modulation*. *Science*, 1998. **281**(5381): p. 1305-8.
26. Nagata, S., *Fas ligand-induced apoptosis*. *Annu Rev Genet*, 1999. **33**: p. 29-55.
27. Peter, M. and P. Krammer, *The CD95(APO-1/Fas) DISC and beyond*. *Cell Death Differ*, 2003. **10**(1): p. 26-35.
28. Green, D.R. and G. Kroemer, *The pathophysiology of mitochondrial cell death*. *Science*, 2004. **305**(5684): p. 626-9.
29. Kan, O., S.A. Baldwin, and A.D. Whetton, *Apoptosis is regulated by the rate of glucose transport in an interleukin 3 dependent cell line*. *J Exp Med*, 1994. **180**(3): p. 917-23.
30. Stuart, R.A. and P. Rehling, *Mitochondrial biogenesis: is an old dog still teaching us new tricks?. Meeting on the Assembly of the Mitochondrial Respiratory Chain*. *EMBO Rep*, 2008. **9**(1): p. 33-8.
31. Ferri, K.F. and G. Kroemer, *Mitochondria--the suicide organelles*. *Bioessays*, 2001. **23**(2): p. 111-5.
32. Joza, N., et al., *Essential role of the mitochondrial apoptosis-inducing factor in programmed cell death*. *Nature*, 2001. **410**(6828): p. 549-54.
33. Youle, R.J., *Mitochondrial fission in apoptosis*. *Nature Reviews*, 2005.
34. Kroemer, G., L. Galluzzi, and C. Brenner, *Mitochondrial membrane permeabilization in cell death*. *Physiol Rev*, 2007. **87**(1): p. 99-163.
35. Jurgensmeier, J.M., et al., *Bax directly induces release of cytochrome c from isolated mitochondria*. *Proc Natl Acad Sci U S A*, 1998. **95**(9): p. 4997-5002.
36. Luo, X., et al., *Bid, a Bcl2 interacting protein, mediates cytochrome c release from mitochondria in response to activation of cell surface death receptors*. *Cell*, 1998. **94**(4): p. 481-90.
37. Kuwana, T., et al., *Bid, Bax, and lipids cooperate to form supramolecular openings in the outer mitochondrial membrane*. *Cell*, 2002. **111**(3): p. 331-42.
38. Crompton, M., et al., *The mitochondrial permeability transition pore*. *Biochem Soc Symp*, 1999. **66**: p. 167-79.
39. Hajnóczky, G. and J.B. Hoek, *Cell signaling. Mitochondrial longevity pathways*. *Science*, 2007. **315**(5812): p. 607-9.
40. Muñoz-Pinedo, C., et al., *Different mitochondrial intermembrane space proteins are released during apoptosis in a manner that is coordinately initiated but can vary in duration*. *Proc. Natl. Acad. Sci. U.S.A.*, 2006. **103**(31): p. 11573-8.

41. Leist, M. and M. Jaattela, *Four deaths and a funeral: from caspases to alternative mechanisms*. Nat Rev Mol Cell Biol, 2001. **2**(8): p. 589-98.
42. Yedavalli, V.S., et al., *Human immunodeficiency virus type 1 Vpr interacts with antiapoptotic mitochondrial protein HAX-1*. J. Virol., 2005. **79**(21): p. 13735-46.
43. Adams, J.M. and S. Cory, *Life-or-death decisions by the Bcl-2 protein family*. Trends Biochem Sci, 2001. **26**(1): p. 61-6.
44. Walensky, L., *BCL-2 in the crosshairs: tipping the balance of life and death*. Cell Death Differ, 2006. **13**(8): p. 1339-50.
45. Galonek, H.L. and J.M. Hardwick, *Upgrading the BCL-2 network*. Nat Cell Biol, 2006. **8**(12): p. 1317-9.
46. Roy, S.S., et al., *VDAC2 is required for truncated BID-induced mitochondrial apoptosis by recruiting BAK to the mitochondria*. EMBO Rep, 2009. **10**(12): p. 1341-7.
47. Zhou, P., et al., *Mcl-1, a Bcl-2 family member, delays the death of hematopoietic cells under a variety of apoptosis-inducing conditions*. Blood, 1997. **89**(2): p. 630-43.
48. Siegel, R.M., *Caspases at the crossroads of immune-cell life and death*. Nat Rev Immunol, 2006. **6**(4): p. 308-17.
49. Lamkanfi, M., et al., *Caspases in cell survival, proliferation and differentiation*. Cell Death Differ., 2006. **14**(1): p. 44-55.
50. Wang, Y. and X. Gu, *Functional divergence in the caspase gene family and altered functional constraints: statistical analysis and prediction*. Genetics, 2001. **158**(3): p. 1311-20.
51. Kersse, K., et al., *A phylogenetic and functional overview of inflammatory caspases and caspase-1-related CARD-only proteins*. Biochem Soc Trans, 2007. **35**(Pt 6): p. 1508-11.
52. Stennicke, H.R., et al., *Pro-caspase-3 is a major physiologic target of caspase-8*. J Biol Chem, 1998. **273**(42): p. 27084-90.
53. Bao, Q. and Y. Shi, *Apoptosome: a platform for the activation of initiator caspases*. Cell Death Differ., 2006. **14**(1): p. 56-65.
54. Deveraux, Q.L., et al., *IAPs block apoptotic events induced by caspase-8 and cytochrome c by direct inhibition of distinct caspases*. EMBO J, 1998. **17**(8): p. 2215-23.
55. Takahashi, R., et al., *A single BIR domain of XIAP sufficient for inhibiting caspases*. J Biol Chem, 1998. **273**(14): p. 7787-90.
56. Yang, Y.L. and X.M. Li, *The IAP family: endogenous caspase inhibitors with multiple biological activities*. Cell Res, 2000. **10**(3): p. 169-77.
57. Kaufman, R.J., *Stress signaling from the lumen of the endoplasmic reticulum: coordination of gene transcriptional and translational controls*. Genes Dev, 1999. **13**(10): p. 1211-33.
58. Xu, C., B. Bailly-Maitre, and J.C. Reed, *Endoplasmic reticulum stress: cell life and death decisions*. J Clin Invest, 2005. **115**(10): p. 2656-64.
59. Zhang, K. and R.J. Kaufman, *Protein folding in the endoplasmic reticulum and the unfolded protein response*. Handb Exp Pharmacol, 2006(172): p. 69-91.
60. Tirasophon, W., A.A. Welihinda, and R.J. Kaufman, *A stress response pathway from the endoplasmic reticulum to the nucleus requires a novel bifunctional protein*



- kinase/endoribonuclease (Ire1p) in mammalian cells.* Genes Dev, 1998. **12**(12): p. 1812-24.
61. Kersteen, E.A. and R.T. Raines, *Catalysis of protein folding by protein disulfide isomerase and small-molecule mimics.* Antioxid Redox Signal, 2003. **5**(4): p. 413-24.
  62. Walker, K.W., M.M. Lyles, and H.F. Gilbert, *Catalysis of oxidative protein folding by mutants of protein disulfide isomerase with a single active-site cysteine.* Biochemistry, 1996. **35**(6): p. 1972-80.
  63. Mayer, M., et al., *BiP and PDI cooperate in the oxidative folding of antibodies in vitro.* J Biol Chem, 2000. **275**(38): p. 29421-5.
  64. Li, J., et al., *The unfolded protein response regulator GRP78/BiP is required for endoplasmic reticulum integrity and stress-induced autophagy in mammalian cells.* Cell Death Differ, 2008. **15**(9): p. 1460-71.
  65. Zhang, K. and R.J. Kaufman, *The unfolded protein response: a stress signaling pathway critical for health and disease.* Neurology, 2006. **66**(2 Suppl 1): p. S102-9.
  66. Ozcan, U., et al., *Chemical chaperones reduce ER stress and restore glucose homeostasis in a mouse model of type 2 diabetes.* Science, 2006. **313**(5790): p. 1137-40.
  67. Suen, K.C., et al., *Reduction of calcium release from the endoplasmic reticulum could only provide partial neuroprotection against beta-amyloid peptide toxicity.* J Neurochem, 2003. **87**(6): p. 1413-26.
  68. Marciniak, S.J. and D. Ron, *Endoplasmic reticulum stress signaling in disease.* Physiol Rev, 2006. **86**(4): p. 1133-49.
  69. Lin, J.H., P. Walter, and T.S. Yen, *Endoplasmic reticulum stress in disease pathogenesis.* Annu Rev Pathol, 2008. **3**: p. 399-425.
  70. Zinszner, H., et al., *CHOP is implicated in programmed cell death in response to impaired function of the endoplasmic reticulum.* Genes Dev, 1998. **12**(7): p. 982-95.
  71. Dong, D., et al., *Critical role of the stress chaperone GRP78/BiP in tumor proliferation, survival, and tumor angiogenesis in transgene-induced mammary tumor development.* Cancer Res, 2008. **68**(2): p. 498-505.
  72. Wang, X.Z., et al., *Signals from the stressed endoplasmic reticulum induce C/EBP-homologous protein (CHOP/GADD153).* Mol Cell Biol, 1996. **16**(8): p. 4273-80.
  73. Rutkowski, D.T. and R.J. Kaufman, *That which does not kill me makes me stronger: adapting to chronic ER stress.* Trends Biochem Sci, 2007. **32**(10): p. 469-76.
  74. Yoshida, H., [*Molecular biology of the ER stress response*]. Seikagaku, 2004. **76**(7): p. 617-30.
  75. Wu, S., et al., *Ultraviolet light inhibits translation through activation of the unfolded protein response kinase PERK in the lumen of the endoplasmic reticulum.* J Biol Chem, 2002. **277**(20): p. 18077-83.
  76. Yang, Y.P., et al., *Molecular mechanism and regulation of autophagy.* Acta Pharmacol Sin, 2005. **26**(12): p. 1421-34.
  77. Zong, W., et al., *Bax and Bak can localize to the endoplasmic reticulum to initiate apoptosis.* J Cell Biol, 2003. **162**(1): p. 59-69.

78. Krajewski, S., et al., *Investigation of the subcellular distribution of the bcl-2 oncoprotein: residence in the nuclear envelope, endoplasmic reticulum, and outer mitochondrial membranes.* *Cancer Res*, 1993. **53**(19): p. 4701-14.
79. Akao, Y., et al., *Multiple subcellular localization of bcl-2: detection in nuclear outer membrane, endoplasmic reticulum membrane, and mitochondrial membranes.* *Cancer Res*, 1994. **54**(9): p. 2468-71.
80. Ubeda, M., et al., *Stress-induced binding of the transcriptional factor CHOP to a novel DNA control element.* *Mol Cell Biol*, 1996. **16**(4): p. 1479-89.
81. Di Sano, F., et al., *Endoplasmic reticulum stress induces apoptosis by an apoptosome-dependent but caspase 12-independent mechanism.* *J Biol Chem*, 2006. **281**(5): p. 2693-700.
82. Komatsu, M., et al., *Constitutive autophagy: vital role in clearance of unfavorable proteins in neurons.* *Cell Death Differ.*, 2007. **14**(5): p. 887-894.
83. Klionsky, D.J. and S.D. Emr, *Autophagy as a regulated pathway of cellular degradation.* *Science*, 2000. **290**(5497): p. 1717-21.
84. Codogno, P. and A. Meijer, *Autophagy and signaling: their role in cell survival and cell death.* *Cell Death Differ*, 2005. **12 Suppl 2**: p. 1509-18.
85. Gozuacik, D. and A. Kimchi, *Autophagy as a cell death and tumor suppressor mechanism.* *Oncogene*, 2004. **23**(16): p. 2891-906.
86. Shintani, T. and D.J. Klionsky, *Autophagy in health and disease: a double-edged sword.* *Science*, 2004. **306**(5698): p. 990-5.
87. Amano, A., I. Nakagawa, and T. Yoshimori, *Autophagy in innate immunity against intracellular bacteria.* *Journal of Biochemistry*, 2006. **140**(2): p. 161-6.
88. Pattingre, S., et al., *Bcl-2 antiapoptotic proteins inhibit Beclin 1-dependent autophagy.* *Cell*, 2005. **122**(6): p. 927-39.
89. Kim, D.H., et al., *mTOR interacts with raptor to form a nutrient-sensitive complex that signals to the cell growth machinery.* *Cell*, 2002. **110**(2): p. 163-75.
90. Pattingre, S., et al., *Bcl-2 antiapoptotic proteins inhibit Beclin 1-dependent autophagy.* *Cell*, 2005. **122**(6): p. 927-39.
91. Shimizu, S., et al., *Role of Bcl-2 family proteins in a non-apoptotic programmed cell death dependent on autophagy genes.* *Nat Cell Biol*, 2004. **6**(12): p. 1221-8.
92. Takahashi, Y., et al., *Bif-1 interacts with Beclin 1 through UVRAG and regulates autophagy and tumorigenesis.* *Nat. Cell Biol.*, 2007. **9**(10): p. 1142-51.
93. Liang, X.H., et al., *Induction of autophagy and inhibition of tumorigenesis by beclin 1.* *Nature*, 1999. **402**(6762): p. 672-6.
94. Mathew, R., V. Karantza-Wadsworth, and E. White, *Role of autophagy in cancer.* *Nat Rev Cancer*, 2007.
95. Rubinsztein, D.C., et al., *Autophagy and its possible roles in nervous system diseases, damage and repair.* *J Biol Chem*, 2005. **1**(1): p. 11-22.
96. Dunn, W.A., *Studies on the mechanisms of autophagy: formation of the autophagic vacuole.* *J Cell Biol*, 1990. **110**(6): p. 1923-33.
97. Mizushima, N., Y. Ohsumi, and T. Yoshimori, *Autophagosome formation in mammalian cells.* *Cell Struct Funct*, 2002. **27**(6): p. 421-9.
98. Komatsu, M., et al., *Impairment of starvation-induced and constitutive autophagy in Atg7-deficient mice.* *J Cell Biol*, 2005. **169**(3): p. 425-34.
99. Reggiori, F. and D.J. Klionsky, *Autophagy in the eukaryotic cell.* *Eukaryotic Cell*, 2002. **1**(1): p. 11-21.

100. Levine, B. and D.J. Klionsky, *Development by self-digestion: molecular mechanisms and biological functions of autophagy*. Dev Cell, 2004. **6**(4): p. 463-77.
101. Munafó, D.B. and M.I. Colombo, *A novel assay to study autophagy: regulation of autophagosome vacuole size by amino acid deprivation*. Journal of Cell Science, 2001. **114**(Pt 20): p. 3619-29.
102. Zhang, Y., et al., *The Role of Autophagy in Mitochondria Maintenance: Characterization of Mitochondrial Functions in Autophagy-Deficient S. cerevisiae Strains*. J Biol Chem, 2007. **3**(4).
103. Nave, B.T., et al., *Mammalian target of rapamycin is a direct target for protein kinase B: identification of a convergence point for opposing effects of insulin and amino-acid deficiency on protein translation*. Biochem J, 1999. **344 Pt 2**: p. 427-31.
104. Kanazawa, T., et al., *Amino acids and insulin control autophagic proteolysis through different signaling pathways in relation to mTOR in isolated rat hepatocytes*. J. Biol. Chem., 2004. **279**(9): p. 8452-9.
105. Pattingre, S., et al., *Regulation of macroautophagy by mTOR and Beclin 1 complexes*. Biochimie, 2008. **90**(2): p. 313-23.
106. Soulard, A. and M.N. Hall, *SnapShot: mTOR signaling*. Cell, 2007. **129**(2): p. 434.
107. Gohla, A., K. Klement, and B. Nürnberg, *The Heterotrimeric G Protein G(i3) Regulates Hepatic Autophagy Downstream of the Insulin Receptor*. J Biol Chem, 2007. **3**(4).
108. Petiot, A., et al., *Distinct classes of phosphatidylinositol 3'-kinases are involved in signaling pathways that control macroautophagy in HT-29 cells*. J. Biol. Chem., 2000. **275**(2): p. 992-8.
109. Klionsky, D.J., et al., *A unified nomenclature for yeast autophagy-related genes*. Dev Cell, 2003. **5**(4): p. 539-45.
110. Yorimitsu, T. and D.J. Klionsky, *Autophagy: molecular machinery for self-eating*. Cell Death Differ, 2005. **12 Suppl 2**: p. 1542-52.
111. Meijer, A.J. and P. Codogno, *Regulation and role of autophagy in mammalian cells*. Int J Biochem Cell Biol, 2004. **36**(12): p. 2445-62.
112. Mariño, G., et al., *Human autophagins, a family of cysteine proteinases potentially implicated in cell degradation by autophagy*. J. Biol. Chem., 2003. **278**(6): p. 3671-8.
113. Levine, B. and J. Yuan, *Autophagy in cell death: an innocent convict?* J Clin Invest, 2005. **115**(10): p. 2679-88.
114. Yousefi, S., et al., *Calpain-mediated cleavage of Atg5 switches autophagy to apoptosis*. Nat. Cell Biol., 2006. **8**(10): p. 1124-32.
115. George, M.D., et al., *Apg5p functions in the sequestration step in the cytoplasm-to-vacuole targeting and macroautophagy pathways*. Mol. Biol. Cell, 2000. **11**(3): p. 969-82.
116. Wang, C.W., et al., *Apg2 is a novel protein required for the cytoplasm to vacuole targeting, autophagy, and pexophagy pathways*. J. Biol. Chem., 2001. **276**(32): p. 30442-51.
117. Codogno, P. and A.J. Meijer, *Atg5: more than an autophagy factor*. Nat. Cell Biol., 2006. **8**(10): p. 1045-7.
118. Kim, J. and D.J. Klionsky, *Autophagy, cytoplasm-to-vacuole targeting pathway, and pexophagy in yeast and mammalian cells*. Annu Rev Biochem, 2000. **69**: p. 303-42.

119. Klionsky, D.J., *Autophagy: from phenomenology to molecular understanding in less than a decade*. Nat Rev Mol Cell Biol, 2007. **8**(11): p. 931-7.
120. Klionsky, D.J., *The molecular machinery of autophagy: unanswered questions*. Journal of Cell Science, 2005. **118**(Pt 1): p. 7-18.
121. Jia, L., et al., *Inhibition of autophagy abrogates tumour necrosis factor alpha induced apoptosis in human T-lymphoblastic leukaemic cells*. Br J Haematol, 1997. **98**(3): p. 673-85.
122. Mills, K.R., et al., *Tumor necrosis factor-related apoptosis-inducing ligand (TRAIL) is required for induction of autophagy during lumen formation in vitro*. Proc Natl Acad Sci U S A, 2004. **101**(10): p. 3438-43.
123. Thorburn, J., et al., *Selective inactivation of a Fas-associated death domain protein (FADD)-dependent apoptosis and autophagy pathway in immortal epithelial cells*. Mol Biol Cell, 2005. **16**(3): p. 1189-99.
124. Liang, C., et al., *Autophagic and tumour suppressor activity of a novel Beclin1-binding protein UVRAG*. Nat. Cell Biol., 2006. **8**(7): p. 688-99.
125. Suzuki, Y., et al., *HAX-1, a novel intracellular protein, localized on mitochondria, directly associates with HS1, a substrate of Src family tyrosine kinases*. J. Immunol., 1997. **158**(6): p. 2736-44.
126. Han, Y., et al., *Overexpression of HAX-1 protects cardiac myocytes from apoptosis through caspase-9 inhibition*. Circ. Res., 2006. **99**(4): p. 415-23.
127. Shaw, J. and L.A. Kirshenbaum, *HAX-1 represses postmitochondrial caspase-9 activation and cell death during hypoxia-reoxygenation*. Circ. Res., 2006. **99**(4): p. 336-8.
128. Gallagher, A.R., et al., *The polycystic kidney disease protein PKD2 interacts with Hax-1, a protein associated with the actin cytoskeleton*. Proc. Natl. Acad. Sci. U.S.A., 2000. **97**(8): p. 4017-22.
129. Yin, H., et al., *Evidence that HAX-1 is an interleukin-1 alpha N-terminal binding protein*. Cytokine, 2001. **15**(3): p. 122-37.
130. Ortiz, D.F., et al., *Identification of HAX-1 as a protein that binds bile salt export protein and regulates its abundance in the apical membrane of Madin-Darby canine kidney cells*. J. Biol. Chem., 2004. **279**(31): p. 32761-70.
131. Radhika, V., et al., *Galpha13 stimulates cell migration through cortactin-interacting protein Hax-1*. J. Biol. Chem., 2004. **279**(47): p. 49406-13.
132. Cilenti, L., et al., *Regulation of HAX-1 anti-apoptotic protein by Omi/HtrA2 protease during cell death*. J. Biol. Chem., 2004. **279**(48): p. 50295-301.
133. Vafiadaki, E., et al., *Phospholamban interacts with HAX-1, a mitochondrial protein with anti-apoptotic function*. J. Mol. Biol., 2007. **367**(1): p. 65-79.
134. Vafiadaki, E., et al., *The anti-apoptotic protein HAX-1 interacts with SERCA2 and regulates its protein levels to promote cell survival*. Mol. Biol. Cell, 2009. **20**(1): p. 306-18.
135. Kawaguchi, Y., et al., *Interaction of Epstein-Barr virus nuclear antigen leader protein (EBNA-LP) with HS1-associated protein X-1: implication of cytoplasmic function of EBNA-LP*. J. Virol., 2000. **74**(21): p. 10104-11.
136. Dufva, M., M. Olsson, and L. Rymo, *Epstein-Barr virus nuclear antigen 5 interacts with HAX-1, a possible component of the B-cell receptor signalling pathway*. J. Gen. Virol., 2001. **82**(Pt 7): p. 1581-7.

137. Sharp, T.V., et al., *K15 protein of Kaposi's sarcoma-associated herpesvirus is latently expressed and binds to HAX-1, a protein with antiapoptotic function*. J. Virol., 2001. **76**(2): p. 802-16.
138. Al-Maghrebi, M., et al., *The 3' untranslated region of human vimentin mRNA interacts with protein complexes containing eEF-1gamma and HAX-1*. Nucleic Acids Res., 2002. **30**(23): p. 5017-28.
139. Sarnowska, E., et al., *Hairpin structure within the 3'UTR of DNA polymerase beta mRNA acts as a post-transcriptional regulatory element and interacts with Hax-1*. Nucleic Acids Res., 2007. **35**(16): p. 5499-510.
140. Dale, D.C., et al., *Mutations in the gene encoding neutrophil elastase in congenital and cyclic neutropenia*. Blood, 2000. **96**(7): p. 2317-22.
141. Klein, C., H. Bueler, and R.C. Mulligan, *Comparative analysis of genetically modified dendritic cells and tumor cells as therapeutic cancer vaccines*. J Exp Med, 2000. **191**(10): p. 1699-708.
142. Paisan-Ruiz, C., et al., *Homozygosity mapping through whole genome analysis identifies a COL18A1 mutation in an Indian family presenting with an autosomal recessive neurological disorder*. Am J Med Genet B Neuropsychiatr Genet, 2009. **150B**(7): p. 993-7.
143. Kollner, I., et al., *Mutations in neutrophil elastase causing congenital neutropenia lead to cytoplasmic protein accumulation and induction of the unfolded protein response*. Blood, 2006. **108**(2): p. 493-500.
144. Duan, Z. and M. Horwitz, *Gfi-1 oncoproteins in hematopoiesis*. Hematology, 2003. **8**(5): p. 339-44.
145. Hippe, A., et al., *Expression and tissue distribution of mouse Hax1*. Gene, 2006. **379**: p. 116-26.
146. Narita, M., et al., *Bax interacts with the permeability transition pore to induce permeability transition and cytochrome c release in isolated mitochondria*. Proc. Natl. Acad. Sci. U.S.A., 1998. **95**(25): p. 14681-6.
147. Green, D.R., *Apoptotic pathways: ten minutes to dead*. Cell, 2005. **121**(5): p. 671-4.
148. Bouchier-Hayes, L., L. Lartigue, and D.D. Newmeyer, *Mitochondria: pharmacological manipulation of cell death*. J Clin Invest, 2005. **115**(10): p. 2640-7.
149. Liu, B.F., et al., *Consequences of functional expression of the plasma membrane Ca<sup>2+</sup> pump isoform 1a*. J Biol Chem, 1996. **271**(10): p. 5536-44.
150. Verhagen, A.M., et al., *Identification of DIABLO, a mammalian protein that promotes apoptosis by binding to and antagonizing IAP proteins*. Cell, 2000. **102**(1): p. 43-53.
151. Lee, A.Y., et al., *HS 1-associated protein X-1 is cleaved by caspase-3 during apoptosis*. Mol Cells, 2008. **25**(1): p. 86-90.
152. Tajeddine, N., et al., *Hierarchical involvement of Bak, VDAC1 and Bax in cisplatin-induced cell death*. Oncogene, 2008.
153. Takahashi, Y., et al., *Loss of Bif-1 suppresses Bax/Bak conformational change and mitochondrial apoptosis*. Mol. Cell. Biol., 2005. **25**(21): p. 9369-82.
154. Gillick, K. and M. Crompton, *Evaluating cytochrome c diffusion in the intermembrane spaces of mitochondria during cytochrome c release*. J Cell Sci, 2008. **121**(Pt 5): p. 618-26.

155. Letai, A., *Pharmacological manipulation of Bcl-2 family members to control cell death*. J Clin Invest, 2005. **115**(10): p. 2648-55.
156. Hegde, R., et al., *Identification of Omi/HtrA2 as a mitochondrial apoptotic serine protease that disrupts inhibitor of apoptosis protein-caspase interaction*. J. Biol. Chem., 2002. **277**(1): p. 432-8.
157. Lithgow, T., et al., *The protein product of the oncogene bcl-2 is a component of the nuclear envelope, the endoplasmic reticulum, and the outer mitochondrial membrane*. Cell Growth Differ, 1994. **5**(4): p. 411-7.
158. Nguyen, M., et al., *Role of membrane anchor domain of Bcl-2 in suppression of apoptosis caused by E1B-defective adenovirus*. J Biol Chem, 1994. **269**(24): p. 16521-4.
159. Gurlay, C.W. and K.R. Ayscough, *The actin cytoskeleton: a key regulator of apoptosis and ageing?* Nat Rev Mol Cell Biol, 2005. **6**(7): p. 583-9.
160. Giorgio, M., et al., *Electron transfer between cytochrome c and p66Shc generates reactive oxygen species that trigger mitochondrial apoptosis*. Cell, 2005. **122**(2): p. 221-33.
161. Trinei, M., et al., *A p53-p66Shc signalling pathway controls intracellular redox status, levels of oxidation-damaged DNA and oxidative stress-induced apoptosis*. Oncogene, 2002. **21**(24): p. 3872-8.
162. Yu, L., et al., *Autophagic programmed cell death by selective catalase degradation*. Proc. Natl. Acad. Sci. U.S.A., 2006. **103**(13): p. 4952-7.
163. Ferri, K.F. and G. Kroemer, *Organelle-specific initiation of cell death pathways*. Nat Cell Biol, 2001. **3**(11): p. E255-63.
164. Oh, S.Y., et al., *Autophagy-related proteins, LC3 and Beclin-1, in placentas from pregnancies complicated by preeclampsia*. Reprod Sci, 2008. **15**(9): p. 912-20.
165. Cao, Y. and D.J. Klionsky, *Physiological functions of Atg6/Beclin 1: a unique autophagy-related protein*. Cell Res, 2007. **17**(10): p. 839-49.

# Abbreviations

<b>#</b>	number
<b>APC</b>	Allophycocyanin
<b>APS</b>	Ammonium persulphate
<b>BM</b>	Bone marrow
<b>°C</b>	Degree Celsius
<b>CD</b>	Cluster of differentiation
<b>DCs</b>	Dendritic cells
<b><math>\Delta\Psi_m</math></b>	Mitochondrial membrane potential
<b>ddH<sub>2</sub>O</b>	Double distilled water
<b>DTT</b>	Dithiothreitol
<b>EDTA</b>	Ethylene diamine tetrasodium acetate
<b>FACS</b>	Fluorescence activated cell sorting
<b>FCS</b>	Fetal calf serum
<b>FITC</b>	Flourescein iso thiocyanate
<b>Flt3L</b>	Fms like tyrosine kinase 3 Ligand
<b>FSC</b>	Forward scatter
<b>GFP</b>	Green fluorescent protein
<b>RFP</b>	Red fluorescent protein
<b>G-CSF</b>	Granulocyte colony stimulating factor
<b>GM-CSF</b>	Granulocyte macrophage colony stimulating factor
<b>GMFI</b>	Geo mean fluorescence intensity
<b>GMFIi</b>	Geo mean fluorescence intensity index
<b>H<sub>2</sub>O<sub>2</sub></b>	Hydrogen peroxide.
<b>Hr</b>	Hour
<b>HSC</b>	Hematopoietic stem cells
<b>IL</b>	Interleukin
<b>IRES</b>	Internal ribosome entry site
<b>KDa</b>	kilo daltons
<b>Lin</b>	Lineage
<b>MAb</b>	Monoclonal antibody
<b>MHC</b>	Major histo compatibility complex
<b>Min</b>	Minute
<b>MOI</b>	Multiplicity of infection
<b>MOMP</b>	Mitochondrial outer membrane potential
<b>MQ H<sub>2</sub>O</b>	milli Q water
<b>NaCl</b>	Sodium chloride
<b>NH<sub>4</sub>Cl</b>	Ammonium Chloride
<b>PB</b>	Peripheral blood
<b>PBS</b>	Phosphate buffered Saline
<b>PE</b>	Phycoerythrin
<b>Per CP</b>	Peridinium chlorophyll protein
<b>RT-PCR</b>	Reverse Transcriptase Polymerase chain reaction
<b>RT</b>	Room temperature

<b>RBC</b>	Red blood cells
<b>ROS</b>	Reactive oxygen/oxidant species
<b>SSC</b>	Sideward scatter
<b>SCF</b>	Stem cell factor
<b>SCN</b>	Severe Congenital Neutropenia
<b>SDS</b>	Sodium do-decylsulphate
<b>TEMED</b>	N,N,N'N'-Tetramethylenediamine
<b>TGF</b>	Transforming growth factor
<b>TNF</b>	Tumor necrosis factor
<b>TPO</b>	Thrombopoietin
<b>Tris</b>	Tris-(hydroxymethyl)-aminomethane
<b>VSVG</b>	Vesicular Stomatitis Virus Glycoprotein
<b>PMSF</b>	Phenyl methyl sulphonyl fluoride



# Acknowledgements

I am grateful to **Prof. Dr. Christoph Klein** for giving me the opportunity to pursue my PhD in his laboratory. I also take this opportunity to thank him for his guidance, encouragement and support through out my stay in the lab.

I am thankful to **Prof. Dr. Karl Welte** for his support with lab space and his encouragement.

I would like to express my gratitude to **Dr. Chozhavendan Rathinam** for his valuable guidance and support.

I would like to thank **Dr. med Axel Schambach** for providing me with pSUPER and lentiviral plasmid pRRL.PPT.SF.DsRedEx.Pre SnaB1. I would also like to thank the **registry for neutropenia**, Kinderklinik, Hannover Medical School for their support with valuable resources and patient information. I would like to thank **Dr. Gudrun Brandes** for her valuable suggestions and help with electron microscopy studies.

I also thank my **family** for their love, courage and support, in my utmost difficult times.

I would like to thank my dearest friend and colleague **Miss. Anchana Rathinasamy** and **Dr. med. Daniel Kotlarz** for their valuable help, discussions and constant support. I also take this opportunity to thank **Dr. Cornelia Zeidler** for providing me a regular update on the SCN patients. I am thankful to the members of **Christoph Klein laboratory** and **Tummlers laboratory** for their kind help and making my tenure cherishable.

# Curriculum Vitae

**Name:** Giridharan Appaswamy  
**Address:** Raum 217, Karl-Wiechert-Allee 15  
Hannover 30625  
**Geburtsort:** Nagercoil, Tamil Nadu, India.  
**Geburtsdatum:** 07.10.1980 (dd.mm.yyyy)  
**Familienstand:** ledig

## Schulbildung

1985-1997 C.S.I. Matriculation Higher Secondary School, India  
1997-1998 Good Sheperd Matriculation Higher Secondary School, India

## Studium

1998-2001 **(B.Sc.)** Bachelors in Science-Zoology (spl. Biotechnology)  
The American College, Madurai, Tamil Nadu, India  
2001-2003 **(M.Sc.)** Masters in Science-Biotechnology,  
Manonmaniam Sundarnar University, Tirunelveli.  
Tamil Nadu, India

## Dissertation (M.Sc.)

Phytochemical and Molecular Marker Analysis in *Centella asiatica*.  
Comparison of Field Raised and *In Vitro* Raised Tissues.

## Berufstätigkeit:

Dec 2002-May 2003: Project student at the Centre For Biotechnology, **SPIC Science Foundation**, Chennai, India  
Jul 2003-Oct 2003: Project Assistant at **Mitocon Biotech, SPIC Science Foundation**, Centre For Biotechnology, Chennai, India  
Nov 2003-Apr 2005: **(JRF)** Junior Research Fellow at **Centre for Human Genetics**, ITPL, Bangalore, India  
May 2005-Jul 2005: **(SRF)** Senior Research Fellow at **Avestha Gengraine technologies** Private limited, ITPL, Bangalore, India  
Jul 2005-till date: PhD student in **Christoph Klein laboratory**, at the Department of Pediatric Hematology and Oncology, **MHH**, Hannover, Germany

# **Publications**

# HAX1 deficiency causes autosomal recessive severe congenital neutropenia (Kostmann disease)

Christoph Klein<sup>1</sup>, Magda Grudzien<sup>2</sup>, Giridharan Appaswamy<sup>1</sup>, Manuela Germeshausen<sup>1</sup>, Inga Sandrock<sup>1</sup>, Alejandro A Schäffer<sup>3</sup>, Chozhavendan Rathinam<sup>1</sup>, Kaan Boztug<sup>1</sup>, Beate Schwitzer<sup>1</sup>, Nima Rezaei<sup>4</sup>, Georg Bohn<sup>1</sup>, Malin Melin<sup>5</sup>, Göran Carlsson<sup>6</sup>, Bengt Fadeel<sup>7</sup>, Niklas Dahl<sup>5</sup>, Jan Palmblad<sup>8</sup>, Jan-Inge Henter<sup>6</sup>, Cornelia Zeidler<sup>1</sup>, Bodo Grimbacher<sup>2,9,10</sup> & Karl Welte<sup>1,10</sup>

**Autosomal recessive severe congenital neutropenia (SCN)<sup>1</sup> constitutes a primary immunodeficiency syndrome associated with increased apoptosis in myeloid cells<sup>2,3</sup>, yet the underlying genetic defect remains unknown. Using a positional cloning approach and candidate gene evaluation, we identified a recurrent homozygous germline mutation in *HAX1* in three pedigrees. After further molecular screening of individuals with SCN, we identified 19 additional affected individuals with homozygous *HAX1* mutations, including three belonging to the original pedigree described by Kostmann<sup>1</sup>. *HAX1* encodes the mitochondrial protein HAX1, which has been assigned functions in signal transduction<sup>4</sup> and cytoskeletal control<sup>5,6</sup>. Here, we show that *HAX1* is critical for maintaining the inner mitochondrial membrane potential and protecting against apoptosis in myeloid cells. Our findings suggest that *HAX1* is a major regulator of genetic control of apoptosis in neutrophil development.**

Individuals with autosomal recessive SCN show a paucity of mature neutrophils in peripheral blood and bone marrow and develop life-threatening bacterial infections<sup>7</sup>. SCN constitutes a heterogeneous group of diseases: about 60% of affected individuals of European and Middle Eastern ancestry have dominant heterozygous mutations in the gene encoding neutrophil elastase (*ELA2*)<sup>7,8</sup>. However, the genes mutated in the 'classical' form of SCN, characterized by autosomal recessive mode of inheritance, have remained unknown since the publication of Kostmann's seminal paper<sup>1</sup> 50 years ago. To define the molecular etiology of autosomal recessive SCN, we initiated a genome-wide linkage scan in three unrelated Kurdish families (Fig. 1).

All four affected individuals in the index families suffered from recurrent infections due to neutropenia characterized by a maturation arrest at the promyelocyte or myelocyte stage in their bone marrow (Fig. 2a). A synopsis of the clinical features is given in Table 1, and further immunological data are presented in Supplementary Table 1 online.

Qualitative analysis of the genome scan genotypes showed that D1S2635 (located 156.0 Mb from 1pter in build 35 of the human genome) was the only genome scan marker at which all four affected individuals were homozygous and at which the unaffected siblings had a different genotype. After all available individuals were genotyped at D1S2635, the LOD score for that marker was +3.17 at a recombination fraction ( $\theta$ ) of 0. However, this marker was imperfect, because the affected individual in SCN-III was homozygous for an allele different from the disease-associated allele in the other two families.

Fine mapping on chromosome 1 identified six other markers that had perfect segregation within families and were informative enough to give a single-marker LOD score above +2.0 (summed over SCN-I to SCN-III): D1S514 (120.0 Mb, score +2.62), D1S2696 (120.2 Mb, +2.39), D1S3466 (147.0 Mb, +2.78), D1S2624 (153.4 Mb, +3.06), D1S1653 (154.7 Mb, +3.08), and D1S2707 (156.9 Mb, +2.75). Two-marker analysis using D1S3466 and D1S2624 gave a peak LOD score of +3.95 with a nearly flat LOD score curve. Adding a third marker, D1S1653, boosted the peak LOD score to +4.15. For the purpose of identifying positional candidate genes, we defined the minimal critical linkage interval as the interval in which consanguineous families SCN-I and SCN-III have their maximum positive scores at  $\theta = 0$ , and the three affected individuals therein are homozygous for the same allele. To obtain a maximal interval, we extended by one marker on each side. The minimal interval is from D1S442 (143.1 Mb) through D1S2624 (153.4 Mb), and the maximal

<sup>1</sup>Department of Pediatric Hematology/Oncology, Hannover Medical School, Carl Neuberg Strasse 1, 30625 Hannover, Germany. <sup>2</sup>Division of Rheumatology and Clinical Immunology, Medical Center, Freiburg University Hospital, Hugstetterstr. 55, 79106 Freiburg, Germany. <sup>3</sup>Computational Biology Branch, National Center for Biotechnology Information, National Institutes of Health, Department of Health and Human Services, Bethesda, Maryland 20894, USA. <sup>4</sup>Immunology, Asthma and Allergy Research Institute, Tehran University of Medical Sciences, Tehran, Iran. <sup>5</sup>Department of Genetics and Pathology, University Children's Hospital, 75185 Uppsala, Sweden. <sup>6</sup>Childhood Cancer Research Unit, Department of Woman and Child Health, Karolinska Institutet, Karolinska University Hospital Solna, 17176 Stockholm, Sweden. <sup>7</sup>Division of Biochemical Toxicology, Institute of Environmental Medicine, Karolinska Institutet, 17177 Stockholm, Sweden. <sup>8</sup>Department of Medicine, Karolinska Institutet, Karolinska University Hospital Huddinge, 14186 Stockholm, Sweden. <sup>9</sup>Present address: Department of Immunology and Molecular Pathology, Royal Free Hospital & University College Medical School, NW3 2QG London, UK. <sup>10</sup>These authors contributed equally to this work. Correspondence should be addressed to C.K. (klein.christoph@mh-hannover.de).

Received 3 August; accepted 13 November; published online 24 December 2006; doi:10.1038/ng1940

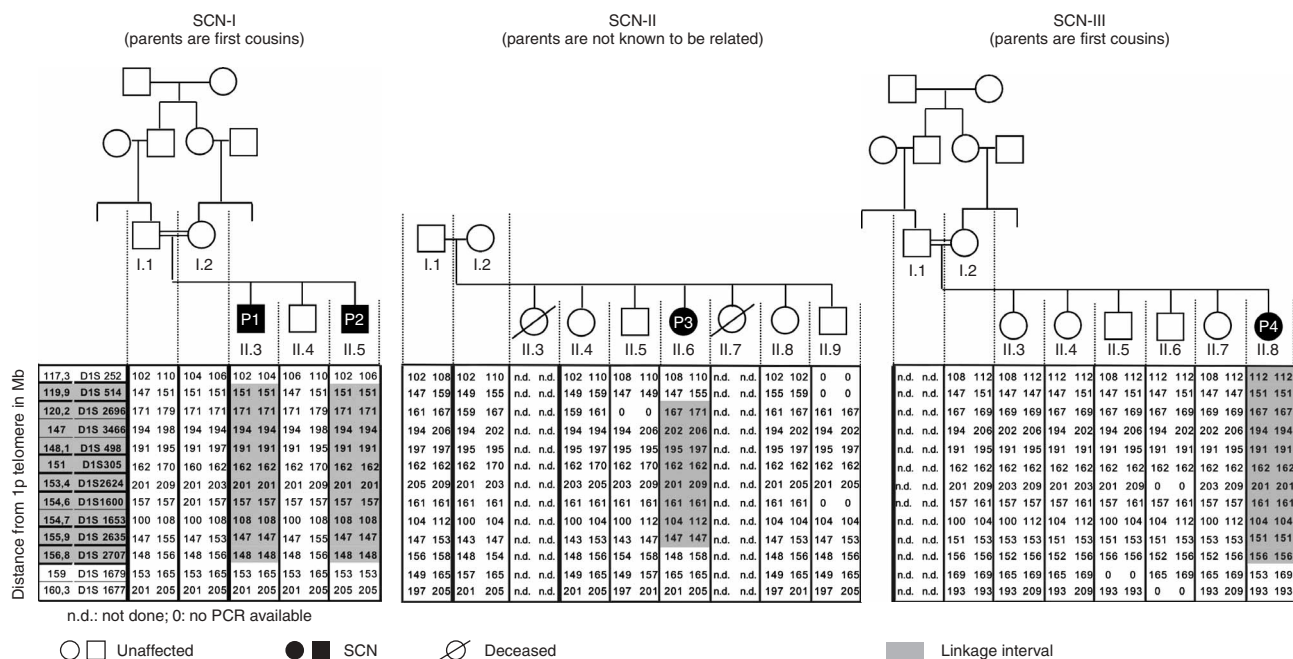


**Figure 1** Haplotypes on chromosome 1q. Pedigrees of three unrelated families with severe congenital neutropenia and allele distribution in affected individuals (filled symbols) and healthy family members (open symbols). P1–P4 refer to numbers of individuals in **Table 1**. The homozygous part of the linkage interval within each family is shown in gray. We considered the minimal linkage interval for the study to be the intersection of the intervals for SCN-I and SCN-III, and we concentrated on the subintervals where the affected individuals shared the same allele. We did not use SCN-II to further restrict the overall linkage interval because the lack of documented consanguinity in SCN-II suggested that the affected individual might have two distinct heterozygous mutations.

interval is D1S2696 (120.2 Mb) through D1S1600 (154.6 Mb). In build 35 of the human genome, there are 234 genes or predicted genes in the minimal interval and an additional 41 genes in the maximal interval.

We identified several functional candidate genes among these 275 genes in the maximal interval. Sequencing of genomic DNA from affected individuals showed some wild-type sequences, including *MAP3IP1* (also known as *HSPC003*), *RAB25* and *IL6R*. We considered *HAX1*, localized at 151.1 Mb from 1pter, as a candidate gene for SCN because *HAX1* participates in B cell receptor-mediated signal transduction<sup>4</sup>, it has the potential to regulate the actin cytoskeleton<sup>5,6</sup> and it is proposed to control apoptosis<sup>9,10</sup>. Increased apoptosis in myeloid progenitor cells has been proposed as a potential mechanism accounting for neutropenia in individuals with SCN<sup>2</sup>. Although intrinsic B cell abnormalities have not previously been reported, defective directed migration and aberrant rearrangement of the cyto-

skeleton of SCN neutrophils have been described<sup>11</sup>. We sequenced *HAX1* (for detailed conditions, see **Supplementary Table 2** online) and identified a homozygous single-nucleotide insertion (position 130-131insA) leading to a premature stop codon (W44X) in all affected individuals (**Fig. 2b**); their healthy siblings and parents had at least one allele with the wild-type sequence. As a consequence, *HAX1* was absent in the cells from affected individuals, as shown by protein blot analysis (**Fig. 2c**). Heterozygous carriers of W44X had no detectable phenotype.

To assess the frequency of *HAX1* mutations within a cohort of sporadic and familial individuals with SCN, we sequenced the gene in 63 additional individuals with SCN associated with a documented myeloid maturation arrest, including 21 individuals with mutations in the gene encoding neutrophil elastase (*ELA2*). Fifteen affected individuals had the same 1-bp insertion as the index families, and one individual had a homozygous single-base pair substitution (256C→T) causing the nonsense change R86X. Three affected individuals from

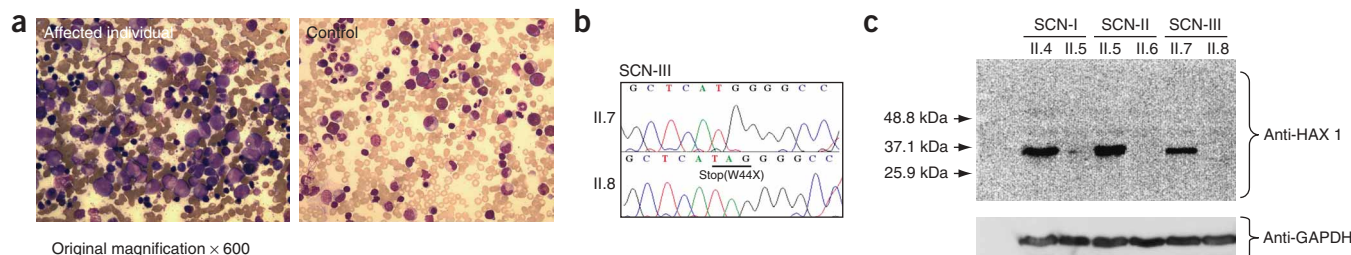


**Figure 2** Bone marrow phenotype, *HAX1* genotype and *HAX1* expression. **(a)** Representative bone marrow phenotype of an individual with SCN (P2) and a healthy individual. Note the characteristic absence of mature neutrophils in the individual with SCN. **(b)** Sequencing of *HAX1* shows a single-nucleotide insertion (A) in exon 2. **(c)** Detection of *HAX1* in EBV B cell lines by protein blot analysis (SCNII-II.5 is individual P2, SCNII-II.6 is individual P3 and SCNIII-II.8 is individual P4).

**Table 1 Clinical and molecular findings**

Individual	Sex	Parental origin	ANC <sup>a</sup>	Bacterial infections	Associated findings	<i>HAX1</i>	<i>ELA2</i>	<i>CSFR3</i>	Therapy <sup>b</sup>	Outcome <sup>c</sup>
1 ('P1')	M	Turkey (K) <sup>d</sup>	224–400	Omphalitis, pneumonia lymphadenitis, sinusitis	β-thalassemia minor, splenomegaly	W44X (G) <sup>e</sup>	WT	WT	G-CSF	Alive, age 11 yrs
2 ('P2')	M	Turkey (K)	192–244	Oral ulcers, otitis, pneumonia, bacteremia	Splenomegaly	W44X (G)	WT	WT	G-CSF	Alive, age 5 yrs
3 ('P3')	F	Turkey (K)	0–410	Pneumonia, skin abscess, stomatitis, tonsillitis	Growth hormone deficiency, splenomegaly	W44X (G)	WT	WT	G-CSF, growth hormone	Alive, age 15 yrs
4 ('P4')	F	Turkey (K)	84–116	Pneumonia, otitis, skin abscess	Tricuspid insufficiency, splenomegaly	W44X (G)	WT	WT	G-CSF	Alive, age 6 yrs
5	M	Turkey (K)	0–464	Lymphadenitis, skin abscess, septicemia, mastoiditis, otitis		W44X (G)	WT	2405C→T (8 yrs after G-CSF)	G-CSF	Alive, age 8 yrs
6	F	Turkey (K)	200	Skin abscess, bronchitis		W44X (G)	WT	WT	G-CSF	Alive, age 6 yrs
7	F	Turkey	535–1,188	Pneumonia, skin abscess, bronchitis	Splenomegaly	W44X	WT	WT	G-CSF	Alive
8	M	Turkey	0–63	Pneumonia, pharyngitis	Splenomegaly, myelodysplasia, extramedullary hematopoiesis	W44X	WT	2423C→T (11 months after G-CSF) <sup>f</sup>	G-CSF, allo-BMT	Alive, age 9 yrs
9	M	Turkey	61	Septicemia, skin abscess		W44X (G)	WT	WT	G-CSF	Alive, age 2 yrs
10	M	Turkey (K)	242	None		W44X (G)	WT	WT	G-CSF	Alive, age 1 yr
11	F	Turkey (K)	0–1,050	Unclassified		W44X (G)	WT	WT	G-CSF	Alive, age 1 yr
12	F	Iran	248	Skin abscess, pneumonia, oral ulcers		W44X	WT	WT	G-CSF	Alive, age 6 yrs
13	M	Iran	608	Omphalitis, skin abscess, oral ulcers, urinary tract infections, pneumonia, otitis		W44X	WT	WT	G-CSF	Alive, age 5 yrs
14	F	Iran	270	Skin abscess, otitis media, pneumonia, oral ulcers	Failure to thrive	R86X	WT	WT	G-CSF	Alive, age 7 yrs
15	M	Turkey	268	Unclassified	Splenomegaly, lymphadenopathy	W44X	WT	WT	G-CSF	Alive, age 14 yrs
16	F	Turkey	200	Gingivitis, pneumonia, otitis		W44X	WT	WT	G-CSF	Alive, age 6 yrs
17	F	Lebanon	0–270	Otitis, enteritis, bronchitis	Splenomegaly	W44X (G)	WT	WT	G-CSF	Alive, age 2 yrs
18	F	Turkey	100–500	Omphalitis, bronchitis		W44X	WT	WT	G-CSF	Alive, age 1 yr
19	M	Lebanon	40–250	Pneumonia, skin abscess, septicemia	46,XY,t(5;9)(q12;p22) in myeloid cells	W44X	WT	2423C→T 2399C→T (13 yrs after G-CSF)	G-CSF	Alive, age 27 yrs
20	F	Turkey	ND	Otitis	Muscular hypotonia	W44X	WT	WT	G-CSF	Alive, age 11 yrs
21	F	Sweden <sup>g</sup>	0–400	Skin abscess, pneumonia, gingivitis, septicemia		Q190X (G)	WT	WT		Died at age 12 yrs
22	F	Sweden <sup>g</sup>	0–270	Otitis, skin abscess, gingivitis, septicemia		Q190X (G)	WT	WT	G-CSF	Alive, age 23 yrs
23	M	Sweden <sup>g</sup>	0–600	Skin abscess, paronychia		Q190X (G)	WT	WT	G-CSF, allo-BMT	Alive, age 22 yrs

Individuals 1,2 (from family SCN-1), 9,10 (siblings) and 21–23 (from the Kostmann family) are the only individuals with an affected relative that we know of. The designations P1, P2, P3 and P4 are used in **Figures 1–4**. BMT, bone marrow transplantation. ND, not done.

<sup>a</sup>ANC: absolute neutrophil count before G-CSF therapy. <sup>b</sup>G-CSF induced increased neutrophil counts in all individuals (required dose, <10 μg/kg body weight). <sup>c</sup>Refers to age in July 2006. <sup>d</sup>(K) = Kurdish origin. <sup>e</sup>(G) = germline transmission proven by parental heterozygosity. <sup>f</sup>Time after initiation of G-CSF therapy. <sup>g</sup>Individuals from the original Kostmann family (individuals 21, 22 and 23 in our study correspond to patients 1, 4 and 5, respectively, in ref. 13).

the original Kostmann family<sup>12</sup> had the homozygous germline mutation 568C→T (Q190X) (**Supplementary Fig. 1** online), providing definitive proof that Kostmann disease is caused by *HAX1* deficiency. None of the individuals with SCN in our cohort was heterozygous for *HAX1* mutations. However, further studies are needed to determine the prevalence of *HAX1* mutations in affected individuals, as our access to SCN samples may have been biased. We screened 200 healthy central European individuals for the presence of the 130-131insA allele

and found none. In a healthy Swedish control population ( $n = 125$ ), we determined the allele frequency of the 568C→T mutation to be 1 out of 250 chromosomes. We also sequenced *ELA2*, previously associated with cyclic<sup>13</sup> and congenital<sup>8</sup> neutropenia, in all affected individuals with *HAX1* mutations. Notably, we did not find any affected individuals with mutations in both *ELA2* and *HAX1* (**Table 1**), suggesting that these genes define two mutually exclusive groups of individuals with SCN.





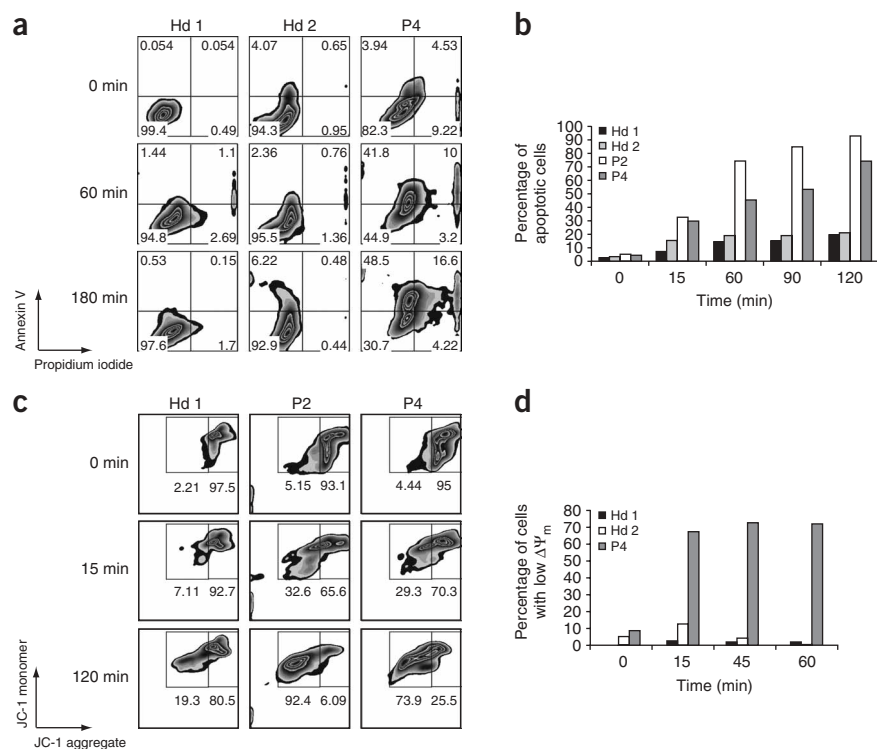


**Figure 3** Apoptosis and mitochondrial membrane potential in HAX1-deficient granulocytes. **(a)** FACS plots showing apoptosis of purified neutrophils upon exposure to TNF $\alpha$ . As an additional control, healthy donor 1 (HD1) received G-CSF. **(b)** Rate of apoptosis after treatment of purified neutrophils with H<sub>2</sub>O<sub>2</sub>. Cells were analyzed by FACS, and the percentage of annexin V-positive, propidium iodide-negative cells was plotted. **(c)** FACS plots showing loss of mitochondrial membrane potential ( $\Delta\Psi_m$ ) upon exposure of purified neutrophils to valinomycin. **(d)** Graphical representation showing progressive loss of  $\Delta\Psi_m$  in HAX1-deficient neutrophils upon treatment with valinomycin. All experiments were performed on at least two independent occasions. Similar results were seen in cells from P1 and P3.

SCN is a premalignant condition, as up to 21% of affected individuals develop a clonal proliferative disease leading to myelodysplastic syndrome or overt acute leukemia<sup>14,15</sup>, often preceded by mutations in the gene encoding the granulocyte colony stimulating factor (G-CSF) receptor (*CSF3R*)<sup>16</sup>. To determine whether *HAX1* mutations predispose to somatic *CSF3R* mutations, we sequenced *CSF3R* in all affected individuals with documented *HAX1* mutations and reanalyzed the data of the SCN registry<sup>7</sup>. In three HAX1-deficient individuals, we identified somatic mutations in *CSF3R* (Table 1). In one of the affected individuals, the onset of a myelodysplastic syndrome led to allogeneic bone marrow transplantation. At this time, it is not clear to what extent the malignant transformation is dependent on the underlying *HAX1* mutation, prolonged exposure to G-CSF or a combination of both factors. Further follow-up studies will be required to estimate the risk posed by HAX1 deficiency with regard to the development of somatic *CSF3R* mutations and myelodysplasia or leukemia.

Mitochondria have been recognized as key regulators of apoptosis in many cell types, including neutrophils<sup>17–19</sup>. Permeabilization of mitochondrial membranes is often a rate-limiting process in apoptotic cell death. Mitochondrial inner membrane permeabilization, manifested as a dissipation of  $\Delta\Psi_m$ , compromises the vital function of mitochondria and leads to cell death. After this trigger, the outer membrane of mitochondria is permeabilized, leading to release of proteins such as cytochrome c, Smac (also known as DIABLO) and

HtrA2 (also known as Omi) from the intermembrane space into the cytosol. Cytochrome c is critical for the formation of the apoptosome, whereas Smac and Omi are negative regulators of inhibitor of apoptosis proteins (IAP) by competing with caspases for IAP binding<sup>20</sup>. The core mitochondrial apoptotic pathway is both executed and regulated by members of the B cell leukemia/lymphoma 2 (BCL2) protein family, which has both antiapoptotic and proapoptotic members and controls cell viability via mitochondrial outer membrane permeabilization<sup>21,22</sup>.

In parallel to other pro-survival members of the BCL2 family, such as Mcl-1 and A1 (also known as Bfl-1), HAX1 contains two domains reminiscent of a BH1 and BH2 domain<sup>4</sup> and thus may be involved in controlling apoptosis at the level of the mitochondria. Of note, mice with a targeted deletion of A1-a manifest accelerated neutrophil apoptosis<sup>23</sup>. To directly assess the role of HAX1 in apoptosis, we analyzed the rate of apoptosis in primary neutrophils of HAX1-deficient individuals. We incubated purified neutrophils from affected individuals and healthy donors in the presence of tumor necrosis factor  $\alpha$  (TNF $\alpha$ ) and analyzed them by FACS for the uptake of propidium iodide and staining with annexin-V. As expected, neutrophils from HAX1-deficient individuals showed a higher amount of both spontaneous and TNF $\alpha$ -induced apoptosis compared with control neutrophils (Fig. 3a and Supplementary Fig. 2 online). We saw similar results

when we induced apoptosis by H<sub>2</sub>O<sub>2</sub> (Fig. 3b) or staurosporine (data not shown). Enhanced neutrophil apoptosis in HAX1-deficient cells was associated with increased cleavage of caspase 3/7 (Supplementary Fig. 2). In summary, these findings may explain why treatment with G-CSF, a cytokine with known antiapoptotic functions<sup>24</sup>, alleviates the neutropenia phenotype in individuals with SCN.

In view of its preferential mitochondrial localization<sup>4</sup>, we reasoned that HAX1 might be involved in stabilizing the mitochondrial membrane potential ( $\Delta\Psi_m$ ) in neutrophils. To visualize  $\Delta\Psi_m$ , we stained neutrophils from affected individuals and healthy controls with the dual-emission indicator dye 5,5',6,6'-tetrachloro-1,1',3,3'-tetraethylbenzimidazol-carbocyanine iodide (JC-1), which accumulates in mitochondria and forms J-aggregates emitting an orange fluorescence. Upon loss of the mitochondrial membrane potential (for instance, on exposure to the specific K<sup>+</sup> ionophor valinomycin), JC-1 adopts a monomeric conformation and emits green fluorescence. Neutrophils isolated from HAX1-deficient individuals showed a rapid dissipation of  $\Delta\Psi_m$ , whereas the inner mitochondrial membrane potential in neutrophils from healthy individuals was maintained (Fig. 3c,d). Similar results were seen in myeloid cells that differentiated *in vitro* (data not shown). These findings are in line with our observation of increased apoptosis in HAX1-deficient neutrophils as well as with the increased release of cytochrome c from these organelles in myeloid progenitor cells<sup>2</sup> and suggest that HAX1 is involved in stabilizing the mitochondrial membrane potential.

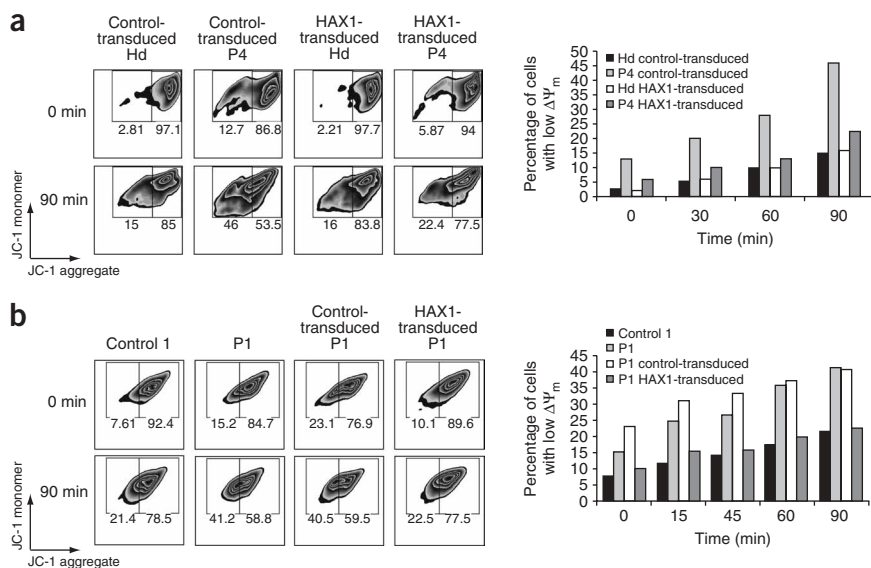


**Figure 4** Reconstitution of  $\Delta\Psi_m$  in myeloid progenitor cells and fibroblasts after retroviral *HAX1* gene transfer. **(a)** Left: representative FACS plots indicating loss of valinomycin-induced  $\Delta\Psi_m$  in myeloid cells that differentiated *in vitro* and reversion of  $\Delta\Psi_m$  upon retroviral *HAX1* gene transfer. Right: graphical representation of  $\Delta\Psi_m$  reconstitution showing all measured time points. **(b)** Left: representative FACS plots indicating loss of valinomycin-induced  $\Delta\Psi_m$  in fibroblasts (P1) and reversion of  $\Delta\Psi_m$  upon retroviral *HAX1* gene transfer. Right: graphical representation of  $\Delta\Psi_m$  reconstitution in fibroblasts upon retroviral *HAX1* gene transfer, showing all measured time points. We observed similar results in two independent experiments.

As *HAX1* is a ubiquitously expressed gene<sup>4</sup>, we were interested to see whether *HAX1* deficiency would be associated with altered membrane potential in non-hematopoietic cells. Compared with fibroblasts from healthy donors, *HAX1*-deficient fibroblasts showed a more rapid loss of their membrane potential when exposed to valinomycin (Supplementary Fig. 3 online), suggesting that the function of *HAX1* in stabilization of the mitochondrial membrane potential may not be limited to neutrophils. Nevertheless, it is mysterious why a seemingly null mutation of a ubiquitously expressed gene causes a myeloid-specific phenotype in individuals with SCN. Perhaps this effect is due to intrinsic differences in the molecular control of apoptosis in neutrophils compared with other cell types. Alternatively, in view of an extremely high cellular turnover rate, neutrophil counts may be particularly sensitive to even slight alterations in the balance of apoptosis.

To unequivocally prove that *HAX1* mutations cause SCN by lowering the threshold for apoptosis upon mitochondrial membrane dissipation, we reconstituted the cellular phenotype of individuals with SCN by retroviral gene transfer. We purified CD34<sup>+</sup> cells from affected individuals and healthy controls, transduced them with bicistronic retroviral vectors encoding *HAX1* and a reporter gene (mouse CD24), cultured them *in vitro* until they differentiated into myeloid progenitor cells and analyzed them for maintenance of  $\Delta\Psi_m$  upon exposure to valinomycin. As expected, cells transduced with the marker gene showed an accelerated loss of  $\Delta\Psi_m$  (Fig. 4a). In contrast, affected individuals' myeloid progenitor cells transduced with *HAX1*-expressing virus showed a significantly delayed loss of  $\Delta\Psi_m$ , similar to wild-type cells that were transduced with a control vector or transduced with *HAX1*-expressing constructs (Fig. 4a). Similarly, maintenance of  $\Delta\Psi_m$  was corrected in *HAX1*-deficient fibroblasts after retroviral gene transfer (Fig. 4b).

Our data indicate that *HAX1* deficiency causes the phenotype of accelerated loss of  $\Delta\Psi_m$  in myeloid cells of individuals with homozygous *HAX1* mutations. Further support for an antiapoptotic function of *HAX1* comes from studies analyzing viral proteins. *HAX1* interacts with a number of viral proteins, such as the K15 protein of Kaposi's sarcoma-associated herpesvirus<sup>9</sup>, Epstein-Barr virus (EBV) nuclear antigen<sup>25</sup>, EBV nuclear antigen leader protein (EBNA-LP)<sup>26</sup>, and human immunodeficiency virus viral protein R1 (Vpr1) (ref. 27), suggesting that viruses may have developed mechanisms to induce or evade apoptosis via *HAX1*.

In conclusion, we have shown for the first time the genetic etiology of autosomal recessive SCN and identified a role for the antiapoptotic molecule *HAX1* in myeloid cell homeostasis. Thus, our findings point to a mechanism involving mitochondrial control of apoptosis as a regulator of myeloid cell homeostasis in humans. Future genetic studies in individuals with SCN may identify mutations in additional genes controlling the survival of neutrophils. Mutations in *HAX1* should be sought in all individuals with autosomal recessive SCN. We expect that, in the future, *HAX1* mutation status will be

used as a variable in large-scale clinical studies as a possible predictor for clinical manifestation, response to treatment, leukemia susceptibility and outcome in individuals with SCN. Our findings may also open up new horizons for clinical and basic research in other premalignant conditions.

## METHODS

**Participants.** Blood, skin, and bone marrow samples were taken upon informed parental consent or participants' consent, according to the guidelines of the local institutional review boards at Hannover Medical School, University of Freiburg and Umeå University Sweden. Participants were referred by pediatric hematologists or identified in our clinic. Central European control samples comprised individuals originating from Germany and Turkey.

**Genotyping.** A total of 217 markers were genotyped on eight individuals (four affected individuals and four unaffected siblings, including at least one from each family). In the only region selected for fine mapping, an additional 15 markers were genotyped on all available individuals, but one marker was dropped owing to inconsistency, and five other markers were uninformative in at least one family. Reagents for genotyping were purchased from Invitrogen Research Genetics, biomers.net and Qiagen. PCR was performed according to published protocols. PCR products were sequenced on an ABI377 sequencer (PE Applied Biosystems), using the COLLECTION and ANALYSIS software. Allele sizes were determined using the GENOTYPER (PE Applied Biosystems) software.

**Genetic linkage analysis.** All genotype data were evaluated qualitatively looking for perfect segregation of a marker with the disease and homozygosity in the affected individuals in families SCN-I and SCN-III. The fine-mapping data on chromosome 1 were also evaluated quantitatively by computing LOD scores. These were computed using FASTLINK version 4.1P (refs. 28,29) assuming 0.001 as disease allele frequency and full penetrance. We used equal marker allele frequencies owing to the small sample size. As this study involved multiple families, and the LOD score computations treated each family



separately, there were at least two aspects in which qualitative analysis provided additional information. First, we preferred markers where affected individuals in different families were homozygous for the same allele rather than markers where they were homozygous for different alleles. Second, we preferred markers where the affected individual in SCN-II was homozygous, even though SCN-II does not have known consanguinity. These preferences arose because we suspected that affected individuals in all three families would have the same mutation in the same gene. However, we defined our linkage intervals based only on SCN-I and SCN-III, and we considered the possibility that the affected individual in the non-consanguineous SCN-II family might be a compound heterozygote.

**Protein blots.** Cell extracts of EBV-immortalized B cell lines were separated by SDS-PAGE, blotted and stained with a monoclonal antibody to HAX1 (BD Biosciences) or antibodies to GAPDH (Santa Cruz). After staining with HRP-conjugated goat antibody to mouse (BD Biosciences), we captured images of chemiluminescence using a Kodak Image Station 440CF.

**Assessment of apoptosis and mitochondrial membrane potential.** Neutrophils were isolated from peripheral blood; exposed to TNF $\alpha$  (50 ng/ml) (Sigma), H<sub>2</sub>O<sub>2</sub> (0.02 M) (Sigma) or staurosporine (5  $\mu$ M) (Sigma) and analyzed by FACS after staining with annexin-V (Molecular Probes) and propidium iodide (Sigma). Cells were gated on intact neutrophils based on forward scatter and side scatter features. Caspase 3/7 activation was determined by FACS using a commercially available kit (the Vybrant FAM caspase-3 and -7 assay kit (Molecular Probes)). Dissipation of the mitochondrial membrane potential ( $\Delta\Psi_m$ ) was determined by FACS after loading the cells with valinomycin (100 nM) (Sigma) and the dye JC-1 (3.5  $\mu$ M) (Molecular Probes).

**Retroviral gene transfer.** The human HAX1 cDNA was cloned into the retroviral vector CMMP<sup>30</sup> containing either GFP or a truncated version of mouse CD24 as a marker gene. Gibbon ape leukemia virus (GALV) envelope pseudotyped retroviruses were generated by tripartite transient transfection of MMP-based transfer vectors together with the envelope plasmid K83.pHCMV-GALVenv and the packaging plasmid pMDgag/pol into the cell line 293T.

CD34<sup>+</sup> cells were purified from bone marrow using magnetic microbeads (Miltenyi Biotec). Separation was performed by AutoMACS devices (Miltenyi Biotec). The cells were expanded for 48–72 h in Stemspan SF medium (StemCell Technologies) supplemented with human stem cell factor (100 ng/ml), Flt-3 ligand (100 ng/ml), thrombopoietin (20 ng/ml) and interleukin-6 (20 ng/ml) (PreproTech) and then were transduced by spinoculation on RetroNectin-coated plates. We sorted cells for mouse CD24 expression 48 h later in a FACSria System (BD Biosciences), and we induced cells to differentiate into myeloid cells using recombinant G-CSF (50 ng/ml) (Amgen) and GM-CSF (50 ng/ml) (Amgen). Functional studies in myeloid cells generated *in vitro* were done after cytokine starvation.

**GenBank accession codes.** HAX1 GeneID, 10456; HAX1 protein, NP\_006109.2; HAX1 cDNA, NM\_006118.3. ELA2 GeneID, 1991; ELA2 protein, NP\_001963.1; ELA2 cDNA, NM\_001972.2. CSF3R GeneID, 1441; CSF3R protein, NP\_000751.1; CSF3R cDNA, NM\_000760.2.

Note: Supplementary information is available on the Nature Genetics website.

#### ACKNOWLEDGMENTS

We are indebted to the participants and their families and to M. Ballmaier and C. Reimers (Central Medical School Hannover, Flow Cytometry Laboratory) for their assistance. We thank all colleagues referring and registering patients at the International SCN Registry. We wish to acknowledge the genetic studies performed by M. Entesarian, K. Ericson and M. Nordenskjöld. Plasmid K83.pHCMV-GALVenv was a gift from C. Baum (Hannover Medical School). This study was supported by a grant from the Deutsche Forschungsgemeinschaft (DFG-KliFo 110), by the German José Carreras Leukemia Foundation, by the Bundesministerium für Bildung und Forschung (Congenital Bone Marrow Failure Syndromes) and in part by the Intramural Research program of the US National Institutes of Health, National Library of Medicine.

#### AUTHOR CONTRIBUTIONS

C.K. designed and directed the study; obtained clinical samples; taught and supervised G.A., I.S., K.B., C.R. and G.B.; provided laboratory resources and

wrote the manuscript with help from B.G. and A.A.S. The manuscript was then reviewed and approved by all authors. M. Grudzien did the genotyping for linkage analysis and sequenced candidate genes. G.A. performed all gene transfer studies and functional assays on myeloid cells and fibroblasts. M. Germeshausen sequenced HAX1, ELA2 and CSF3R and comprehensively analyzed genetic data. I.S. discovered the first HAX1 mutation and performed sequencing and protein blotting. A.A.S. chose markers to genotype in the linkage region and performed linkage analysis computations. K.B. performed functional immunological assays. C.R. performed functional neutrophil studies and taught G.A. C.Z. cared for patients and collected and curated data in the SCN patient registry. B.S. collected and curated data in the SCN patient registry. N.R. treated patients in Iran and ascertained their samples for this study. G.B. performed functional neutrophil studies and sequenced candidate genes. G.C. and J.-I.H. initiated the Swedish Kostmann family project; G.C. treated the patients, and J.-I.H. and J.P. supervised the project with the support of B.F. N.D. was responsible for Swedish Kostmann gene studies. M.M. sequenced genomic samples from the Kostmann family. B.G. provided laboratory resources, organized patient samples, supervised M. Grudzien and assisted A.A.S. K.W. provided laboratory resources and resources for SCN registry and helped to initiate and carry out the study. M. Grudzien and G.A. contributed equally to this work and are considered *acquo loco*.

#### COMPETING INTERESTS STATEMENT

The authors declare that they have no competing financial interests.

Published online at <http://www.nature.com/naturegenetics>

Reprints and permissions information is available online at <http://npg.nature.com/reprintsandpermissions/>

- Kostmann, R. Infantile genetic agranulocytosis (Agranulocytosis infantilis hereditaria): a new recessive lethal disease in man. *Acta Paediatr.* **45** (Suppl.), 1–78 (1956).
- Carlsson, G. *et al.* Kostmann syndrome: severe congenital neutropenia associated with defective expression of Bcl-2, constitutive mitochondrial release of cytochrome c, and excessive apoptosis of myeloid progenitor cells. *Blood* **103**, 3355–3361 (2004).
- Cario, G. *et al.* Heterogeneous expression pattern of pro- and anti-apoptotic factors in myeloid progenitor cells of patients with severe congenital neutropenia treated with granulocyte colony-stimulating factor. *Br. J. Haematol.* **129**, 275–278 (2005).
- Suzuki, Y. *et al.* HAX-1, a novel intracellular protein, localized on mitochondria, directly associates with HS1, a substrate of Src family tyrosine kinases. *J. Immunol.* **158**, 2736–2744 (1997).
- Gallagher, A.R., Cedzich, A., Gretz, N., Somlo, S. & Witzgall, R. The polycystic kidney disease protein PKD2 interacts with Hax-1, a protein associated with the actin cytoskeleton. *Proc. Natl. Acad. Sci. USA* **97**, 4017–4022 (2000).
- Radhika, V., Onesime, D., Ha, J.H. & Dhanasekaran, N. G $\alpha_{13}$  stimulates cell migration through cortactin-interacting protein Hax-1. *J. Biol. Chem.* **279**, 49406–49413 (2004).
- Welte, K., Zeidler, C. & Dale, D. Severe congenital neutropenia. *Semin. Hematol.* **43**, 189–195 (2006).
- Dale, D.C. *et al.* Mutations in the gene encoding neutrophil elastase in congenital and cyclic neutropenia. *Blood* **96**, 2317–2322 (2000).
- Sharp, T.V. *et al.* K15 protein of Kaposi's sarcoma-associated herpesvirus is latently expressed and binds to HAX-1, a protein with antiapoptotic function. *J. Virol.* **76**, 802–816 (2002).
- Cilenti, L. *et al.* Regulation of HAX-1 anti-apoptotic protein by Omi/HtrA2 protease during cell death. *J. Biol. Chem.* **279**, 50295–50301 (2004).
- Elsner, J., Roesler, J., Emmendorffer, A., Lohmann-Matthes, M.L. & Welte, K. Abnormal regulation in the signal transduction in neutrophils from patients with severe congenital neutropenia: relation of impaired mobilization of cytosolic free calcium to altered chemotaxis, superoxide anion generation and F-actin content. *Exp. Hematol.* **21**, 38–46 (1993).
- Carlsson, G. & Fasth, A. Infantile genetic agranulocytosis, morbus Kostmann: Presentation of six cases from the original "Kostmann family" and a review. *Acta Paediatr.* **90**, 757–764 (2001).
- Horwitz, M., Benson, K.F., Person, R.E., Aprikyan, A.G. & Dale, D.C. Mutations in ELA2, encoding neutrophil elastase, define a 21-day biological clock in cyclic haematopoiesis. *Nat. Genet.* **23**, 433–436 (1999).
- Gilman, P.A., Jackson, D.P. & Guild, H.G. Congenital agranulocytosis: prolonged survival and terminal acute leukemia. *Blood* **36**, 576–585 (1970).
- Rosenberg, P.S. *et al.* The incidence of leukemia and mortality from sepsis in patients with severe congenital neutropenia receiving long-term G-CSF therapy. *Blood* **107**, 4628–4635 (2006).
- Dong, F. *et al.* Mutations in the gene for the granulocyte colony-stimulating-factor receptor in patients with acute myeloid leukemia preceded by severe congenital neutropenia. *N. Engl. J. Med.* **333**, 487–493 (1995).
- Green, D.R. & Kroemer, G. The pathophysiology of mitochondrial death. *Science* **305**, 626–629 (2004).

18. Newmeyer, D.D. & Ferguson-Miller, S. Mitochondria: releasing power for life and unleashing the machineries of death. *Cell* **112**, 481–490 (2003).
19. Maianski, N.A. *et al.* Functional characterization of mitochondria in neutrophils: a role restricted to apoptosis. *Cell Death Differ.* **11**, 143–153 (2004).
20. Kroemer, G. & Reed, J.C. Mitochondrial control of cell death. *Nat. Med.* **6**, 513–519 (2000).
21. Gross, A., McDonnell, J.M. & Korsmeyer, S.J. BCL-2 family members and the mitochondria in apoptosis. *Genes Dev.* **13**, 1899–1911 (1999).
22. Opferman, J.T. & Korsmeyer, S.J. Apoptosis in the development and maintenance of the immune system. *Nat. Immunol.* **4**, 410–415 (2003).
23. Hamasaki, A. *et al.* Accelerated neutrophil apoptosis in mice lacking A1-a, a subtype of the *bcl-2*-related A1 gene. *J. Exp. Med.* **188**, 1985–1992 (1998).
24. Maianski, N.A., Mul, F.P.J., van Buul, J.D., Roos, D. & Kuijpers, T.W. Granulocyte colony-stimulating factor inhibits the mitochondria-dependent activation of caspase-3 in neutrophils. *Blood* **99**, 672–679 (2002).
25. Dufva, M., Olsson, M. & Rymo, L. Epstein-Barr virus nuclear antigen 5 interacts with HAX-1, a possible component of the B-cell receptor signalling pathway. *J. Gen. Virol.* **82**, 1581–1587 (2001).
26. Kawaguchi, Y. *et al.* Interaction of Epstein-Barr virus nuclear antigen leader protein (EBNA-LP) with HS1-associated protein X-1: implication of cytoplasmic function of EBNA-LP. *J. Virol.* **74**, 10104–10111 (2000).
27. Yedavalli, V.S. *et al.* Human immunodeficiency virus type 1 Vpr interacts with antiapoptotic mitochondrial protein HAX-1. *J. Virol.* **79**, 13735–13746 (2005).
28. Cottingham, R.W., Jr., Idury, R.M. & Schäffer, A.A. Faster sequential genetic linkage computations. *Am. J. Hum. Genet.* **53**, 252–263 (1993).
29. Schäffer, A.A., Gupta, S.K., Shriram, K. & Cottingham, R.W. Jr. Avoiding recomputation in linkage analysis. *Hum. Hered.* **44**, 225–237 (1994).
30. Klein, C., Bueler, H.R. & Mulligan, R.C. Comparative analysis of genetically modified dendritic cells and tumor cells as therapeutic cancer vaccines. *J. Exp. Med.* **191**, 1699–1708 (2000).

## ORIGINAL ARTICLE

# A Syndrome with Congenital Neutropenia and Mutations in *G6PC3*

Kaan Boztug, M.D., Giridharan Appaswamy, M.Sc., Angel Ashikov, Ph.D., Alejandro A. Schäffer, Ph.D., Ulrich Salzer, M.D., Jana Diestelhorst, B.Sc., Manuela Germeshausen, Ph.D., Gudrun Brandes, M.D., Jacqueline Lee-Gossler, M.Sc., Fatih Noyan, Ph.D., Anna-Katherina Gatzke, M.Sc., Milen Minkov, M.D., Ph.D., Johann Greil, M.D., Christian Kratz, M.D., Theoni Petropoulou, M.D., Isabelle Pellier, M.D., Christine Bellanné-Chantelot, Pharm.D., Ph.D., Nima Rezaei, M.D., Kirsten Mönkemöller, M.D., Noha Irani-Hakimeh, M.D., Hans Bakker, Ph.D., Rita Gerardy-Schahn, Ph.D., Cornelia Zeidler, M.D., Bodo Grimbacher, M.D., Karl Welte, M.D., and Christoph Klein, M.D., Ph.D.

## ABSTRACT

**BACKGROUND**

The main features of severe congenital neutropenia are the onset of severe bacterial infections early in life, a paucity of mature neutrophils, and an increased risk of leukemia. In many patients, the genetic causes of severe congenital neutropenia are unknown.

**METHODS**

We performed genomewide genotyping and linkage analysis on two consanguineous pedigrees with a total of five children affected with severe congenital neutropenia. Candidate genes from the linkage interval were sequenced. Functional assays and reconstitution experiments were carried out.

**RESULTS**

All index patients were susceptible to bacterial infections and had very few mature neutrophils in the bone marrow; structural heart defects, urogenital abnormalities, and venous angiectasia on the trunk and extremities were additional features. Linkage analysis of the two index families yielded a combined multipoint lod score of 5.74 on a linkage interval on chromosome 17q21. Sequencing of *G6PC3*, the candidate gene encoding glucose-6-phosphatase, catalytic subunit 3, revealed a homozygous missense mutation in exon 6 that abolished the enzymatic activity of glucose-6-phosphatase in all affected children in the two families. The patients' neutrophils and fibroblasts had increased susceptibility to apoptosis. The myeloid cells showed evidence of increased endoplasmic reticulum stress and increased activity of glycogen synthase kinase 3 $\beta$  (GSK-3 $\beta$ ). We identified seven additional, unrelated patients who had severe congenital neutropenia with syndromic features and distinct biallelic mutations in *G6PC3*.

**CONCLUSIONS**

Defective function of glucose-6-phosphatase, catalytic subunit 3, underlies a severe congenital neutropenia syndrome associated with cardiac and urogenital malformations.

From Hannover Medical School, Hannover, Germany (K.B., G.A., A.A., J.D., M.G., G.B., J.L.-G., F.N., A.-K.G., H.B., R.G.-S., C.Z., K.W., C. Klein); the National Center for Biotechnology Information, National Institutes of Health, Bethesda, MD (A.A.S.); the University Medical Center Freiburg, Freiburg, Germany (U.S.); St. Anna Children's Hospital, Vienna (M.M.); Children's Hospital, University of Heidelberg, Heidelberg, Germany (J.G.); the University of Freiburg, Freiburg, Germany (C. Kratz); Aghia Sophia Children's Hospital, University of Athens, Athens (T.P.); Centre Hospitalier Universitaire Angers, Angers, France (I.P.); Assistance Publique-Hôpitaux de Paris, Hôpital de la Pitié-Salpêtrière, Paris (C.B.-C.); the Immunology, Asthma, and Allergy Research Institute, Tehran University of Medical Sciences, Tehran, Iran (N.R.); Children's Hospital Amsterdamer Straße, Cologne, Germany (K.M.); Saint Georges University Hospital, Beirut, Lebanon (N.I.-H.); and Royal Free Hospital and University College London, London (B.G.). Address reprint requests to Dr. Klein at the Department of Pediatric Hematology and Oncology, Medical School Hannover, Carl-Neuberg-Straße 1, Hannover D-30625, Germany, or at klein.christoph@mh-hannover.de.

Drs. Appaswamy and Ashikov contributed equally to this article.

N Engl J Med 2009;360:32-43.

Copyright © 2009 Massachusetts Medical Society.

SEVERE CONGENITAL NEUTROPENIA WAS described more than 50 years ago by Kostmann,<sup>1,2</sup> and subsequently the disorder was found to consist of a heterogeneous group of diseases.<sup>3,4</sup> In these syndromes, the neutropenia is associated with life-threatening bacterial infections early in life. Most patients respond to treatment with recombinant human granulocyte colony-stimulating factor (rhG-CSF), which increases neutrophil counts and decreases the frequency and severity of infections.<sup>5</sup> Nonetheless, patients may remain at risk for both infectious complications and the development of clonal disorders of hematopoiesis, such as myelodysplastic syndrome and acute myeloid leukemia.<sup>6</sup>

Considerable progress has been made in identifying the molecular defects that cause congenital neutropenia.<sup>7,8</sup> Many patients with severe congenital or cyclic neutropenia have a heterozygous mutation in *ELA2*, the gene encoding neutrophil elastase.<sup>9-11</sup> We recently identified homozygous mutations in *HAX1*, the gene encoding HCLS1-associated protein X1, in a subgroup of patients with autosomal recessive severe congenital neutropenia.<sup>12</sup> In addition, mutations in *WAS*, the gene encoding the Wiskott-Aldrich syndrome protein,<sup>13,14</sup> and in *GFI1*, the gene encoding the growth factor independent 1 transcription-repressor protein,<sup>15</sup> have been associated with a phenotype resembling Kostmann's syndrome. In many patients with congenital neutropenia, however, the underlying molecular cause remains unknown. Despite insights into the role of apoptosis in congenital neutropenia,<sup>12,16,17</sup> the mechanisms of neutropenia and the risk of leukemia in patients with severe congenital neutropenia are incompletely understood. We report a syndrome consisting of severe congenital neutropenia, other congenital abnormalities, and biallelic mutations in *G6PC3*, the gene encoding glucose-6-phosphatase, catalytic subunit 3.

---

## METHODS

---

### PATIENTS AND CONTROLS

We took blood and bone marrow samples from patients and healthy volunteers with their written informed consent. The study was approved by the institutional review board of Hannover Medical School.

### ANALYTICAL METHODS

We genotyped microsatellite markers in a whole-genome scan for a family with severe congenital neutropenia, with a pedigree identified as SCN-I. The equipment and protocols for genotyping have been described previously.<sup>12</sup> The genetic-linkage analysis was performed with the use of a combination of quantitative and qualitative syllogisms. The quantitative decisions were made with the use of lod scores and optimal recombination fractions computed with Superlink software.<sup>18,19</sup> For calculation of lod scores, we modeled neutropenia as a fully penetrant autosomal recessive disease with no phenocopies and a disease-allele frequency of 0.001. The Marshfield map<sup>20</sup> was used to select usefully positioned markers for fine mapping. For details, see the Supplementary Appendix, available with the full text of this article at NEJM.org.

Exons and flanking intron-exon boundaries from candidate genes were amplified by polymerase chain reaction (PCR) and analyzed with the use of an ABI PRISM 3130 DNA Sequencer and DNA Sequencing Analysis software, version 3.4 (Applied Biosystems), and Sequencer, version 3.4.1 (Gene Codes Corporation). See the Supplementary Appendix for primer sequences and details of the restriction-length-polymorphism analysis of the frequency of the R253H mutation in healthy controls.

Promyelocytes were sorted by fluorescence-activated cell sorting, as described previously,<sup>17</sup> with minor modifications. Analysis of the expression of the *G6PC3* and *HSPA5/BiP/Grp78* genes was performed with the use of a Roche LightCycler 2.0 (see the Supplementary Appendix).

The complete open reading frames of wild-type and mutant *G6PC3* were amplified by PCR and cloned in pYES-cup1 (modified from pYES-NT [Invitrogen]), as described by Ashikov et al.,<sup>21</sup> and expressed in *Saccharomyces cerevisiae*. Centrifugation at 100,000×g produced a microsomal fraction that was assayed for hydrolysis of glucose-6-phosphate to glucose by the addition of <sup>14</sup>C-glucose-6-phosphate (MP Biomedicals). Released <sup>14</sup>C-glucose was separated from glucose-6-phosphate by anion exchange and measured in the eluate by liquid scintillation.

Whole-cell lysates from primary granulocytes were separated by sodium dodecyl sulfate-polyacrylamide-gel electrophoresis (SDS-PAGE), blot-

**Table 1. Clinical and Molecular Findings in Patients with G6PC3 Deficiency.\***

Patient No.	Sex	Race or Ethnic Group and Country of Origin†	Absolute Neutrophil Count‡ <i>per mm<sup>3</sup></i>	Infections	Other Findings
1	M	Aramean, Turkey	60–246	Neonatal sepsis, otitis media	Type 2 atrial septal defect, cryptorchidism, prominent superficial venous pattern, intermittent thrombocytopenia, hepatosplenomegaly
2	F	Aramean, Turkey	54–240	Neonatal pneumonia and sepsis	Cor triatriatum, malformation of pulmonary veins, prominent superficial venous pattern, hepatosplenomegaly
3	F	Aramean, Turkey	0–61	Pneumonia, sepsis	Type 2 atrial septal defect, mitral insufficiency, prominent superficial venous pattern, intermittent thrombocytopenia, hepatosplenomegaly
4	M	Aramean, Turkey	0–322	Neonatal sepsis	Type 2 atrial septal defect, cryptorchidism, prominent superficial venous pattern
5	M	Aramean, Turkey	25–84	Neonatal sepsis	Prominent superficial venous pattern, intermittent thrombocytopenia
6	F	Turkish, Turkey	90–612	Pneumonia, sepsis	Type 2 atrial septal defect, pulmonary valve stenosis, panniculitis, prominent superficial venous pattern
7	F	White, Greece	30–1280¶	Perianal abscesses, recurrent urinary tract infections	Inner-ear hearing loss, prominent superficial venous pattern
8	F	White, Germany	75–210	Omphalitis, recurrent urinary tract infections, oral ulcers	Type 2 atrial septal defect, urachal fistula, microcephaly, prominent superficial venous pattern, intermittent thrombocytopenia
9	F	White, France	200–500	Upper and lower respiratory tract infections	Myopathy, prominent superficial venous pattern
10	M	White, Germany	0–3000	Urinary tract infection	Type 2 atrial septal defect, cryptorchidism, genital dysplasia, microcephaly, inner-ear hearing loss, prominent superficial venous pattern, intermittent thrombocytopenia
11	M	Persian, Iran	250–440	Neonatal sepsis, urinary tract infection	Type 2 atrial septal defect, patent ductus arteriosus
12	M	Arab, Lebanon	615–2000¶	Perianal abscesses, pneumonia, recurrent lower respiratory tract infections	Cryptorchidism, bilateral inguinal hernia, cleft palate

\* G-CSF denotes granulocyte colony-stimulating factor.

† Race or ethnic group was self-assessed.

‡ Absolute neutrophil counts were determined before the start of treatment with G-CSF.

§ Percentiles of height and weight were based on German reference data for white patients from Greece, Germany, and France and on Turkish reference data for other patients.

¶ During infectious episodes, an occasional increase in neutrophil counts was observed.

ted, and stained with antibodies against phospho-Mcl-1 (Ser159/Thr163), total glycogen synthase kinase 3 $\beta$  (GSK-3 $\beta$ ), phospho-GSK-3 $\beta$  (Ser9) (all from Cell Signaling Technology/New England Biolabs), Bip/Grp78 (BD Biosciences), and glyceralde-

hyde-3-phosphate dehydrogenase (GAPDH) (Santa Cruz Biotechnology) (see the Supplementary Appendix).

Bone marrow samples from patients and healthy control subjects were subjected to hypo-



Genotype	Therapy	Current Age yr	Current Height and Weight Percentiles§	
			Height	Weight
c.[758G→A]+[758G→A], p.[Arg253His]+[Arg253His]	G-CSF, cardiac surgery	6	25–50	3–10
c.[758G→A]+[758G→A], p.[Arg253His]+[Arg253His]	G-CSF, cardiac surgery	3	25	10–25
c.[758G→A]+[758G→A], p.[Arg253His]+[Arg253His]	G-CSF, awaiting corrective cardiac procedure	11	10–25	10–25
c.[758G→A]+[758G→A], p.[Arg253His]+[Arg253His]	G-CSF, cardiac surgery	6	8 cm below 3rd percentile	1.3 kg below 3rd percentile
c.[758G→A]+[758G→A], p.[Arg253His]+[Arg253His]	G-CSF	4	3	1.0 kg below 3rd percentile
c.[554T→C]+[554T→C], p.[Leu185Pro]+[Leu185Pro]	G-CSF, awaiting corrective cardiac procedure	12	50	75
c.[141C→G]+[141C→G], p.[Tyr47X]+[Tyr47X]	G-CSF	13	25–50	50–75
c.[784G→C]+[784G→C], p.[Gly262Arg]+[Gly262Arg]	G-CSF, cardiac surgery	7	3–10	10
c.[677+1 G→A]+[829C→T], p.[?]+[Gln277X]	G-CSF	13	3–10	10
c.[778G→C]+[778G→C], p.[Gly260Arg]+[Gly260Arg]	G-CSF, cardiac surgery	17	4 cm below 3rd percentile	8 kg below 3rd percentile
c.[935dupT]+[935dupT], p.[Asn313fs]+[Asn313fs]	G-CSF, awaiting corrective cardiac procedure	10	10–25	10–25
c.[144C→A]+[144C→A], p.[Tyr48X]+[Tyr48X]	G-CSF	5	3–10	3–10

tonic lysis. Fixation and electron microscopy were performed as described previously.<sup>22</sup>

Human G6PC3 complementary DNA (cDNA) was cloned into a bicistronic retroviral vector (MMP)<sup>23</sup> containing murine *cd24* as a marker gene. RD114-pseudotyped retroviral particles were generated by tripartite transfection of MMP-based vectors together with the envelope plasmid and the packaging plasmid mPD.old.gag/pol into a human embryonic kidney-cell line (HEK293T). Trans-

duction of CD34+ cells and myeloid differentiation were performed as described previously.<sup>12</sup>

Apoptosis in peripheral-blood neutrophils or in cells that were differentiated into myeloid cells in vitro was induced with the use of tumor necrosis factor  $\alpha$  (TNF- $\alpha$ ) (50 ng per milliliter), thapsigargin (10  $\mu$ M), or tunicamycin (5  $\mu$ g per milliliter) (all from Sigma) and assessed by staining with annexin V (Invitrogen) and propidium iodide (Sigma). In fibroblasts, apoptosis was induced with

the use of 5 mM dithiothreitol (Roche). Caspase 3/7 activation was assessed as described previously<sup>12</sup> (see the Supplementary Appendix).

## RESULTS

### CLINICAL FINDINGS

Table 1 lists the main features of the five patients we studied. Patients 1 and 2, who were siblings born to consanguineous parents of Aramean descent, presented with neonatal sepsis. Their extended pedigree is denoted SCN-I (see Fig. 1 in the Supplementary Appendix). Their workup in the first year of life found severe neutropenia with a paucity of mature neutrophils in the peripheral blood and bone marrow. Bone marrow smears contained few granulocytes beyond the stage of promyelocytes or myelocytes (Fig. 1A and 1B, and Table 1 in the Supplementary Appendix). Erythrocyte counts were normal. Platelet counts in Patient 1 ranged from 73,000 to 425,000 per cubic millimeter, whereas Patient 2 had normal platelet counts. Both patients had unusually prominent subcutaneous veins, venous angiectasia, or both (Fig. 1C); Patient 1 had a type 2 atrial septal defect (Fig. 1D), and Patient 2 had cor triatriatum and hepatosplenomegaly. Genealogic investigations revealed that the SCN-I pedigree could be extended to include two additional sibships, each with one child affected by severe congenital neutropenia and type 2 atrial septal defect (Patients 3 and 4 in Fig. 1 in the Supplementary Appendix). We also identified a child with severe congenital neutropenia in a second consanguineous pedigree (SCN-II) from the same ethnic background (Patient 5 in Fig. 1 in the Supplementary Appendix). All patients received rhG-CSF, which resulted in an increase in neutrophil counts.

### GENETIC STUDIES

Mutations in both *ELA2*<sup>10</sup> and *HAX1*<sup>12</sup> were excluded in all five index patients. Linkage analysis provided statistical evidence that the gene of interest in SCN-I is located on chromosome 17q21 between D17S1299 (36.2 Mb, 62.0 cM) and D17S1290 (53.7 Mb, 82.0 cM) (Fig. 2A, and the Supplementary Appendix). We carried out a series of fine mapping steps in SCN-I and SCN-II and were able to genotype an additional 13 microsatellite markers between D17S1299 and D17S1290 in SCN-I and 11 of these 13 microsatellite markers in SCN-II. Table 2 in the Supplementary Appendix shows the

single-marker lod scores. On the assumption that the same gene is mutated in all five affected children, the maximal linkage interval spanned from D17S1789 (39.1 Mb, 63.1 cM) to D17S791 (42.2 Mb, 64.2 cM). With the use of D17S932, D17S950, and D17S806, the peak multipoint lod score in SCN-I alone was 4.98, and the peak two-pedigree multipoint lod score was 5.74.

Several candidate genes were identified in the SCN-I linkage interval (see Table 3 in the Supplementary Appendix). Of these, *G6PC3*, which encodes glucose-6-phosphatase, catalytic subunit 3, and is located in the narrowest possible linkage interval, was a plausible candidate, because abnormal glucose metabolism has been implicated in the neutropenia of type Ib glycogen storage disease.<sup>24</sup> DNA sequencing revealed a homozygous missense mutation in exon 6 of the *G6PC3* gene (c.G758A, p.R253H) (Fig. 2B). This mutation was found in all four affected children in SCN-I and in the one affected child in SCN-II. All parents were heterozygous for the mutation, a finding consistent with autosomal recessive inheritance of a germ-line missense mutation. According to restriction-site analysis, the R253H allele of the *G6PC3* gene was not found in 192 healthy central European persons. An *in silico* sequence analysis using the program Sorting Intolerant from Tolerant (SIFT)<sup>25</sup> calculated that the probability that this mutation is benign is 0.01. Analysis with the program PolyPhen<sup>26</sup> predicted that the R253H change probably interferes with the function of glucose-6-phosphatase. The wild-type protein is conserved in mammals, amphibians, bony fish, and insects.

### FUNCTIONAL STUDIES

#### *Enzymatic Activity of G6PC3 with the R253H Mutation*

Wild-type *G6PC3* and *G6PC3* with the R253H mutation were expressed in *S. cerevisiae*. Microsomes were isolated from yeast transfected with wild-type *G6PC3* or *G6PC3* with the R253H mutation and assayed for phosphatase activity. Wild-type *G6PC3* hydrolyzed glucose-6-phosphate and the universal substrate p-nitrophenylphosphate (pNPP), as demonstrated by radioactive (Fig. 2C) and spectrometric (Fig. 3 in the Supplementary Appendix) assays, respectively. In contrast, the level of enzymatic activity of *G6PC3* with the R253H mutation did not exceed the level of phosphatase activity in yeast transfected with an empty vector.

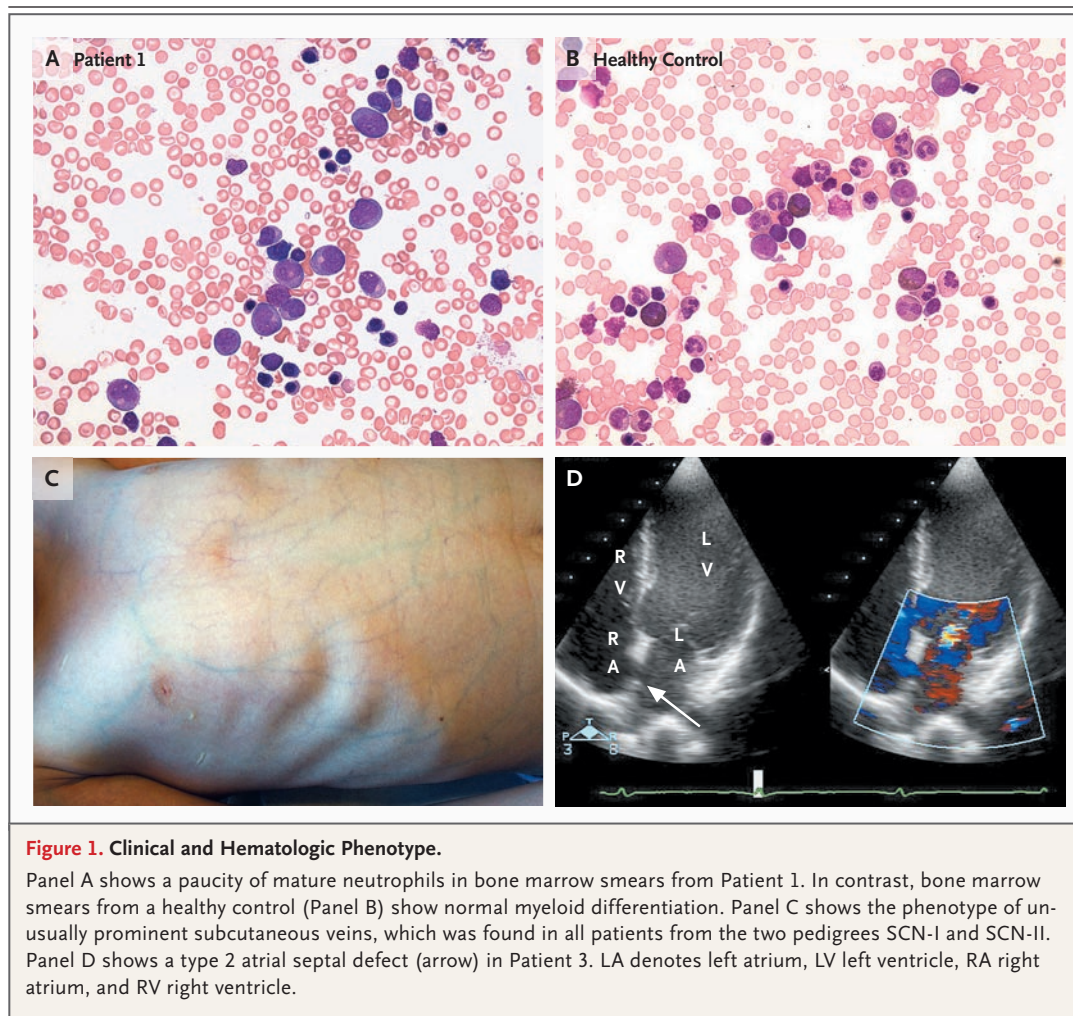


**Figure 1. Clinical and Hematologic Phenotype.**

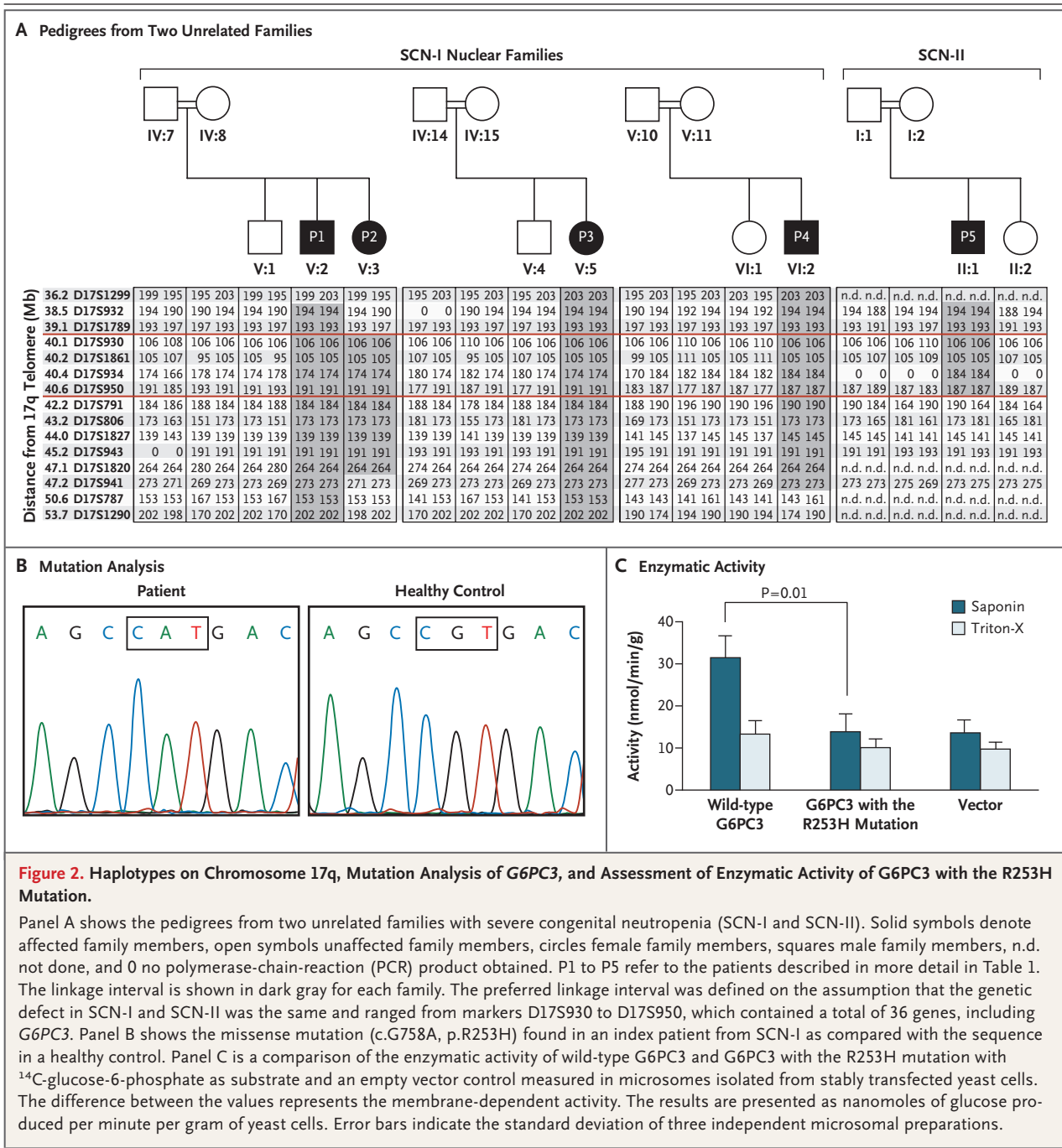
Panel A shows a paucity of mature neutrophils in bone marrow smears from Patient 1. In contrast, bone marrow smears from a healthy control (Panel B) show normal myeloid differentiation. Panel C shows the phenotype of unusually prominent subcutaneous veins, which was found in all patients from the two pedigrees SCN-I and SCN-II. Panel D shows a type 2 atrial septal defect (arrow) in Patient 3. LA denotes left atrium, LV left ventricle, RA right atrium, and RV right ventricle.

### Apoptosis

Like neutrophils from patients with mutations in *ELA2*<sup>10</sup> or *HAX1*,<sup>12</sup> peripheral-blood neutrophils from our patients had an increased rate of spontaneous apoptosis. Apoptosis of neutrophils was markedly accelerated after induction with  $\text{TNF-}\alpha$  (Fig. 3A) or tunicamycin (data not shown), as assessed by annexin V staining and a test for activation of caspase 3/7, respectively (see Fig. 4 in the Supplementary Appendix). Since *G6PC3* is ubiquitously expressed and since the phenotype of our patients was not restricted to the hematopoietic system, we tested nonhematopoietic cells for susceptibility to apoptosis. Skin fibroblasts from patients with a deficiency of *G6PC3* had an increased susceptibility to apoptosis after dithiothreitol-induced stress to the endoplasmic reticulum (Fig. 3B).

To provide further evidence that this form of severe congenital neutropenia is caused by mutations in *G6PC3*,  $\text{CD34}^+$  hematopoietic stem cells from two patients were isolated and transduced with retroviral constructs containing either the wild-type *G6PC3* cDNA sequence and murine *cd24* as a reporter gene (MMP-*G6PC3*-mcd24) or the reporter gene only (MMP-mcd24). After in vitro differentiation in the presence of rhG-CSF and recombinant human granulocyte-macrophage colony-stimulating factor (rhGM-CSF), cells were exposed to tunicamycin to induce apoptosis and analyzed by flow cytometry by gating on mcd24-positive cells. In control-transduced cells from a patient, exposure to tunicamycin induced a high degree of apoptosis (30.0% of annexin V-positive cells and 4.6% of annexin V and propidium iodide-double-positive cells underwent apoptosis). By con-



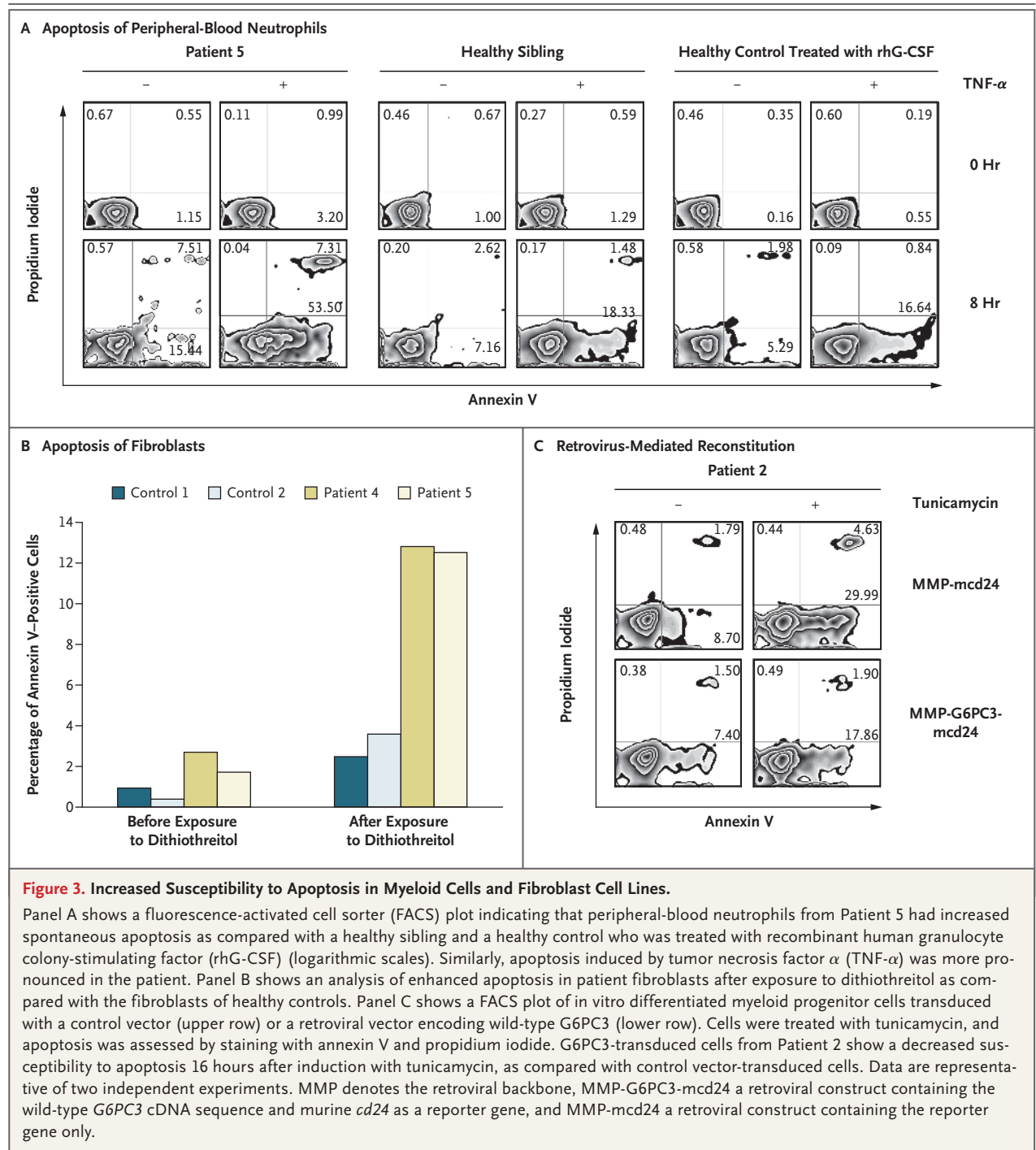


trast, in G6PC3-transduced cells, the percentage of cells undergoing apoptosis was lower (17.9% of annexin V-positive cells and 1.9% of double-positive cells) (Fig. 3C, and Fig. 5 in the Supplementary Appendix). We tested the function of neutrophils in G6PC3-deficient neutrophils. Both phagosomal lysis of *Escherichia coli* and the oxidative burst were similar to those in neutrophils

from healthy control subjects (Fig. 6 in the Supplementary Appendix).

*Endoplasmic Reticulum Stress*

Endoplasmic reticulum stress and the unfolded-protein response have been linked to the pathophysiology of aberrant organogenesis,<sup>27</sup> including structural heart defects<sup>28</sup> and congenital neutropenia



caused by mutations in *ELA2*.<sup>17,29</sup> Transmission electron microscopy of bone marrow cells from four patients with *G6PC3* deficiency showed an enlarged rough endoplasmic reticulum in myeloid progenitor cells as compared with the rough endoplasmic reticulum in corresponding cells from a healthy subject (Fig. 4A and 4B, and Fig. 7 in the

Supplementary Appendix). This finding is consistent with increased endoplasmic reticulum stress. BiP messenger RNA (mRNA), a member of the chaperone family and another marker of endoplasmic reticulum stress, was measured by quantitative real-time PCR in bone marrow promyelocytes that had been isolated by flow cytometry.

The level of BiP mRNA was increased in promyelocytes from the two patients we tested as compared with that in promyelocytes from healthy subjects (Fig. 4C).

### GSK-3 $\beta$

A signaling circuit linking glucose, GSK-3 $\beta$ , and Mcl-1 has been previously established<sup>30,31</sup> in which GSK-3 $\beta$  controls glycogen metabolism, Wnt signaling, and apoptosis.<sup>32</sup> Mcl-1, an antiapoptotic member of the Bcl-2 family, is involved in the maintenance of neutrophil viability.<sup>33</sup> GSK-3 $\beta$  phosphorylates Mcl-1, thus facilitating its degradation in the proteasome.<sup>30</sup> We performed Western blot studies to estimate the levels of GSK-3 $\beta$ , BiP, and Mcl-1 proteins in neutrophils exposed to tunicamycin, an agent that induces endoplasmic reticulum stress. Neutrophils from the two patients we examined had increased levels of BiP (Fig. 4E), an increase in the enzymatically active dephosphorylated form of GSK-3 $\beta$  (Fig. 4D, and Fig. 8 in the Supplementary Appendix), and increased phosphorylation of Mcl-1 (Fig. 4E). To investigate whether intracellular glucose deprivation causes dephosphorylation of GSK-3 $\beta$ , we inhibited glucose metabolism in neutrophils from two healthy subjects with the use of 2-deoxyglucose. Treatment with 2-deoxyglucose induced dephosphorylation of GSK-3 $\beta$  (Fig. 4F) and increased apoptosis of neutrophils (Fig. 4G), whereas CD3-positive T lymphocytes were resistant to the effects of 2-deoxyglucose (Fig. 4G).

### G6PC3 MUTATIONS IN OTHER PATIENTS

We assessed the frequency and variety of *G6PC3* mutations in a cohort of patients with genetically unclassified severe congenital neutropenia. Of 104 such patients, 7 had distinct biallelic mutations in *G6PC3* (Table 1). The mutations include nonsense mutations (Y47X and Y48X) that would abolish the function of the protein if the truncated mRNA was translated. The three other missense mutations were predicted to be deleterious to the protein by SIFT<sup>22</sup> analysis, with probabilities of being benign of 0.03 for L185P, 0.00 for G262R, and 0.00 for G260R. None of these additional patients with *G6PC3* mutations had mutations in *ELA2* or *HAX1*, a finding suggesting that these three genetic defects are distinct variants of severe congenital neutropenia. None of the patients with *G6PC3* deficiency had hypoglycemia or lactic acidosis (see Table 4 in the Supplementary Appendix), as is seen in glycogen storage disorders.

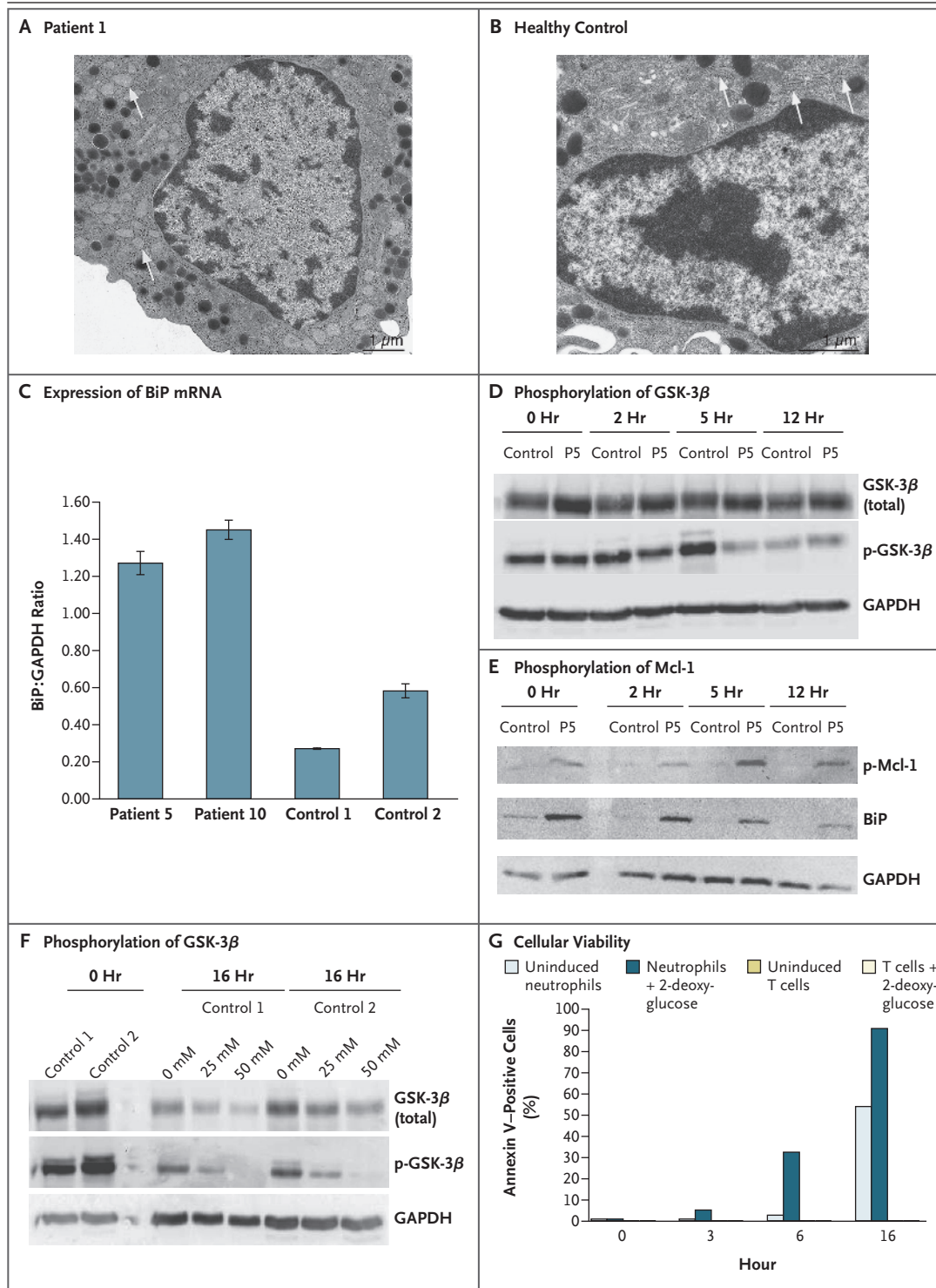
### Figure 4 (facing page). Pathophysiologic Consequences of G6PC3 Deficiency.

Panel A is a transmission electron micrograph showing the aberrantly enlarged rough endoplasmic reticulum (arrows) in a myeloid progenitor cell of a patient with G6PC3 deficiency. Panel B shows the rough endoplasmic reticulum (arrows) in a cell from a healthy subject. Panel C illustrates increased endoplasmic reticulum stress in patients with G6PC3 deficiency, as documented by increased expression levels of BiP messenger RNA in purified promyelocytes. Error bars indicate the standard deviation. GAPDH denotes glyceraldehyde-3-phosphate dehydrogenase. Panel D is a Western blot showing an increase in the enzymatically active, dephosphorylated form of glycogen synthase kinase 3 $\beta$  (GSK-3 $\beta$ ) in Patient 5 (P5) after induction with tunicamycin (p-GSK-3 $\beta$  denotes phosphorylated GSK-3 $\beta$ ). Panel E shows increased phosphorylation of Mcl-1 and increased levels of BiP in neutrophils from Patient 5 (P5) with G6PC3 deficiency at different time points after induction with tunicamycin (p-Mcl-1 denotes phosphorylated Mcl-1). Panel F shows 2-deoxyglucose-induced dephosphorylation of GSK-3 $\beta$  in two healthy donors. Panel G shows that healthy neutrophils, but not CD3-positive T cells, are susceptible to apoptosis on pharmacologic glucose depletion with the use of 2-deoxyglucose. Some values are too small to appear clearly.

A clinical review of all 12 patients with G6PC3 deficiency found variation in clinical features. Of the 12 patients, 8 had various cardiac malformations and 10 had a phenotype of unusually prominent subcutaneous veins, venous angiectasia, or both (Fig. 1, and Fig. 2 in the Supplementary Appendix). Five patients had urogenital malformations, including cryptorchidism and urachal fistula (the urachus is a channel between the bladder of the fetus and the allantois). Two patients had inner-ear hearing loss, and two had delayed growth but no dysmorphic features (Table 1).

### DISCUSSION

We have described a congenital neutropenia syndrome with biallelic mutations in *G6PC3*. Like patients with mutations in *HAX1*<sup>12</sup> or *ELA2*,<sup>16</sup> patients with G6PC3 deficiency lacked mature neutrophils in the bone marrow and had increased susceptibility to apoptosis in peripheral neutrophils. Of 12 patients, 8 had structural heart defects (e.g., type 2 atrial septal defect, cor triatriatum, or pulmonary stenosis) and 5 had urogenital defects (e.g., cryptorchidism or urachal fistula). In most patients, an atypical, increased visibility of the superficial veins, angiectasia, or both was prominent. The spectrum of developmental aberrations may



depend on factors other than the mutant *G6PC3*. Perhaps increased susceptibility to apoptosis also affects cardiac or urogenital development in patients with *G6PC3* deficiency. There is clinical variation in other neutropenia syndromes, such as Co-

hen syndrome and cartilage-hair hypoplasia, even though the two syndromes are genetically homogeneous.<sup>8</sup> All patients in our cohort had a response to treatment with rhG-CSF, and to date no patient has had a clonal hematopoietic disorder.



Three human genes mediating glucose-6-phosphatase activity have been discovered: *G6PC1*, *G6PC2*, and *G6PC3*. *G6PC1*, the classic glucose-6-phosphatase in the liver, kidney, and small intestine, catalyzes the hydrolysis of glucose-6-phosphate, an essential step in the gluconeogenic and glycogenolytic pathways. Patients without *G6PC1* activity have type Ia glycogen storage disease.<sup>34</sup> *G6PC2* is expressed only in pancreatic islet cells<sup>35,36</sup> and may be involved in glucose-dependent insulin secretion by controlling free glucose levels.<sup>37</sup> Statistically significant associations between non-coding polymorphisms in or near *G6PC2* and the level of glucose after an overnight fast have been shown.<sup>38,39</sup> In contrast to *G6PC1* and *G6PC2*, *G6PC3* is ubiquitously expressed.<sup>40,41</sup> Glucose-6-phosphate is transported to the endoplasmic reticulum by a glucose-6-phosphate transporter (*G6PT*).<sup>42</sup> The stoichiometry and topologic relationships between the catalytic subunits of glucose-6-phosphatase and *G6PT* are unclear, but they do have a functional link.<sup>42-44</sup> The complex formed between *G6PT* and *G6PC1* (and perhaps also the complex between *G6PT* and *G6PC2*) appears to maintain normoglycemia. Our data show that *G6PC3* is needed to maintain neutrophil viability and suggest an important role for glucose in the homeostasis of human neutrophils.

Cheung et al. recently described the phenotype of *g6pc3*-deficient mice that was generated by gene targeting.<sup>45</sup> These mice had neutropenia and neutrophil dysfunction; another group had previously shown that murine *g6pc3* deficiency results in lowered plasma cholesterol and elevated glucagon levels.<sup>46</sup> We could not identify any consistent aberration in neutrophil function or any metabolic aberrations in patients with *G6PC3* deficiency. The underlying mechanism of increased apoptosis of neutrophils in the absence of *G6PC3* involves increased endoplasmic reticulum stress, which is usually seen in cases of deficient protein folding in the endoplasmic reticulum. In an attempt to counteract potentially toxic effects that can ensue from abnormally folded proteins, cells initiate a rescue program that, if ineffective, leads to apoptosis.<sup>47</sup> We have provided evidence that *GSK-3 $\beta$* , a key enzyme that regulates cellular differentiation and apoptosis,<sup>32</sup> is implicated in this pathway. In the absence of intracellular glucose, *GSK-3 $\beta$*  is activated and thus can phosphorylate the antiapoptotic molecule *Mcl-1*, thereby mediating its degradation.<sup>30,31</sup> Neutrophils from patients with *G6PC3* deficiency have higher levels of nonphos-

phorylated *GSK-3 $\beta$*  and phosphorylated *Mcl-1* than do neutrophils from unaffected people, a finding suggesting that a decrease in antiapoptotic *Mcl-1* accounts for increased apoptosis in *G6PC3*-deficient neutrophils. These alterations may be in part responsible for the phenotype of *G6PC3* deficiency.

Although we cannot rule out the possibility that additional mechanisms could contribute to the increase in apoptosis in *G6PC3*-deficient neutrophils, our data suggest that *G6PC3* acts by a pathway involving *GSK-3 $\beta$*  to maintain the viability of neutrophils. Evidence of increased endoplasmic reticulum stress has previously been reported in patients with mutations in *ELA2*,<sup>17,29</sup> and premature apoptosis of neutrophils is known to cause the phenotype of congenital neutropenia.<sup>12,16,17</sup> Thus, *G6PC3* deficiency is another example of how increased apoptosis of neutrophil granulocytes can cause congenital neutropenia.

Five arguments support our claim that *G6PC3* deficiency causes neutropenia. Distinct biallelic *G6PC3* mutations were found in two pedigrees and seven singleton patients with congenital neutropenia; sequence analysis predicted that all four missense mutations are likely to affect the function of *G6PC3*; expression of wild-type *G6PC3* and *G6PC3* with the R253H mutation in yeast showed that the R253H mutation abrogates enzymatic activity; *g6pc3*<sup>-/-</sup> knockout mice have neutropenia and increased myeloid-cell apoptosis; and the susceptibility to apoptosis in *G6PC3*-deficient myeloid cells was reduced by retroviral transfer of the wild-type *G6PC3* gene.

Supported by grants from the Deutsche Forschungsgemeinschaft (DFG KliFo 110-2, to Dr. Klein), the Junior Research Group "Glycomics" (to Dr. Gerardy-Schahn), the Bundesministerium für Bildung und Forschung Bone Marrow Failure Syndromes (to Drs. Welte and Klein), and the European Union (MEXT-CT-2006-042316, to Dr. Grimbacher); and by the Intramural Research Program of the National Institutes of Health, National Library of Medicine (for Dr. Schäffer). Dr. Boztug is a recipient of an Else Kröner Memorial Fellowship. Drs. Klein and Gerardy-Schahn are members of REBIRTH, a Deutsche Forschungsgemeinschaft Cluster of Excellence.

Dr. Welte reports owning equity in Amgen and receiving royalties on a patent for rhG-CSF. No other potential conflict of interest relevant to this article was reported.

We thank the patients and their families for supporting our study; all colleagues referring and registering patients at the Severe Chronic Neutropenia International Registry; François-Loïc Cosset for the kind gift of the RD114 plasmid; Edelgard Odenwald for analysis of bone marrow smears; Thomas Jack for his help with echocardiography; Jessica Pfannstiel, Maren Sievers, Marie Böhm, Marly Dalton, Martina Wackerhahn, Tanja Reinke, and Gwendoline Leroy for technical assistance; and Dr. Jean Donadieu at the Pediatric Hematology Oncology Service, Hôpital Trousseau, Paris, and Dr. Roula Farah at the Department of Pediatrics, Saint Georges Hospital, Balamand University, Beirut, Lebanon, for excellent collaboration.

## REFERENCES

- Kostmann R. Hereditär reticulos — en ny systemsjukdom. Svenska Laekartidningen 1950;47:2861-8. (In Swedish.)
- Idem*. Infantile genetic agranulocytosis; agranulocytosis infantilis hereditaria. Acta Paediatr 1956;45:Suppl:1-78.
- Welte K, Zeidler C, Dale DC. Severe congenital neutropenia. Semin Hematol 2006;43:189-95.
- Boztug K, Welte K, Zeidler C, Klein C. Congenital neutropenia syndromes. Immunol Allergy Clin North Am 2008;28:259-75.
- Bonilla MA, Gillio AP, Ruggeiro M, et al. Effects of recombinant human granulocyte colony-stimulating factor on neutropenia in patients with congenital agranulocytosis. N Engl J Med 1989;320:1574-80.
- Rosenberg PS, Alter BP, Bolyard AA, et al. The incidence of leukemia and mortality from sepsis in patients with severe congenital neutropenia receiving long-term G-CSF therapy. Blood 2006;107:4628-35.
- Boxer LA, Newburger PE. A molecular classification of congenital neutropenia syndromes. Pediatr Blood Cancer 2007;49:609-14.
- Schäffer AA, Klein C. Genetic heterogeneity in severe congenital neutropenia: how many aberrant pathways can kill a neutrophil? Curr Opin Allergy Clin Immunol 2007;7:481-94.
- Horwitz M, Benson KF, Person RE, Aprikyan AG, Dale DC. Mutations in *ELA2*, encoding neutrophil elastase, define a 21-day biological clock in cyclic haematopoiesis. Nat Genet 1999;23:433-6.
- Dale DC, Person RE, Bolyard AA, et al. Mutations in the gene encoding neutrophil elastase in congenital and cyclic neutropenia. Blood 2000;96:2317-22.
- Horwitz MS, Duan Z, Korkmaz B, Lee HH, Mealiffe ME, Salipante SJ. Neutrophil elastase in cyclic and severe congenital neutropenia. Blood 2007;109:1817-24.
- Klein C, Grudzien M, Appaswamy G, et al. HAX1 deficiency causes autosomal recessive severe congenital neutropenia (Kostmann disease). Nat Genet 2007;39:86-92.
- Devriendt K, Kim AS, Mathijs G, et al. Constitutively activating mutation in WASP causes X-linked severe congenital neutropenia. Nat Genet 2001;27:313-7.
- Ancliff PJ, Blundell MP, Cory GO, et al. Two novel activating mutations in the Wiskott-Aldrich syndrome protein result in congenital neutropenia. Blood 2006;108:2182-9.
- Person RE, Li F-Q, Duan Z, et al. Mutations in proto-oncogene *GFI1* cause human neutropenia and target *ELA2*. Nat Genet 2003;34:308-12.
- Carlsson G, Aprikyan AA, Tehranchi R, et al. Kostmann syndrome: severe congenital neutropenia associated with defective expression of Bcl-2, constitutive mitochondrial release of cytochrome c, and excessive apoptosis of myeloid progenitor cells. Blood 2004;103:3355-61.
- Grenda DS, Murakami M, Ghatak J, et al. Mutations of the *ELA2* gene found in patients with severe congenital neutropenia induce the unfolded protein response and cellular apoptosis. Blood 2007;110:4179-87.
- Fishelson M, Geiger D. Exact genetic linkage computations for general pedigrees. Bioinformatics 2002;18:Suppl 1:S189-S198.
- Idem*. Optimizing exact genetic linkage computations. J Comput Biol 2004;11:263-75.
- Broman KW, Murray JC, Sheffield VC, White RL, Weber JL. Comprehensive human genetic maps: individual and sex-specific variation in recombination. Am J Hum Genet 1998;63:861-9.
- Ashikov A, Routier F, Fuhlrott J, et al. The human solute carrier gene *SLC35B4* encodes a bifunctional nucleotide sugar transporter with specificity for UDP-xylose and UDP-N-acetylglucosamine. J Biol Chem 2005;280:27230-5.
- Bohn G, Allroth A, Brandes G, et al. A novel human primary immunodeficiency syndrome caused by deficiency of the endosomal adaptor protein p14. Nat Med 2007;13:38-45.
- Klein C, Bueler H, Mulligan RC. Comparative analysis of genetically modified dendritic cells and tumor cells as therapeutic cancer vaccines. J Exp Med 2000;191:1699-708.
- Beaudet AL, Anderson DC, Michels VV, Arion WJ, Lange AJ. Neutropenia and impaired neutrophil migration in type IB glycogen storage disease. J Pediatr 1980;97:906-10.
- Ng PC, Henikoff S. Accounting for human polymorphisms predicted to affect function. Genome Res 2002;12:436-46.
- Ramensky V, Bork P, Sunyaev S. Human non-synonymous SNPs: server and survey. Nucleic Acids Res 2002;30:3894-900.
- Lin JH, Walter P, Yen TS. Endoplasmic reticulum stress in disease pathogenesis. Annu Rev Pathol 2008;3:399-425.
- Glembotski CC. The role of the unfolded protein response in the heart. J Mol Cell Cardiol 2008;44:453-9.
- Köllner I, Sodeik B, Schreck S, et al. Mutations in neutrophil elastase causing congenital neutropenia lead to cytoplasmic protein accumulation and induction of the unfolded protein response. Blood 2006;108:493-500.
- Maurer U, Charvet C, Wagman AS, Dejardin E, Green DR. Glycogen synthase kinase-3 regulates mitochondrial outer membrane permeabilization and apoptosis by destabilization of MCL-1. Mol Cell 2006;21:749-60.
- Zhao Y, Altman BJ, Coloff JL, et al. Glycogen synthase kinase 3 $\alpha$  and 3 $\beta$  mediate a glucose-sensitive antiapoptotic signaling pathway to stabilize Mcl-1. Mol Cell Biol 2007;27:4328-39.
- Cohen P, Frame S. The renaissance of GSK3. Nat Rev Mol Cell Biol 2001;2:769-76.
- Dzhagalov I, St John A, He YW. The antiapoptotic protein Mcl-1 is essential for the survival of neutrophils but not macrophages. Blood 2007;109:1620-6.
- Lei K-J, Shelly LL, Pan C-J, Sidbury JB, Chou JY. Mutations in the glucose-6-phosphatase gene that cause glycogen storage disease type 1a. Science 1993;262:580-3.
- Martin CC, Bischof LJ, Bergman B, et al. Cloning and characterization of the human and rat islet-specific glucose-6-phosphatase catalytic subunit-related protein (IGRP) genes. J Biol Chem 2001;276:25197-207.
- Arden SD, Zahn T, Steegers S, et al. Molecular cloning of a pancreatic islet-specific glucose-6-phosphatase catalytic subunit-related protein. Diabetes 1999;48:531-42.
- Petrolonis AJ, Yang Q, Tummino PJ, et al. Enzymatic characterization of the pancreatic islet-specific glucose-6-phosphatase-related protein (IGRP). J Biol Chem 2004;279:13976-83.
- Bouatia-Naji N, Rocheleau G, Van Lommel L, et al. A polymorphism within the *G6PC2* gene is associated with fasting plasma glucose levels. Science 2008;320:1085-8.
- Chen W-M, Erdos MR, Jackson AU, et al. Variations in the *G6PC2/ABCB11* genomic region are associated with fasting glucose levels. J Clin Invest 2008;118:2620-8.
- Martin CC, Oeser JK, Svitek CA, Hunter SI, Hutton JC, O'Brien RM. Identification and characterization of a human cDNA and gene encoding a ubiquitously expressed glucose-6-phosphatase catalytic subunit-related protein. J Mol Endocrinol 2002;29:205-22.
- Guionie O, Clottes E, Stafford K, Burchell A. Identification and characterisation of a new human glucose-6-phosphatase isoform. FEBS Lett 2003;551:159-64.
- van Schaftingen E, Gerin I. The glucose-6-phosphatase system. Biochem J 2002;362:513-32.
- Lei K-J, Chen H, Pan C-J, et al. Glucose-6-phosphatase dependent substrate transport in the glycogen storage disease type-1a mouse. Nat Genet 1996;13:203-9.
- Melis D, Fulceri R, Parenti G, et al. Genotype/phenotype correlation in glycogen storage disease type 1b: a multicentre study and review of the literature. Eur J Pediatr 2005;164:501-8.
- Cheung YY, Kim SY, Yiu WH, et al. Impaired neutrophil activity and increased susceptibility to bacterial infection in mice lacking glucose-6-phosphatase- $\beta$ . J Clin Invest 2007;117:784-93.
- Wang Y, Oeser JK, Yang C, et al. Deletion of the gene encoding the ubiquitously expressed glucose-6-phosphatase catalytic subunit-related protein (UGRP)/glucose-6-phosphatase catalytic subunit- $\beta$  results in lowered plasma cholesterol and elevated glucagon. J Biol Chem 2006;281:39982-9.
- Ron D, Walter P. Signal integration in the endoplasmic reticulum unfolded protein response. Nat Rev Mol Cell Biol 2007;8:519-29.

Copyright © 2009 Massachusetts Medical Society.